Universiteit Utrecht

if

Combining geothermal energy with CO_2 storage

Feasibility study of low temperature geothermal electricity production using carbon dioxide as working and storage fluid

Master thesis report
Sustainable development – Track energy and resources
Dave Janse
3293459
April 1st 2010

Combining geothermal energy with CO2 storage

Feasibility study of low temperature geothermal electricity production using carbon dioxide as working and storage fluid

Utrecht University:

Heidelberglaan 8
Postbus 80125
3584 CS Utrecht
www.uu.nl

Student: Name: D.H.M. Janse
Student nr: 3293459
Master: Sustainable Development – Track Energy and Resources
Address: Pastoor Leytenstraat 50
Postal code: 4854 KP Bavel
Telephone: 06-10672397
ECTS thesis: 45

Supervisor: Name: dr. E. Nieuwlaar
Telephone: 030-2537607

IF Technology:

Velperweg 37
Postbus 605
6800 AP Arnhem
www.iftechnology.nl

Supervisor: Name: dr. M. Gutierrez-Neri
Telephone: 026-3535564

Abstract

One of the emerging solutions for today's excess of carbon dioxide emissions, which is one of the major causes of global warming, is the geological storage of carbon dioxide in geothermal reservoirs as depleted gas and oil fields or saline aquifers. The carbon dioxide is captured and pumped into a reservoir which is closed when the reservoir is full. Using this method a certain amount of carbon dioxide is avoided from being emitted to the atmosphere and prevented from contributing to global warming. Another solution is through the usage of renewable energy sources such as geothermal energy. This green energy also uses geothermal reservoirs but in a different way as is the case with carbon dioxide storage. At depths varying from several hundreds of meters to several kilometers geothermal energy is used to provide heat. From a depth of 6 kilometers and deeper geothermal energy is used to produce electricity by means of superheated steam.

This study aims to use the best of two worlds by combining carbon dioxide storage and geothermal energy and integrate them in a system where carbon dioxide is used as working fluid for a geothermal system at a depth of 2 to 3 kilometers which produces electricity. However, before this can be realized a clear understanding of carbon dioxide and its behavior when exposed to geothermal pressure and temperature is required.

A clear result from this research is that carbon dioxide is suitable as working fluid for geothermal energy, mainly because of its low critical point, which lies at 73.8 bar and 304.1 K. Using average conditions in the Netherlands a depth of 718 meters is required to change carbon dioxide from liquid to supercritical. At supercritical phase carbon dioxide has a much lower viscosity than water at the same pressure and temperature which allows for a larger flow in a geothermal reservoir. Compared to water, carbon dioxide has a lower heat capacity and therefore requires more flow to extract the same amount of energy.

It is possible to produce geothermal electricity using carbon dioxide as working fluid at average conditions in the Netherlands. The chosen base reservoir depth is 2000 meter which allows for a temperature of 345 kelvin. This choice is based on the fact that it is deep enough to produce a decent amount of heat while it does not come near the depths for geothermal power production. A reservoir at 2000 meter depth allows for a geothermal electricity production of 0.49 MW_e which can be maintained for at least 50 years using a distance of 1400 meter between the injection and recovery well. When more ideal properties are used such as a depth of 3000 meter or a temperature gradient of 50 degrees per kilometer the electricity production can rise to 4.95 MW_e per doublet. If the reservoir is large enough multiple doublets could be placed which greatly enhances the overall power production.

A geothermal carbon dioxide system can be placed on an empty reservoir or on a reservoir which has already been filled with carbon dioxide as a result of a carbon storage project. This has no effect on the electricity output but determines to a large extent the costs of the system. If a reservoir still needs to be filled with carbon dioxide extra investment costs occur due to the need of injection wells, transport

costs and compression costs. On the contrary, more revenues are earned by gaining carbon credits for the stored carbon dioxide.

At average conditions in the Netherlands it is not economically feasible to produce electricity using a geothermal system with carbon dioxide as working fluid if the reservoir still needs to filled with carbon dioxide. When the reservoir is already filled, the pay back period varies from 38 years and more. However, in more ideal circumstances, the pay back period reduces to 5 to 11 years. This reduction in pay back period is mainly caused by higher electricity sales but also by higher incomes from carbon credits due to carbon neutral electricity production.

This research shows that using carbon dioxide as geothermal working fluid is very promising. The production of a geothermal carbon dioxide system allows for electricity production without the need of going to large depths. It uses techniques which have been used for decades. The system is applicable at nearly every gas field below 800 meters. Depending on the reservoir the system can pay itself back as early as 5 years. And the system can contribute to combating climate change by the production of carbon neutral electricity.

Table of contents

Preface

This report has been written as master thesis report for the master program Sustainable Development, track Energy and Resources at the University Utrecht. During a period of 9 months I have been working on this study at IF technology, a leading company in consultancy and engineering in geothermal energy for the Netherlands and abroad.

In particular, I would like to thank dr. Evert Nieuwlaar from the Utrecht University for supervising this project. He spent a lot of time on this project and was always available to share his expertise.

Also, I would like to thank dr. Mariene Gutierrez-Neri and drs. Guus Willemsen from IF Technology. They assisted and guided me in this project, made time when I had questions and shared their expertise when I needed it.

Finally, I would like to thank Prof. dr. Ruud Schotting from the Utrecht University. Despite his full agenda he made time available to answer my questions and share his knowledge.

I wish everyone an enjoyable time reading this report.

Dave Janse

April 1st 2010

1 Introduction

1.1 Background information

One of the major problems of today's society is the risk of climate change caused by, among others, large scale emission of CO_2 as shown in figure 1.1. The result of this production will have both short and long term effects, of which the magnitude still needs to be assessed. Therefore, a large number of countries have agreed to reduce their emissions, according to rules stated within the Kyoto protocol. For the Netherlands, this means an emission reduction of 6% per year in the period of 2008-2012(Ministerie van VROM, 2006). However, it does not end after 2012, since the Kyoto 2 agreement starts in 2013, demanding further reductions and imposing fines to those countries that failed to meet their 2012 targets.

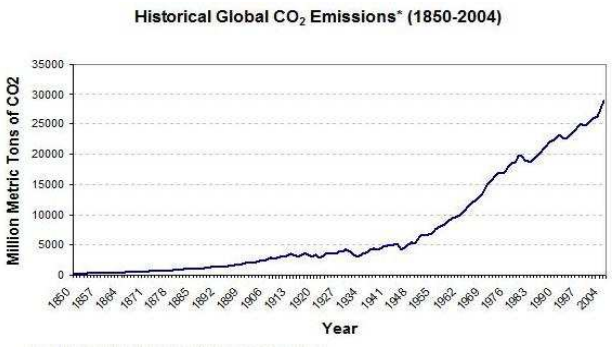

Figure 1-1. Historical global carbon dioxide emissions (Marland 2007)

Besides the Kyoto protocol, more recent agreements are playing an important role to stimulate action against climate change. The first is the Climate action program by the European Union, where they state a so called 20/20/20 commitment. The 20/20/20 commitment aims to have a 20% overall emissions reduction in 2020 compared to the 1990 level and to have a 20% share of renewables in total energy use(European Environment Commission, 2010). The second recent agreement has been made by the G8 top in L'Aquila, Italy. The G8 top has agreed to limit the temperature rise to a maximum of 2°C globally(De Volkskrant, 2009). Besides the temperature, the G8 also agreed to reduce emissions by 80% in the year 2050 for the industrialized countries, with the aim to reduce global emissions by 50% in 2050. A very important factor in the struggle against climate change is the role of the United States, being the country with nearly the largest emission per capita(Nationmaster.com, 2003). The United States signed the Kyoto protocol in 1998, but never ratified, making the agreement non-binding, but now the newly elected president Barack Obama has agreed to comply with the G8 commitment.

One of the emerging technologies for this problem is carbon capture and storage(CCS)(Broek, et al., 2008). CCS has a large potential, especially in the Netherlands, where gas fields are running empty and clearing large storage spaces. The carbon dioxide reduction that CCS can achieve in the Netherlands can go up to 15% in 2020 and 50% in 2050, compared to 1990 targets(Broek, et al., 2008). However, this will require a large investment in a carbon dioxide transport infrastructure and still has much uncertainties and long term risks(Damen, et al., 2006). In the past, a sudden escape of large amounts of carbon dioxide in Lake Nyos in Cameroon caused death by suffocation for 1700 people and thousands of animals. This alone proves that the risks should not be taken lightly.

The earth's soil consists of several different layers, of which some have the ability to hold fluids because of a higher situated impermeable layer. During the past several millions of years, natural gas has been formed in such layers, which we currently burn in our houses and industry. The withdrawal of natural gas results in a lower pressure underground, which can cause landslides, erosion, loss of soil productivity and more(Commissie bodemdaling, 2010). The properties of this layer and the withdrawal of the natural gas clears potential storage space for fluids.

What also has to be considered is the depth of these layers, and with it an increased temperature. There is technology available to withdraw this heat from the earth's soil and use it for

domestic heating or for electricity production, although the latter requires depths of 6 kilometers and more when conventional geothermal systems with water as working fluid are used.

Much research has been done on underground storage of CO_2, with the prospect of large scale application in the Netherlands within 10 years(Broek, et al., 2008)(Damen, et al., 2006). More research has been done: additional purposes for carbon dioxide storage such as ECBM (enhanced coal bed methane), where carbon dioxide is injected in coal beds to produce methane(Hamelink, et al., 2001); increased flow of natural gas or oil recovery from gas and oil fields, where CO_2 is injected in low quantity gas and oil fields to optimize the gas and oil recovery by increasing the pressure(Hovorka, et al., 2008); and the mitigation of carbon dioxide by dissolving the carbon dioxide in water used in geothermal wells(Willemsen, et al., 2008). However, no research has been done on the direct production of electricity from carbon dioxide storage, which will be the main subject of this master thesis research.

This research focuses on the production of electricity instead of heat. Reasons for this choice are: electricity can be transported with fewer losses than water and is therefore less dependent on geographical location; producing heat with carbon dioxide as a working fluid has already been researched(Pruess, 2006); producing electricity with carbon dioxide as working fluid is possible at much smaller depths compared to conventional water based geothermal power production; and geothermal power production is one of the few sustainable technologies which can produce electricity without being dependent on other effects as sunlight, wind or tides.

1.2 Problem definition

As stated above, the current society emits a large amount of greenhouse gasses, mainly carbon dioxide. To prevent environmental disaster, actions have to be taken to reduce these emissions. One of these actions is the Kyoto protocol, as described above. To comply with the agreements of the Kyoto protocol, several measures are being taken to cope with these goals, like for instance CCS, a promising technology which reduces emissions to the environment(Broek, et al., 2008).

However CCS is a temporary solution for large scale greenhouse gas emissions. For example, if we continue with the hypothetical case that there are no emission targets, also stated as the business as usual (BAU) case, the carbon dioxide emissions in the power sector alone would equal 113-117 Mt/yr(Broek, et al., 2008) in the year 2050. As stated by the same authors, CCS can avoid 63 MT CO_2/yr, equaling a reduction of 53% in the electricity production sector. The total available storage space equals nearly 3000 Mt $CO_{2(\text{Broek, et al., 2008})}$. Using a gradual increase in carbon dioxide injection, the storage space will be depleted by the year 2071, negating any further carbon dioxide mitigation by CCS. Therefore, on the longer term, if no action is taken to actually reduce emissions, further measures have to be taken, such as measures which reduce the consumption of energy and measures which produce energy in a sustainable way.

When the CO_2 is stored underground, thermal energy is transferred to the carbon dioxide, namely geothermal heat from the earth. The fact that this amount of heat is significant enough to withdraw is seen in the technology and application of geothermal energy. There are studies that combine carbon dioxide and geothermal energy by replacing water as working fluid with carbon dioxide (Pruess, 2006). carbon dioxide is shown as a promising working fluid of geothermal systems compared to water, because of properties as a larger expansivity and lower viscosity of supercritical CO_2. However, as discussed in(Pruess, 2006), losses equal to 1 ton/s are stated, but failed to explain where this amount of carbon dioxide disappears to.

One of the most used techniques for electricity production is the usage of the so called Rankine cycle. This cycle uses water and steam to drive a turbine which produces electricity. An alternative to this is the Organic Rankine cycle (ORC) which uses organic fluids instead of water(Qouilin, 2007). A

second alternative is the Carbon Dioxide Transcritical Power Cycle(CO_2 TPC)(Chen, et al., 2006), which uses the differences between the supercritical and subcritical phase of carbon dioxide. Due to its large expansivity, increased temperature in CCS and wide availability, carbon dioxide as a working fluid for both geothermal energy and electricity production with an ORC or CO_2 TPC is worth investigating.

1.3 Research question

The following research question has been defined to analyze the potential of the combination of underground stored CO_2 and electricity production by means of geothermal energy:

- **Is it possible, and if possible to which extent, to combine CO_2 storage and geothermal energy for the production of sustainable electricity using CO_2 as working fluid, based on technical feasibility, environmental impact and economical viability?**

Additional questions to this research will be as follows:

1. **What is the current knowledge of CO_2 storage and geothermal energy, based mainly on technical feasibility and environmental impact both in the Netherlands and abroad?**

2. **How does CO_2 behave when stored underground with increased temperature and pressure, when pumped into the soil and when recovered from the soil?**

3. **What are the costs for geothermal CO_2, what are the risks of using CO_2 in geothermal systems for the environment and the nearby population and how can these be minimized?**

4. **Which properties of geological locations are best for optimizing the output of geothermal CO_2, maximizing the safety for the environment and minimizing the investment costs?**

1.4 Report composition

The report starts in chapter 2 by describing carbon dioxide. Chapter 2 consists of a general explanation of carbon dioxide followed by a set of calculation which describes the following properties of carbon dioxide:

- Pressure
- Temperature
- Density
- Compressibility factor
- Fugacity coefficient
- Viscosity
- Specific enthalpy
- Heat capacity
- Specific volume

Chapter 2 ends with a validation where the equations and their results are compared with literature.

Chapter 3 then continues with an explanation of the system including a small introduction to give an impression of the magnitude of the system. All the different parts will be explained followed by the different used equations in the system. Chapter 3 also ends with a validation where the system is compared with literature.

Chapter 4 describes the process to combine all the equations from chapters 2 and 3 into a theoretical model. Every step in the model is visualized using a pressure-enthalpy diagram, a temperature-entropy diagram and a systematic representation.

Chapter 5 describes the results of the model. First a base case is defined which uses average values for the Netherlands. The base case is then used in a sensitivity analysis where the effect of several variables has been analyzed. The results from the sensitivity analysis are then used to define an optimal case which uses the positive outcomes from the sensitivity analysis within realistic boundaries. Chapter 5 ends with a validation where the results are compared with literature.

Chapter 6 contains the safety, environment and financial analysis. This chapter gives a rough estimation on the potential safety risks, the effects on the environment and the financial credibility.

Chapter 7 uses the theoretical model from chapter 4 and the financial analysis from chapter 6 and uses it to calculate the results and effects if a geothermal carbon dioxide projects as stated in this report is used at the empty gas field of Barentdrecht Ziedwij.

Chapter 8 contains the conclusions of the report and chapter 9 discusses the assumptions and limitations of the system and will give some proposals for future work.

2 Carbon dioxide properties

This chapter describes the properties of carbon dioxide which are relevant in the context of this research. The properties of carbon dioxide are calculated and compared to other sources in the range for 30 to 400 bars and 250 to 500 K. This range has been chosen from consideration of reality. The pressure of the system described later in this research will never go below 30 bars since it costs much energy to compress or cool the carbon dioxide to liquid state. The limit of 400 bars is chosen because the depth required will be in the vicinity of 4 kilometers(TNO Bouw en Ondergrond, 2009), which comes near conventional geothermal power systems while the aim of this research is to design a geothermal power system with limited depth.

The temperature range has been set at 250 to 500 K. Carbon dioxide will be cooled by surface water which will never reach 250 K, making it a realistic boundary. A high geothermal gradient and a large depth is required to reach the temperature of 500 K, which falls outside the aim of this research as stated above.

2.1 What is carbon dioxide?

Scientifically, carbon dioxide is a colorless and odorless gas consisting of a single carbon atom connected with 2 double bonded oxygen atoms. Carbon dioxide is nearly harmless to humans, where only high concentrations can cause problems (Air Products Industry Co., Ltd, 2009).

Biologically, carbon dioxide plays a major role in formation and decomposition of sugars. Plants, using photosynthesis, break down CO2 to produce organic compounds, while humans produce CO2 by breaking down sugar, fats and more(EMC, 2007).

Environmentally, carbon dioxide is a trace gas, making up for less than 0.1% of the gas in the atmosphere. Furthermore, carbon dioxide is a greenhouse gas, currently responsible for about 60% of the greenhouse effect caused by human influences(BBC, 2009).

Before the potential of using carbon dioxide as a working fluid in low temperature geothermal electricity production can be analyzed, a clear understanding of the behavior and properties of carbon dioxide is required.

2.2 Carbon dioxide phases

Carbon dioxide has been chosen as a working fluid mainly because of its critical point. Carbon dioxide can exist in four phases being solid, liquid, gas and supercritical. The solid phase is not relevant for this study, because it either requires a very low temperature, a very high pressure or a combination of both. The required temperatures and pressures are not even close to the ranges of the system and the solid phase will therefore not be taken into account.

Carbon dioxide has a critical pressure of 73.8 bar and a critical temperature of 304.1 kelvin(Dean, 1999). Both the critical pressure and the critical temperature are easily reached in geothermal power systems.

For example, on average the temperature increase in the underground in the Netherlands equals 31 degrees per kilometer(Lokhorst, et al., 2007) and the average surface temperature equals 283.5 K(Koninklijk Nederlands Meteorologisch Instituut, 2010). Furthermore, hydrostatic pressure in geothermal reservoirs is roughly estimated as having a pressure increase of 100 bars per kilometer(Meer, et al., 2009). In the Netherlands using average values for temperatures, supercritical carbon dioxide is obtained in a reservoir with a depth starting from 728 meter.

2.3 Carbon dioxide properties: General

A small remark on the units used in this chapter is that all the units are mentioned as they are stated in the references cited. During the calculation process there are constants used to convert the units to SI units. An overview of all used equations and parameters can be found in appendix 1.

EOS: Equations of state

In the start of the research on the properties of carbon dioxide, two main problems aroused. First of all, carbon dioxide is far from an ideal gas, while ideal gasses make up for a major part of the calculations found in literature. The second problem resulted from the first, since there is no exact formula describing the relationship between pressure, temperature, density and volume for carbon dioxide. To solve these problems an equation of state (EOS) is used. An EOS is an equation which describes the relation between various state variables of a certain substance. Using an EOS, it is possible to calculate these variables. However, an EOS is also nothing more than a mere approximation.

There are many articles available covering an EOS for carbon dioxide(Fedyunina, et al., 1992) (Duan and Sun, 2002) (Duan, Moller & Waere, 1992)(Sterner, et al., 1994)(Vukolovich, et al., 1963)(Sandri, et al., 1969)(Tsiklis, 1969). However, while these EOS cover very wide ranges up to 20000 K and 8000 bar the range near phase transitions is crucial for this project and often gives large deviations. These EOS are analyzed and compared with tabulated experimental data to find the optimal EOS for the chosen pressure and temperature range.

There are two EOS which give good results in the chosen range. However, both gave problems around the gas-liquid boundary. The EOS from Duan(Duan, Moller & Waere, 1992), further addressed as EOS Duan, gave some deviation on the liquid side while the EOS from Sterner(Sterner, et al., 1994), further addressed as EOS Sterner, gave deviation on the gas side. Therefore, a choice has been made to use multiple EOS. First, the density is calculated using the EOS from Duan. The density from Duan is then used to calculate the specific enthalpy. Whenever the specific enthalpy is higher than the specific enthalpy at the critical point, the density will be recalculated using the EOS from Sterner.

This is shown in figure 2.1, where the red line represents the specific enthalpy at the critical point. On the left side of that line the EOS from Sterner is used while on the right side of that line the EOS from Duan is used.

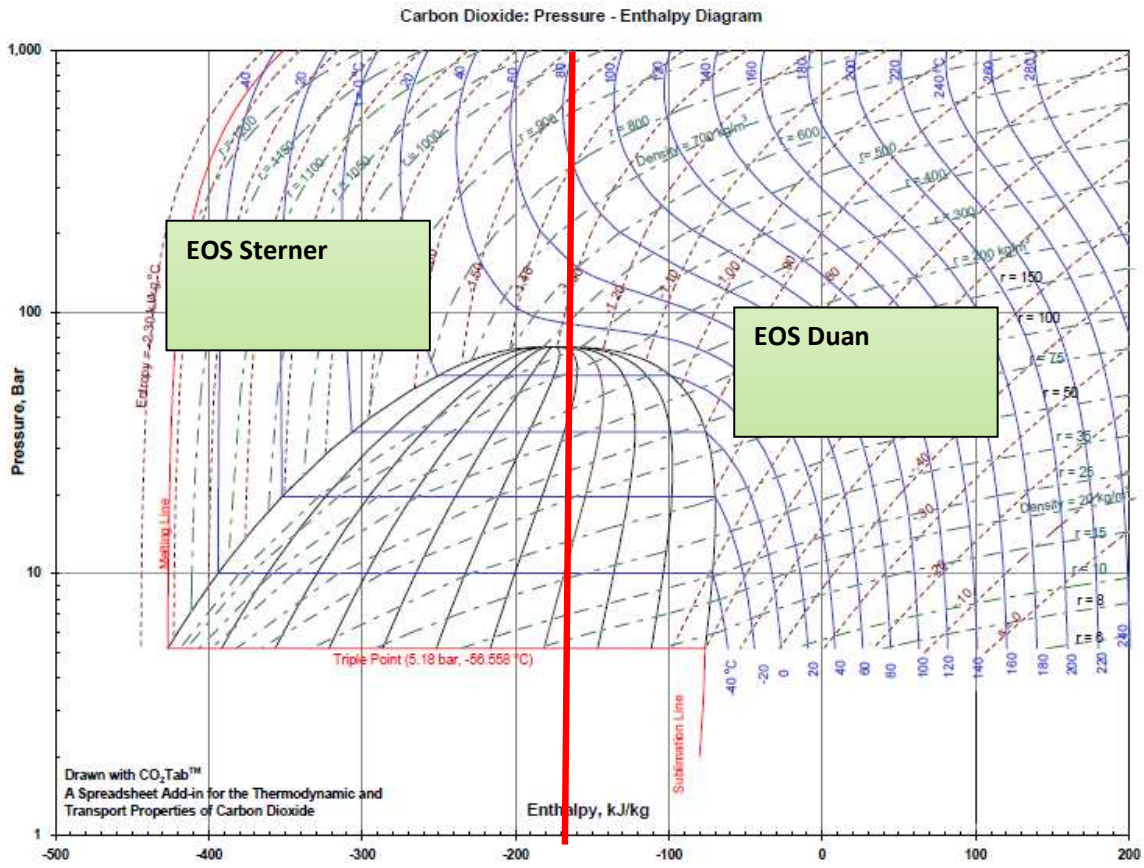

Figure 2-1. Division of EOS from Sterner and Duan shown on a pressure-enthalpy diagram. Reproduced with permission. (Chemalogic Corporation, 2009)

The equation of state from Sterner is formulated as follows (Sterner, et al., 1994).

$$\frac{P}{RT} = \rho + b_1\rho^2 - \rho^2\left(\frac{b_3 + 2b_4\rho + 3b_5\rho^2 + 4b_6\rho^3}{(b_2 + b_3\rho + b_4\rho^2 + b_5\rho^3 + b_6\rho^4)^2}\right) + b_7\rho^2 e^{-b_8\rho} + b_9\rho^2 e^{-b_{10}\rho}$$

(Eq. 1)

where:

P= Pressure (Pa)
T= Temperature (K)
ρ= Density (mol m^{-3})
R= Gas constant (8.314472 J K^{-1} mol^{-1})
b_x= Parameter from Appendix 1

The equation of state from Duan is formulated as follows(Duan, et al., 1992)

$$Z=\frac{PV}{RT}=\frac{P_r V_r}{T_r}=1+\frac{B}{V_r}+\frac{C}{V_r^2}+\frac{D}{V_r^4}+\frac{E}{V_r^5}+\frac{F}{V_r^2}\left(\beta+\frac{\gamma}{V_r^2}\right)e^{\left(-\frac{\gamma}{V_r^2}\right)} \qquad \text{(Eq. 2)}$$

where:

$$B=c_1+\frac{c_2}{T_r^2}+\frac{c_3}{T_r^3} \qquad D=c_7+\frac{c_8}{T_r^2}+\frac{c_9}{T_r^3} \qquad F=\frac{c_{13}}{T_r^3}$$

$$C=c_4+\frac{c_5}{T_r^2}+\frac{c_6}{T_r^3} \qquad E=c_{10}+\frac{c_{11}}{T_r^2}+\frac{c_{12}}{T_r^3}$$

where:

Z = Compressibility factor
P= Pressure (Pa)
V= Molar volume (dm3/mol)
T= Temperature (K)
c_x= Parameter from appendix 1
P_r = Reduced pressure = P/P_c
V_r = Reduced volume = V/V_c
T_r = Reduced temperature = T/T_c
P_c = Critical pressure = 73.8 bar
V_c = $\frac{RT_c}{P_c}$
T_c = Critical temperature = 304.1 K

Using both EOS, the density and volume of carbon dioxide can be calculated for the whole pressure and temperature range of the system. Besides density and volume, other properties of carbon dioxide are also calculated.

Pressure

The pressure is one of the two properties that are used as a base for calculating the rest of the properties.

Temperature

Temperature is the other property that is used as a base for the other properties.

Density

Density is the amount of moles or mass of carbon dioxide per unit of volume. It can be seen in figure 2.2 and 2.3 that carbon dioxide has a low density at low pressure and high temperature. In this region, carbon dioxide is gas. When carbon dioxide reaches a pressure of 73.8 bars the phase changes to supercritical where carbon dioxide is considered to be neither a gas nor a liquid. When the temperature drops below 304.1 K, the carbon dioxide becomes a liquid, which can be seen near the red area of figure 2.2 and 2.3.

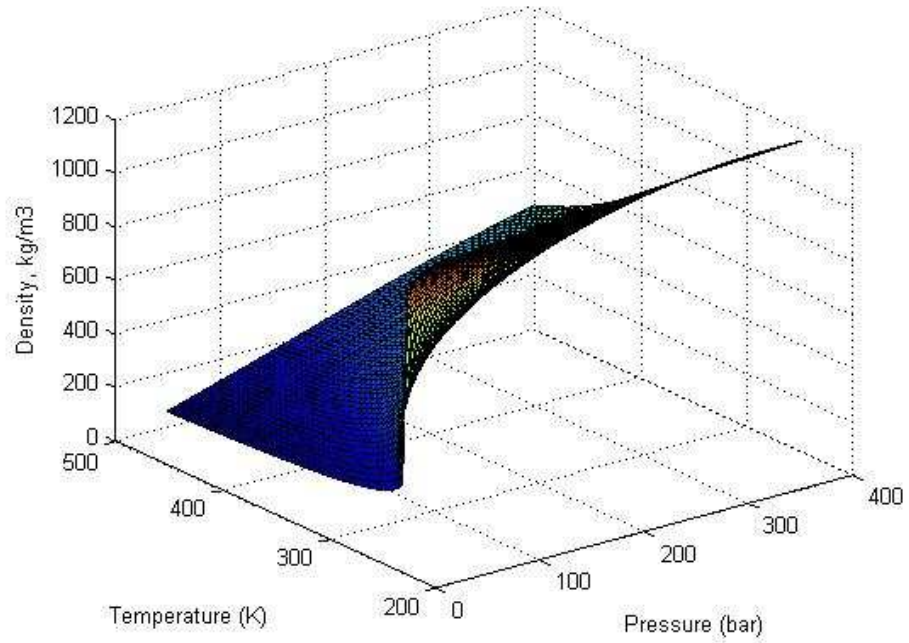

Figure 2-2. Density as a function of pressure and temperature

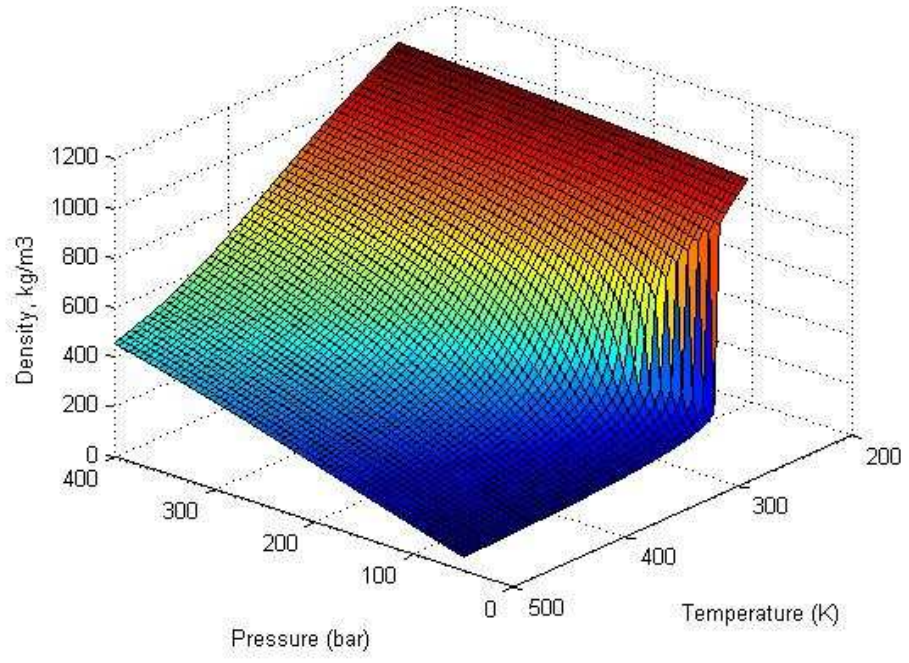

Figure 2-3. Density as a function of pressure and temperature. Axes have been changed to increase visibility.

Compressibility factor

The compressibility factor is a property which is implemented to modify the ideal gas law. The compressibility factor is used in many different equations for real gasses, such as the fugacity coefficient, enthalpy and entropy calculations in this report. A compressibility factor close to 1 approaches an ideal gas. The difference between the compressibility factor and fugacity coefficient, where the latter will be described later, is that the compressibility focuses more on volume and intermolecular forces while the fugacity coefficient focuses on pressure effects.

The compressibility factor is calculated as follows(Duan, et al., 1992).

$$Z = \frac{P_r V_r}{T_r} \qquad \text{(Eq. 3)}$$

where:

The compressibility factor as a function of pressure and temperature is shown in figure 2.4.

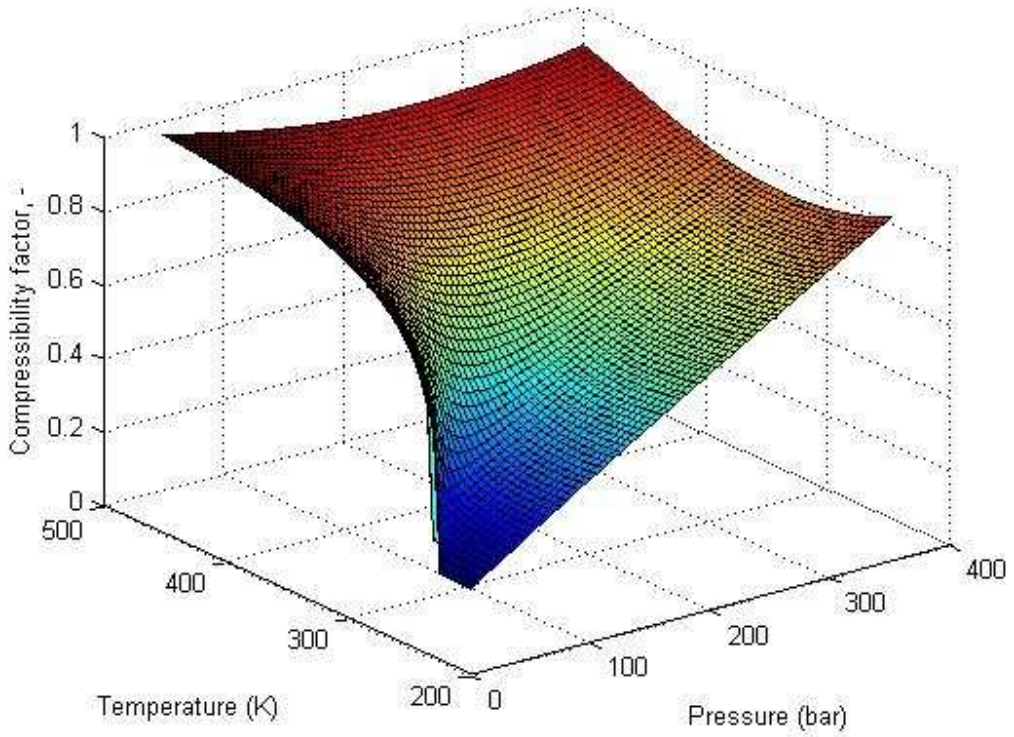

Figure 2-4. Compressibility versus pressure and temperature

Fugacity coefficient

While calculations often assume a gas to be ideal, this is often not the case. The fugacity of a gas is used quantify the deviation from an ideal gas due to pressure effects.. The fugacity coefficient relates the fugacity to the pressure by (Daubert, 1986):

$$\phi = \frac{f}{P} \qquad \text{(Eq. 4)}$$

where:
ϕ = Fugacity coefficient, -
f = Fugacity, -

When a substance has a low pressure and a high temperature, ideal gas properties are approached, showing a fugacity coefficient of nearly 1.

The fugacity coefficient is calculated using an equation from (Daubert, 1986):

$$\ln(\phi) = \ln(\phi)^{(1)} - \frac{\omega^{(1)}}{\omega^{(2)}}\left(\ln(\phi)^{(2)} - \ln(\phi)^{(1)}\right) \qquad \text{(Eq. 5)}$$

where:

ω=Acentric factor for either (1) carbon dioxide or (2) reference fluid. A value for a specific substance to account for the characteristics of its molecular structure, which is defined by (Pitzer, et al., 1955):

$$\omega = -log_{10}\left(\frac{P_{sat}}{P_c}\right) - 1 \quad \text{at} \quad T_r=0.7 \qquad \text{(Eq. 6)}$$

where:

P_{sat}= Saturated pressure, bar

$$\ln(\phi)^{(i)} = Z^{(i)} - 1 - \ln\left(Z^{(i)}\right) + \frac{Bz}{V_r} + \frac{Cz}{2V_r^2} + \frac{Dz}{5V_r^5} + \frac{e_{i,8}}{2T_r^3 e_{i,12}}\left(e_{i,11} + 1 - \left(e_{i,11} + 1 + \frac{e_{i,12}}{V_r^2}\right)\right)e^{-\frac{e_{i,12}}{V_r^2}} \qquad \text{(Eq. 7)}$$

(Eq. 7)

where:

$$Bz = e_{i,1} - \frac{e_{i,2}}{T_r} - \frac{e_{i,3}}{T_r^3} - \frac{e_{i,4}}{T_r^3} \qquad \text{(Eq. 8)}$$

$$Cz = e_{i,5} - \frac{e_{i,6}}{T_r} + \frac{e_{i,7}}{T_r^3} \qquad \text{(Eq. 9)}$$

$$Dz = e_{i,9} + \frac{e_{i,10}}{T_r} \quad \text{(Eq. 10)}$$

$e_{i,j}$ = parameters from Daubert(Daubert, 1986)

Figure 2.5 shows the fugacity as a function of pressure and temperature.

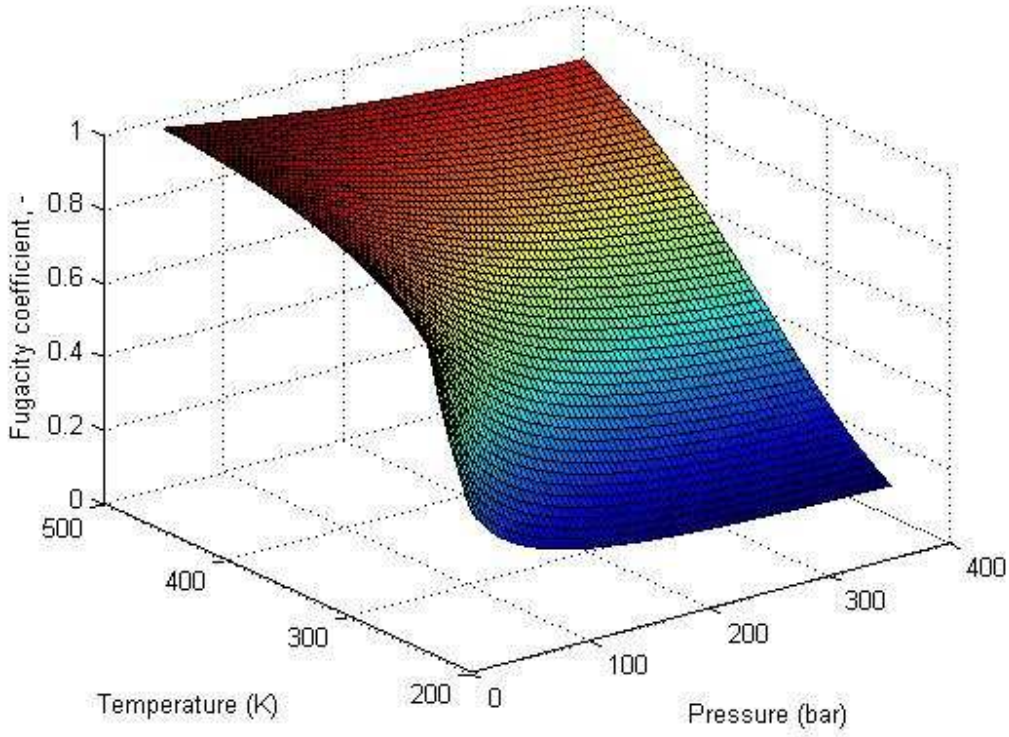

Figure 2-5. Fugacity coefficient versus pressure and temperature

Viscosity

Viscosity for carbon dioxide plays a role in calculating the flow. The larger the viscosity of carbon dioxide, the larger the effect of friction will be, reducing the overall flow of the system. Sovová proposed the following relation to calculate the viscosity of carbon dioxide(Sonová, et al., 1993):

$$\mu = \mu_0 e^{\sum_{i=1}^{4}\sum_{j=0}^{1}\frac{a_{ij}\rho_r^i}{T_r^j}} \qquad \text{(Eq. 11)}$$

where:
μ = Viscosity, Pa s
μ_0 = Viscosity ideal gas, Pa s
ρ_r = Reduced density, -
T_r = Reduced temperature, -
a_{ij} = Parameter from Sonová and Prochoázka (Sonová, et al., 1993)

2.4 Carbon dioxide properties: Thermodynamics

Specific enthalpy

The specific enthalpy is described as the amount of enthalpy per unit of mass. It is uncommon to use and calculate the absolute specific enthalpy, since in most cases the absolute specific enthalpy does not have much meaning. Mostly the difference in the specific enthalpy of two states is used. The enthalpy at 1 bar and 273 K is used as a reference in the calculation of the specific enthalpy. All calculated specific enthalpies are calculated as the enthalpy difference between pressure P and temperature T and the reference state.

The second problem that occurred is that there is no formula that describes the specific enthalpy of carbon dioxide, much like the usage of the EOS as mentioned above. Daubert poses a formula in his book which can be used to approach the specific enthalpy of carbon dioxide. The specific enthalpy is obtained as follows(Daubert, 1986):

$$h = h_0 - \frac{RT_c}{M}\left(\frac{\overline{H}^0 - \overline{H}}{RT_c}\right) \qquad \text{(Eq. 12)}$$

where:

- h= Specific enthalpy at pressure P and temperature T, kJ/kg
- h_0= Enthalpy of the ideal gas at 1 bar and temperature T, kJ/kg

$$h_0 = A + BT + CT^2 + DT^3 + ET^4 + FT^5 \qquad \text{(Eq. 13)}$$

- A,B,C,D,E,F = Parameters from Daubert
- R= Gas constant, 8.314 kJ/kmol/K (Dean, 1999)
- Tc= critical temperature, 304.1 K (Dean, 1999)
- M=Molar mass, 44.01 g/mol (Dean, 1999)
- $\left(\frac{\overline{H}^0 - \overline{H}}{RT_c}\right)$ = Dimensionless pressure effect on enthalpy, as defined by (Daubert, 1986):

$$\left(\frac{\overline{H}^0-\overline{H}}{RT_c}\right)=\left(\frac{\overline{H}^0-\overline{H}}{RT_{c,0}}\right)^{(1)}+\frac{\omega^{(1)}}{\omega^{(2)}}\left(\left(\frac{\overline{H}^0-\overline{H}}{RT_{c,h}}\right)^{(2)}-\left(\frac{\overline{H}^0-\overline{H}}{RT_{c,0}}\right)^{(1)}\right) \quad \text{(Eq. 14)}$$

ω=Acentric factor for either (1) carbon dioxide or (2) reference fluid

$$\left(\frac{\overline{H}^0-\overline{H}}{RT_{c,0}}\right)^{(i)}=-T_r\left(z^{(i)}-1-\frac{\mathrm{e_{i,2}}+\frac{2\mathrm{e_{i,3}}}{T_r}+\frac{3\mathrm{e_{i,4}}}{T_r^2}}{T_rV_r}-\frac{e_{\mathrm{i,6}}+\frac{3\mathrm{e_{,3}}}{T_r^2}}{2T_rV_r^2}-\frac{\mathrm{e_{i,10}}}{5T_rV_r^5}+\frac{3\mathrm{e_{i,8}}}{2T_r^3\mathrm{e_{i,12}}}\left(\mathrm{e_{i,11}}+1-\left(\mathrm{e_{i,11}}+1+\frac{\mathrm{e_{i,12}}}{V_r^2}\right)e^{\left(-\frac{\mathrm{e_{i,12}}}{V_r^2}\right)}\right)\right)$$

(Eq. 15)

Where:

$$z^{(i)}=\frac{\mathrm{P_rV_r}}{\mathrm{T_r}}=1+\frac{\mathrm{Bz}}{\mathrm{V_r}}+\frac{\mathrm{Cz}}{\mathrm{V_r^2}}+\frac{\mathrm{Dz}}{\mathrm{V_r^5}}+\frac{\mathrm{e_{i,8}}}{\mathrm{T_r^3V_r^2}}\left(\mathrm{e_{i,11}}+\frac{\mathrm{e_{i,12}}}{\mathrm{V_r^2}}\right)e^{-\frac{e_{i,12}}{V_r^2}} \quad \text{(Eq. 16)}$$

$$Bz=\mathrm{e_{i,1}}+\frac{\mathrm{e_{i,2}}}{\mathrm{T_r}}+\frac{\mathrm{e_{i,3}}}{T_r^3}+\frac{\mathrm{e_{i,4}}}{T_r^3} \quad \text{(Eq. 17)}$$

$$Cz=\mathrm{e_{i,5}}+\frac{\mathrm{e_{i,6}}}{\mathrm{T_r}}+\frac{\mathrm{e_{i,7}}}{T_r^3} \quad \text{(Eq. 18)}$$

$$Dz=\mathrm{e_{i,9}}+\frac{\mathrm{e_{i,10}}}{\mathrm{T_r}} \quad \text{(Eq. 19)}$$

$e_{i,j}$ = parameters from Daubert (Daubert, 1986)

Figure 2.6 shows the specific enthalpy as a function of pressure and temperature. The specific enthalpy will be used to calculate the electricity production in chapter 5.

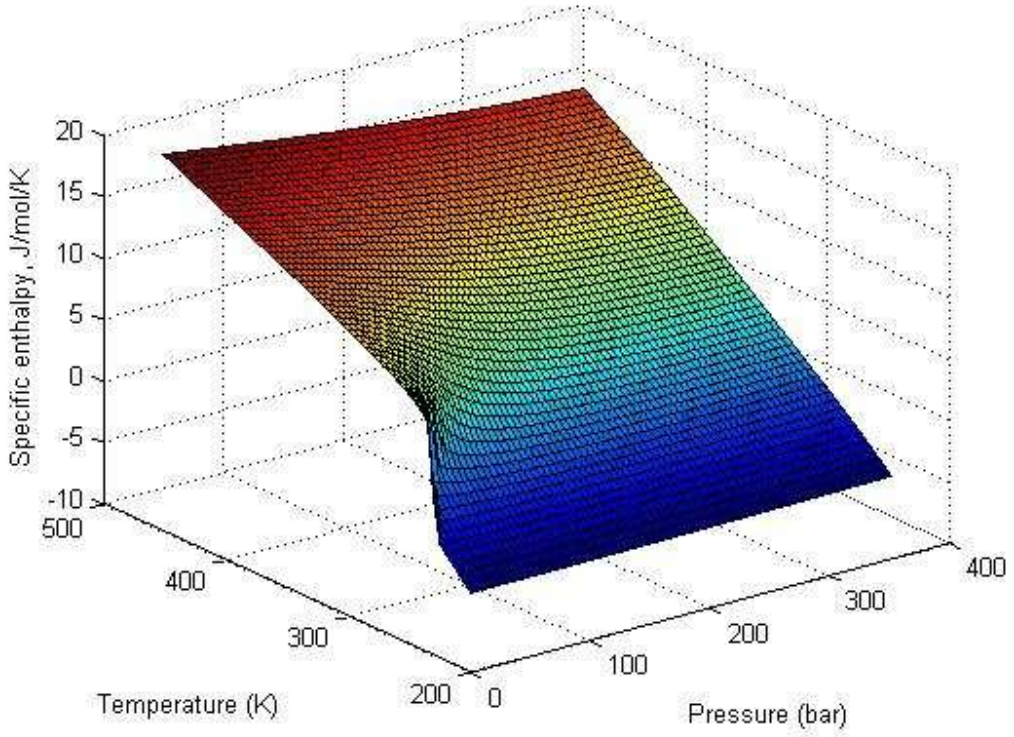

Figure 2-6. Specific enthalpy versus pressure and temperature

Heat capacity

Heat capacity is defined as the change in enthalpy at constant pressure(Cp) or the change in internal energy at constant volume(Cv)(Atkins, 2002). For this study, only the heat capacity at constant pressure(Cp) will be considered. The main reason for this choice is the formulation of the EOS, which uses temperature and pressure as input and has volume as output, which makes is much easier to use the Cp than the Cv.

The heat capacity for an ideal gas is calculated using a formula from (Daubert, 1986), being:

$$Cp_0 = B + 2CT + 3DT^2 + 4ET^4 + 5FT^4 \qquad \text{(Eq. 20)}$$

where:

- A,B,C,D,E,F = The same parameters from (Daubert, 1986) as used for the ideal gas enthalpy
- Cp_0 = Heat capacity at constant pressure for the ideal gas at 1 bar, kJ/kg/K

The heat capacity for a real gas has been calculated as follows:

$$Cp = \left(\frac{dH}{dT}\right)_P \approx \frac{(H_{T=T} - H_{T=T-1})_P}{\Delta T_{(=1)}} \qquad \text{(Eq. 21)}$$

Specific entropy

The following equation has been used to calculate the specific entropy of carbon dioxide(Daubert, 1986):

$$S = S_0 - \frac{R}{M}\left(\frac{\overline{S}^0 - \overline{S}}{R}\right) \qquad \text{(Eq. 22)}$$

where:

- S= Specific entropy, kJ/kg/K
- S_0= Entropy of an ideal gas at 1 bar, kJ/kg/K

$$S_0 = S_{0,298K} + \int_{298}^{T} \frac{C_{P0}\,dT}{T} \qquad \text{(Eq. 23)}$$

- $S_{0,298K}$ = 213.74 kJ/kmol/K, given in Daubert
- R= Gas constant, 8.314 kJ/kmol/K
- Tc= critical temperature, 304.1 K
- M=Molar mass, 44.01 g/mol
- $\left(\frac{\overline{S}^0 - \overline{S}}{R}\right)$ = Dimensionless pressure effect on entropy from (Daubert, 1986)

$$\left(\frac{\overline{S}^0 - \overline{S}}{R}\right) = \left(\frac{\overline{H}^0 - \overline{H}}{RT_c}\right)\frac{Tc}{T} + \ln(\phi) + \ln(P) \qquad \text{(Eq. 24)}$$

- $\ln(\phi)$ = Fugacity coefficient
- P = Pressure, kPa
- $\left(\frac{\overline{H}^0 - \overline{H}}{RT_c}\right)$ = Dimensionless pressure effect on enthalpy, as stated above

The entropy graph can be found in figure 2.7.

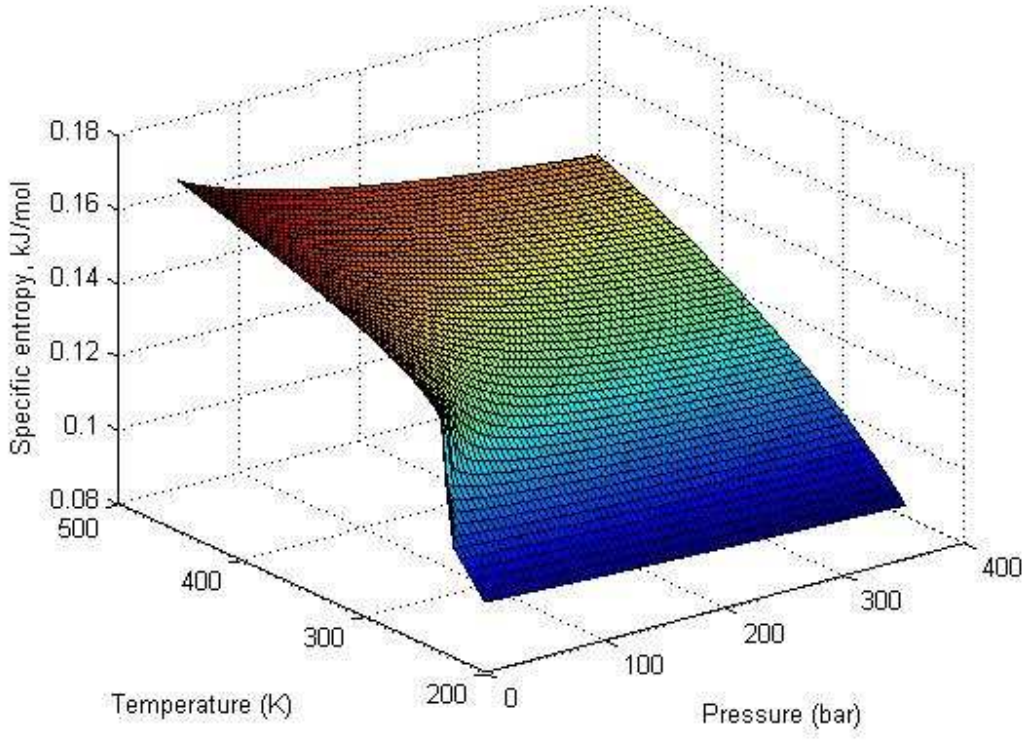

Figure 2-7. Specific entropy versus pressure and temperature

2.5 Contaminants

While the system in chapter 3 is designed as a closed cycle steady state, where there are no other substances except carbon dioxide in the system, there will be some contaminants in the system. Compared to water based geothermal there is only one major difference, which is the reaction between carbon dioxide and water to carbonic acid(Appelo, et al., 2005).

$$CO_2 + H_2O \leftrightarrow H_2CO_3$$

The production of carbonyl acid in the working fluid can cause corrosion in the metal parts of the system such as the wells and the turbine. The amount of corrosion depends mainly on the concentration of carbonyl acid in the working fluid, which is limited since the equilibrium of the reaction is favored for carbon dioxide and water opposed to carbonyl acid(Appelo, et al., 2005).

However, since the current system is designed as a closed cycle, meaning no mass exchange with its surroundings, no further research has been done on possible contaminants in the working fluid.

2.6 Validation

Over the posed range, the results for density, enthalpy and entropy have been compared with the online database from the Duan research group(Zhenhao Duan Research Group, 2006) and the database from the National Institute of Standards and Technology(National Institute of Standards and Technology, 2008).

The deviation in the density calculation shows a maximum below 1% deviation, with the majority of the deviations below 0.5%. Therefore it is concluded that the density calculation is valid for the posed region.

A value has been added to both the enthalpy and entropy, since both are stated as differences with a reference state. To compare the enthalpy and entropy results with the online databases the reference state needs to be the same. Both the enthalpy and the entropy showed a deviation up to 2.5% when compared to (National Institute of Standards and Technology, 2008). However, the enthalpy had a maximum deviation of 1% when compared to (Zhenhao Duan Research Group, 2006). The entropy has not been compared to (Zhenhao Duan Research Group, 2006) since no entropy is given in that database.

The main difference and advantage of the method described in this chapter is its deviation related to the range. Many EOS have a lower overall deviation but describe a range up 20000 K. The method described in this chapter is able to calculate the properties of carbon dioxide around the critical point with a maximum deviation of 2.5%.

3 Geothermal power cycle

This chapter describes the theoretical geothermal power cycle. Before every aspect of the cycle is described in detail with equations a general description of the system and used assumptions are given. This description is only meant to give an impression of the magnitude of the individual components and an impression of the system as a whole.

3.1 General system design

The base system, which will be used as the base for the sensitivity analysis later in this report, consists of a doublet: a single injection and a single recovery well; a reservoir; a turbine and a condenser, as shown in figure 3.1.

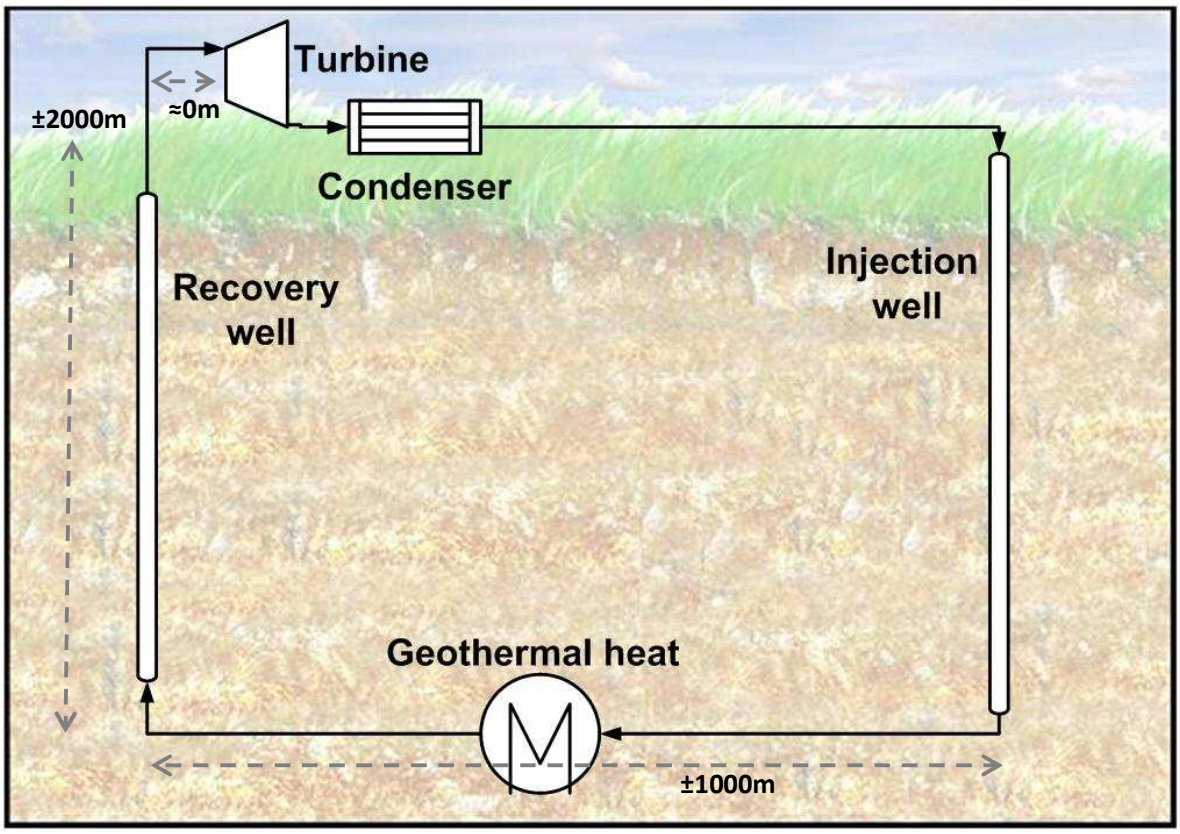

Figure 3-1. Systematic representation of system cycle. The distances are only shown to give an impression and can vary for each different location. The turbine and condenser are placed on the surface while the wells are placed in the subsurface. The geothermal heat is shown as a small heat exchanger while the heat is extracted over the whole range between the wells.

The whole system is designed as a steady state closed cycle. This means that before the system starts operating there already is a reservoir filled with carbon dioxide. Also, no carbon dioxide losses to the surroundings have been taken into account. The following paragraph gives an impression of the

magnitude of the system, of which the values are calculated further in the project. The numbers are rounded and can change for different locations.

System magnitude impression

The liquid carbon dioxide flows through the injection well to the reservoir at 2000 m depth with a flow of 230 kg/s. At this depth, the temperature will increase with 31 degrees per kilometer to around 345 K(Lokhorst, et al., 2007). In the reservoir the carbon dioxide is heated up and changes from liquid state to supercritical state. Due to this phase change the density of carbon dioxide drops with a factor of 1.5, which results in a higher volumetric flow. The supercritical carbon dioxide then flows through the recovery well back to the surface where it enters the turbine with a pressure of around 100 bar. The turbine expands the carbon dioxide while producing electricity of around 0.49 MW_e. After the turbine, the carbon dioxide needs to be cooled down in the condenser to transform it into a liquid. After transforming into a liquid the carbon dioxide re-enters the injection well and the cycle starts over again.

3.1.1 Injection well

The injection well is a tube of around 20 cm diameter and around 2000 m height. The injection well is used to transport the carbon dioxide to the reservoir. The current system design takes an initial value for the pressure and temperature, which are obtained from the outlet of the condenser and uses those initial values to calculate the density at the top of the well. This allows for a top-down calculation for density and pressure increase which will be discussed in section 3.2.

3.1.2 Reservoir

The reservoir is a porous medium located underground through which the carbon dioxide flows and where it gets heated up. This study focuses on depleted gas fields as reservoir. While the reservoir is a component of the system which cannot be modified since it is a geological location, there are calculations required. One of the major results from the reservoir is the calculation of the flow rate. Using the pressures at the injection and recovery wells, the flow rate can be calculated, which is in direct relationship with the output of the system, electricity.

Using several boundary conditions such as the lifetime of the system, the temperature of the reservoir, the temperature of the carbon dioxide and more, it is possible to calculate the amount of energy that can be extracted or the spacing between the injection and recovery well required to extract a certain amount of energy. The spacing between the wells is the only property that physically can be changed by placing the injection well and recovery well at varying distances.

3.1.3 Recovery well

The recovery well is used to extract the carbon dioxide from the reservoir to the turbine. It is assumed that the recovery well has the same calculations as the injection well, with the sole exception that the carbon dioxide is flowing in another direction. The major difference between the injection and recovery well would be the physical state of the carbon dioxide as the physical state of carbon dioxide is altered by the gained heat in the reservoir.

3.1.4 Turbine

In the turbine part, the carbon dioxide is adiabatically expanded. The output of this component is electricity generation.

3.1.5 Condenser

Carbon dioxide is cooled down using water as heat exchange fluid until a phase change from gas to liquid occurs.

3.1.6 Property changes

The properties of carbon dioxide change along its way through the system. Table 3.1 shows which properties change at the different parts of the system. The numbers in the table refer to the numbers in figure 3.2. The table does not show numbers but shows either a plus or a minus for an increase or decrease. A double plus or double minus refers to a big increase or decrease. A zero means that there is no change.

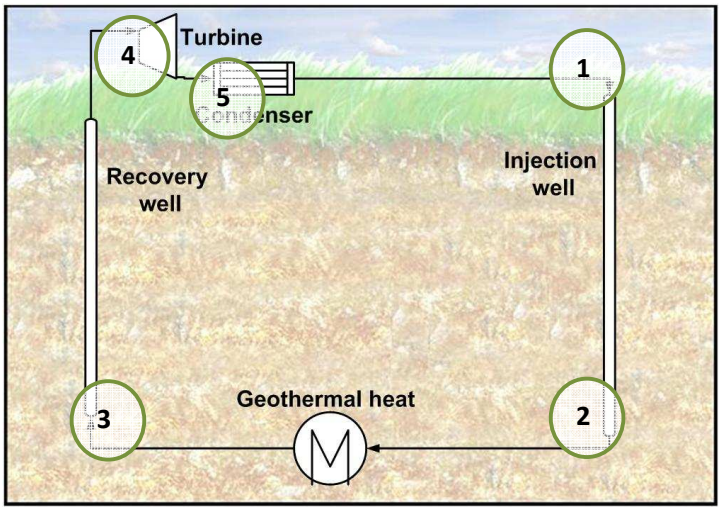

Figure 3-2. Graphical representation for the system, including numbers for the different system locations.

TABLE 3.1. Property changes in a geothermal system

Number	Location	Pressure	Temperature	Enthalpy	Entropy	Phase
1	Injection well	++	+	0	-	Liquid
2	Reservoir	-	++	++	++	Liquid
3	Recovery well	--	-	0	+	Supercritical
4	Turbine	--	--	-	+	Supercritical
5	Condenser	0	--	--	--	Supercritical / gas

3.2 Calculations

All calculations are done using Matlab scripting(The MathWorks, 2010). Matlab .m files allowed for easy and efficient calculation of a large amount of calculation steps. All used Matlab .m files can be found in appendix 2.

All of the abovementioned calculations made in this study assume a steady state for the whole system. This includes the fact that the reservoir is full with carbon dioxide already. The evolution of the properties of carbon dioxide is calculated in stepwise for every single meter, or another step size if desired. All of the initial properties are calculated, using the initial pressure and temperature for the first meter. The results of a single step will be the initial conditions for the next step, continuing until the end of the well. It is known that this method has a slight deviation from the differential equation approach.

To analyze the impact of this choice, two calculations have been performed for the entire well with a step size difference of a factor 100. The resulting deviation was found to be about 0.7 %. For the final calculation, a small step size will be taken.

As will be shown in the following section, the governing equations for carbon dioxide have a strong coupling, sometimes resulting in circular relations. Chapter 5 describes how these equations are linked and how the circular relations are treated by Matlab scripting.

An extended overview of all used equations and parameters can be found in appendix 1.

3.2.1 Carbon dioxide properties

The Matlab .m file *CO2properties.m* is created to model and calculate the properties of carbon dioxide as stated in chapter 2. This file requires only pressure and temperature as input and gives several of the properties of carbon dioxide as output. CO2properties.m uses iterations to calculate the reduced volume and density using the EOS from Duan and Sterner

3.2.2 Injection well:

As mentioned above the calculation of the wells is done stepwise.

Pressure increase

The temperature and pressure at the top of the well are known and used to calculate the properties of carbon dioxide using the Matlab script named rhocalc6.m. The hydrostatic component of the pressure increase is defined as follows (Paterson, et al., 2008):

$$\frac{dP}{dh} = -\rho_{P,T} g - \frac{f \rho v^2}{2D} \qquad \text{(Eq. 25)}$$

where:
P = Pressure, bar
h = height, m
ρ = density, kg/m^3
g = gravitational constant, 9.81 m/s^2
f = friction factor, -
v = velocity, m/s
D = diameter, m

The friction factor f is defined as follows (TNO Bouw en Ondergrond, 2009):

$$\mathrm{f} = \left[1.14 - 2\log\left(\frac{\varepsilon}{\mathrm{D}} + \frac{21.25}{\mathrm{Re}^{0.9}}\right)\right]^{-2} \qquad \text{(Eq. 26)}$$

where:

ε = roughness factor, ε/D = 0.00015
Re= Reynolds number =

$$Re = \frac{Dv\rho}{\mu} \quad \text{(Eq. 27)}$$

where
μ = viscosity, Pa s

For the stepwise calculation, the equation for pressure difference is approximated as

$$\Delta P = -\rho_{P,T} g \Delta h - \Delta h \frac{f \rho v^2}{2D} \quad \text{(Eq. 28)}$$

with Δh being the stepsize. For the final results in chapter 5, a step size of -1m has been taken.

As can be seen in the equations, the pressure increase is dependent on the velocity, which has not yet been elaborated. This issue will further be discussed in chapter 4.2.

Temperature increase

Temperature change in the well has 2 sources being temperature change due to heat exchange with the surroundings and temperature change due to expansion or compression of the carbon dioxide.

To analyze the temperature change due to heat exchange with the surroundings, the following equation has been evaluated (Paterson, et al., 2008):

$$q_{w,well} = \frac{4\pi k_{i,g}(\Delta T_{av})}{ln\left(\frac{4\alpha_{t,g}t}{\sigma r_c^2}\right)} \quad \text{(Eq. 29)}$$

where
$q_{w,well}$ = Heat loss per unit of length, W/m
$k_{i,g}$ = Thermal conductivity of the rock, 3 W/m/K
ΔT_{av}= Average temperature difference between fluid and rock over the entire well, K
α = Thermal diffusivity coefficient of the rock, 1.2 * 10^-6 m^2/s
σ = e^{γ} = 1.781072
t = Time since start of the flow, s
r_c = Radius of the well including casing, m

and (Paterson, et al., 2008)

$$\frac{dT}{dh} = \frac{q_{w,well}}{Q_m C_p} \quad \text{(Eq. 30)}$$

Q_m = Mass flow, kg/s

C_p= Heat capacity carbon dioxide, kJ/kg/K

When using an average temperature difference of 37 °C, a time of 1 year and a radius of 0.2m including casing, the temperature difference over the entire well is less than 1 °C. Therefore, it has been chosen to neglect the temperature difference in the wells due to heat exchange with the surroundings.

The temperature difference due to expansion and compression plays a larger role than due to heat exchange with the surroundings. When carbon dioxide flows to the reservoir it will be compressed, lowering intermolecular velocity. The increased pressure also increases the density of the carbon dioxide which lowers its specific volume and volumetric flow. The lower the carbon dioxide gets in the reservoir, the lower its gravitational energy will be. There are in total thus 3 processes resulting in a lowering of energy which have to be compensated by something internal, as there are no heat exchanges with the surroundings. The only possibility is changes in temperature.

An article by Pruess has been used to calculate this change in temperature, where he states *"A more realistic outlook on longer-term P, T-conditions in flowing injection and production well can be obtained by approximating fluid flow in the wellbore as isenthalpic"*(Pruess, 2006). Therefore, the wells in the system are calculated as being isenthalpic, using enthalpy and pressure to calculate the temperature change.

3.2.3 Reservoir:

Due to the earth's core temperature the reservoir has a higher temperature than the surface temperature. Depending on the geological location the geothermal gradient varies from 30 degrees per kilometer to 80 degrees per kilometer. Figure 3.3 shows the heat flow from the earth's core which is in proportion to the geothermal gradient. However, the majority of all locations have a low geothermal gradient and the higher gradients are often only found in either volcanic area's or on a border of a tectonic plate, as can be seen in figure 3.3 which shows the global heat flow distribution. The average temperature of the Netherlands equals 10.5 ^{o}C on the surface and increases by 31 degrees per kilometer below the surface(Lokhorst, et al., 2007).

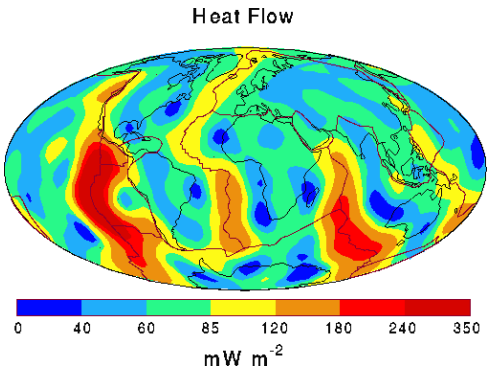

Figure 3-3. Heat flow distribution over the earth

Heat transfer rate

In the reservoir carbon dioxide gets heated up. However, the question arises how fast the carbon dioxide is heated up. The reservoir consists of porous media resulting in a large contact area for only a small volume of liquid. Therefore, the current chosen heat flow rate is infinite, where the carbon dioxide is assumed to heat up from low to high temperature in a very short time and space.

$$\frac{dQ}{dt} = \infty \qquad \text{(Eq. 31)}$$

where:
Q = Heat transfer, J
t = Time, s

Energy recovery

The amount of energy that can be recovered from the reservoir equals the amount of energy currently present in the reservoir combined with the heat flow from the earth's core. However, the heat flow

from the earth's core is very small. The energy from the earth's core equals around 38 TW, which has to be spread out over the entire surface of the earth, resulting in a 0.063 W/m^2(Hofmeister, 2004). When using a reservoir of 1 square kilometer, the entire added heat flow equals 63 kW, which is very small compared to the non flow heat already present in the well and is therefore ignored.

The following equation is used to calculate the total energy being extracted per year (U.S. Department of Energy, 2001):

$$\mathrm{E} = Q_v t_f \Delta T C_{p,f} \quad \text{(Eq. 32)}$$

where:
E = Energy extracted per year, J
Q_v = Volumetric flow rate, m^3/hr
t_f = Equivalent running hours, hr/yr
ΔT = Temperature difference between injected carbon dioxide and initial reservoir temperature
$C_{p,f}$ = Volume related heat capacity working fluid, J/m^3/K

Flow

Conventional geothermal power plants use a pump as driving force for the flow. In the current design, the flow of carbon dioxide through the reservoir does not use a pump as driving force, but uses the pressure difference at the recovery and injection well to drive the flow. This is possible due to the large difference in density between the wellheads, which can go up to a factor 2. To calculate the flow, the following equation is used by TNO (TNO Bouw en Ondergrond, 2009):

$$\Delta P = Q_v \frac{\mu}{2\pi k h_r R n}\left(ln\left(\frac{L}{r}\right)\right) \quad \text{(Eq. 33)}$$

The equation is rearranged to be able to solve it for flow:

$$Q_v = \frac{\Delta P}{\frac{\mu}{2\pi k h_r R n}\left(ln\left(\frac{L}{r}\right)\right)} \quad \text{(Eq. 34)}$$

where:
k = Permeability, m^2
h_r = Height of the reservoir, m
R_n = Net/gross fraction, factor between theoretical reservoir height and actual available reservoir height, -
L = Length of the reservoir, well spacing, m
r = Well diameter, m

Well spacing

As mentioned above, the flow in the system is determined by the size of the wells. A larger well diameter allows the fluid to enter the reservoir in a larger area. When more carbon dioxide travels through the reservoir, more area is required to allow for the same lifetime of the system. Therefore, the size of the reservoir is also dependent on the flow, resulting in a circular relation.

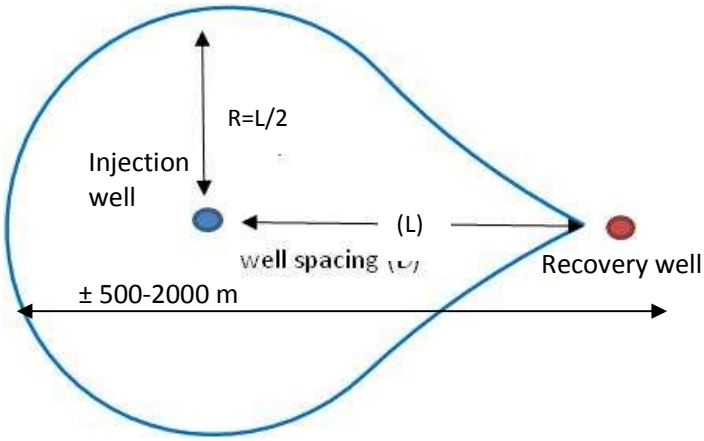

Figure 3-4. Graphical representation of thermal front which develops between an injection and recovery well. (U.S. Department of Energy, 2001)

When carbon dioxide flow through well, the temperature distribution in the reservoir will look like figure 3.4, where the blue line represents the thermal front. Using the equation for well spacing below, which includes flow as a variable, it is possible to calculate how much space is required for a certain lifetime of the project. The well spacing described in the figure represents the distance between the injection and recovery well (U.S. Department of Energy, 2001).

$$L = \sqrt{\frac{3T_l Q_v t_f}{\pi h_r f_{ret} \phi}} \qquad \text{(Eq. 35)}$$

where:
L = Well spacing, m
R = Thermal radius, L/2, m
T_l = Lifetime of the system, yr
t_f = Running fraction, hours/yr
h_r = Height of the reservoir, m
ϕ = Porosity, -
f_{ret} = Retardation factor, factor between mass flow and heat flow through the reservoir (U.S. Department of Energy, 2001), -

$$f_{ret} = 1 + \frac{(1-\phi)C_p}{\phi C_{p,r}} \qquad \text{(Eq. 36)}$$

Where
$C_{p,r}$ = Heat capacity rock, J/m^3/K

3.2.4 Recovery well:

The equations used for the recovery well are exactly the same as the equations for the injection well with the only difference that the recovery well is calculated from the reservoir to the surface.

3.2.5 Turbine:

The turbine is where the actual electricity is being produced. As part of the transcritical power cycle, in the turbine the carbon dioxide expands from supercritical state to gas. Without entropy losses, the output of the turbine can be calculated using enthalpy differences and mass flow(Nieuwlaar, et al., 2007-2009):

$$\dot{W}_p = \mathrm{Q_m}(\Delta \mathrm{h}) \qquad \text{(Eq. 37)}$$

where:
Q_m = Mass flow rate, kg/s
W_p = Electrical output, kW_e
Δh = Enthalpy difference, kJ/kg

The equation for specific enthalpy is elaborated in chapter 2. The procedure to calculate the enthalpy difference in the turbine is elaborated in chapter 4.2.4.

Efficiency

While the equation for electrical output above is valid for isentropic expansion, this will never be possible in reality. No matter how efficient the turbine is, there will always be some losses, especially when using low temperatures. In the temperature range of 289 to 353 K, a maximum isentropic efficiency of 80% is achievable(Cayer, et al., 2008)(Feher, 1968)(Yamaguchi, et al., 2006). The equation of the specific entropy is given in chapter 3.

3.2.6 Surface transportation losses

As stated in chapter 3.2.4 there is a certain amount of distance required between the wells to guarantee the production of energy over the entire lifetime of the project. However, the required distance for the wells applies to both subsurface and surface.

There are 2 possible losses when the carbon dioxide is transported from the recovery well to the injection well, being pressure losses and temperature losses. However, the surface piping is not limited to a certain diameter as the wells allowing for larger diameters and lower pressure losses. Therefore, the pressure losses in surface piping are ignored(TNO Bouw en Ondergrond, 2009).

There are no temperature losses when the carbon dioxide is transported from the condenser to the injection well. Since the carbon dioxide is already cooled down to surface water temperature there will be only a small temperature difference between the surrounding air and the flowing carbon dioxide. However, when the carbon dioxide is transported from the recovery well to the turbine, the temperature difference with the surrounding is much larger. For a recovery well temperature of 353 K the heat loss equals around 6.5 W/m (The Engineering Toolbox, 2005). When the recovery well temperature increases to 405 K the heat loss increases to around 49 W/m (The Engineering Toolbox, 2005).

The temperature losses can be negated by placing the turbine near the recovery well. However, as will be elaborated in chapter 6.3, this is not always possible.

3.2.7 Condenser:

The carbon dioxide is gaseous after it exits the turbine. To maximize the pressure difference in the reservoir the pressure increase in the injection well has to be high. Injection the carbon dioxide as liquid results in a larger pressure increase in the injection well. Therefore, an additional step has to be taken to convert gaseous carbon dioxide into liquid carbon dioxide. To do this, a large jump in specific enthalpy has to take place, which requires large amounts of cooling.

In the current scenario, surface water has been chosen as cooling medium due to its large availability and because it requires no additional energy. However, this sets a limit to the minimum temperature, as you cannot go below the surface water temperature. To make sure liquid carbon dioxide is obtained at the start of the injection well, sufficient cooling has to be done. To this end, an end temperature of the turbine has been chosen to be at least 10 degrees above the average surface water temperature in the Netherlands, which equals 288 K(Lokhorst, et al., 2007), resulting in a turbine end temperature of minimal 298 K. To achieve sufficient cooling and guarantee the forming of a liquid in the condenser with realistic size, a temperature drop of 2 degrees has been chosen, resulting in the 296 K.

The temperature of 298 K is chosen as absolute minimum at the end of the turbine. It is possible that the end temperature of the turbine is higher when the pressure in the turbine is high enough to form a liquid before the temperature of 298 K is reached.

No further calculations have been done on the condenser, as it is assumed that enough surface water is available to achieve sufficient cooling in the available amount of time and space.

3.2.8 Pump absence

A pump is nearly always present in water based geothermal systems to drive the flow. In this project however no pump is required. The main difference between a water based system and a carbon dioxide based system is found in the properties of carbon dioxide. At the injection well water has a density of around 1010 kg/m^3 and carbon dioxide has a density of around 980 kg/m^3(National Institute of Standards and Technology, 2008). Both substances will be heated up to the temperature of the reservoir. If the base system is used with a reservoir temperature of 353 K the end density of water equals 986 kg/m^3, while the density of carbon dioxide equals 725 kg/m^3. Because of this large difference in density for carbon dioxide it is also possible to gain a large pressure difference in the well due to the fact that the hydrostatic pressure component in the recovery well is lower than the hydrostatic pressure component in the injection well. If balanced, which will be elaborated in the following chapter, this pressure difference is enough to drive to flow of the system and replace a pump.

3.2.9 Validation

The system as described in this chapter has been compared with the geothermal system described by TNO(TNO Bouw en Ondergrond, 2009); the study to compare water and carbon dioxide as geothermal working fluid by Pruess(Pruess, 2006); the numerical modeling of carbon dioxide wells by Paterson(Paterson, et al., 2008); and the supercritical power cycle by Feher(Feher, 1968). While none of these studies on itself describe a system similar to this study, the combination of these studies covers a large part of the system.

It is not possible to define an exact deviation where the articles posed above specify their results in graphs. However, the system shows similar effects in the case of pressure and temperature change in the wells and reservoir. Also the adiabatic expansion in the turbine shows a similar effect as posed by Feher(Feher, 1968). Therefore it is concluded that the calculations as described in this chapter does not have large deviations from calculations described in the literature posed above and can therefore be used to calculate the properties and results of a geothermal carbon dioxide system.

4 Modeling

As shown in the previous chapter there is a strong coupling in the governing equations for carbon dioxide in the system. For example the pressures at the wellheads are dependent on the flow while the flow is dependent on the pressures at the wellheads. This chapter will discuss the modeling to solve these interlinked relations. The Matlab codes can be found in Appendix 2.

4.1 Carbon dioxide properties

The properties of carbon dioxide can vary with pressure and temperature which are independent of the location in the geothermal system. However, as pressure and temperature are used as input in the equation, it is not possible to write the EOS given in chapter 2 in an explicit form for density as a function of pressure and temperature due to the large number of parameters. Therefore, an iterative method is used to solve the equation.

4.1.1 Density

The density of carbon dioxide is calculated using two different EOS. As explained in chapter 2 a boundary is drawn between the two EOS. After the correct EOS has been set, an initial value for the density has to be given. This density will be used to calculate the pressure at a given temperature, which is compared to the actual pressure.

If the calculated pressure is too low or too high, the density is changed by a factor and a new pressure P1 is calculated. This is repeated until the actual pressure and the calculated pressure have an acceptable difference. This specifically mentions acceptable since an iteration process almost never reaches its limit, although the result might come very close. To solve this, the actual pressures and the calculated pressure are rounded and multiplied by a factor before they are compared. Adjusting the factor allows for increasing the accuracy but also increasing the calculation time.

4.1.2 Enthalpy

The calculation for the specific enthalpy is also done iteratively. All the parameters for the equations are known, but the reduced volume is still unknown.

An initial value for the reduced volume is entered to start the iteration process. Thereafter the known reduced pressure and the calculated reduced pressure are compared and the reduced volume is adapted accordingly. The difference with the calculation of the density is the factor, which is higher because the reduced pressure has a much smaller absolute quantity than density.

4.1.3 Fugacity coefficient and specific entropy

While the fugacity coefficient and the specific entropy have large equations alike the equation for specific enthalpy, they are much easier to calculate in this stage since the reduced volume has already been calculated. Therefore, the fugacity coefficient and specific enthalpy can be calculated without iterations.

4.1.4 Other properties

The other properties of carbon dioxide are calculated in a normal way as the equations show no unknown variables or large number of parameters.

4.2 Power cycle

The power cycle consists of 5 parts as mentioned before: Injection well, reservoir, recovery well, turbine and condenser. Also, several of the equations stated in previous chapter have circular relations. This chapter describes the Matlab codes written to solve these circular relations. The codes can be found in appendix 2. For every step, where applicable, both a pressure-enthalpy and a temperature-entropy graph are shown.

4.2.1 Step 1: The flow

The flow plays a role in only 3 out of 5 parts in the system being the wells and the reservoir. However, flow plays the largest role in the wells and the calculation of the pressure difference in the wells.

Step 1a: Pressure distribution

The pressure change is distributed among 4 parts in the system, being the wells, the reservoir and the turbine. Out of those 4 parts, only the injection well has a pressure increase. The balance looks like:

$$\Delta P_{Injection} = \Delta P_{Reservoir} + \Delta P_{Recovery} + \Delta P_{Turbine} \quad \text{(Eq. 38)}$$

The pressure difference in the turbine is independent of the flow. The remaining three unknown pressure differences are dependent on the flow, but not in the same quantity. However, the pressure differences in the wells are related by the same equation.

Step 1b: Adding a flowfactor variable

To manipulate the pressure differences in the wells, an additional variable has been introduced named flowfactor:

$$f_{flow} = 100\frac{\Delta P_{recovery}}{\Delta P_{injection}} = 100\frac{\Delta P_{recovery,hydrostatic}+\Delta P_{recovery,flow}}{\Delta P_{injection,hydrostatic}+\Delta P_{injection,flow}} \quad \text{(Eq. 39)}$$

This flowfactor is introduced to calculate the maximum allowed flow in the system. The flow has no effect on the hydrostatic component of the pressure difference. The effect of flow on the pressure is visualized in figure 4.1. Figure 4.1 uses an initial pressure of 70 bar for the injection well and an end pressure of 120 bar for the recovery well.

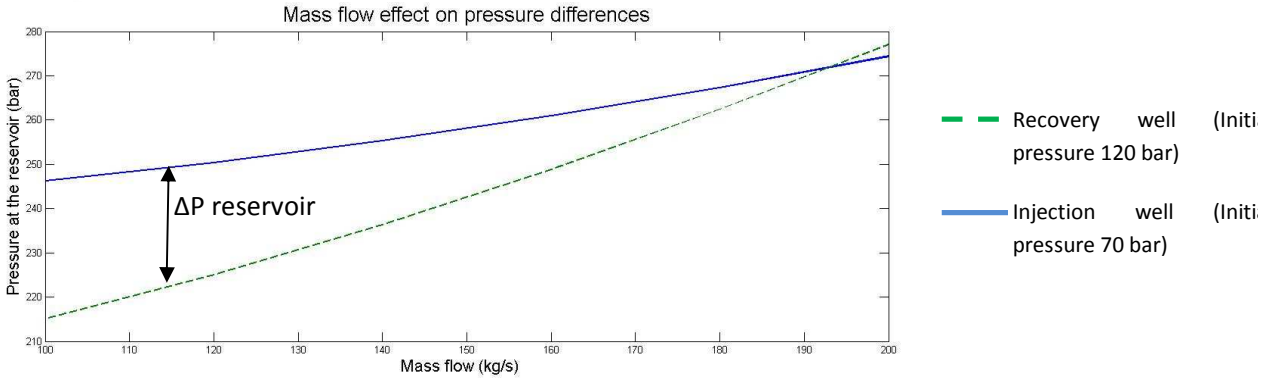

Figure 4-1. Mass flow effect on pressure. The dotted green line represents recovery well end pressure at a starting pressure of 120 bar. Continuous blue line represents injection well end pressure at a starting pressure of 70 bar. The difference between the lines equals the pressure difference in the reservoir.

Figure 4.1 shows the effect of mass flow on the pressure of both wells. The higher the flow becomes, the smaller the difference between both wells becomes. However, when the flow becomes larger, the pressure difference in the reservoir drops causing the flow to drop. The flowfactor is used to balance this circular relationship.

An initial flowfactor of 60 has been chosen. This means that for the first cycle the pressure difference in the recovery well is 60% of the pressure difference in the injection well. The flowfactor will be further elaborated in chapter 4.2.6 Balancing the system.

4.2.2 Step 2: The reservoir

When the pressure in the wells and the flow are calculated, enough data is available to calculate the properties of the reservoir. The flow can be used to calculate the pressure difference and the well spacing using equations from chapter 3 and the temperature can be calculated from the average surface temperature and the geothermal gradient. Figure 4.2 shows the taken step in a pressure-enthalpy, a temperature-entropy diagram and a graphical representation of the system.

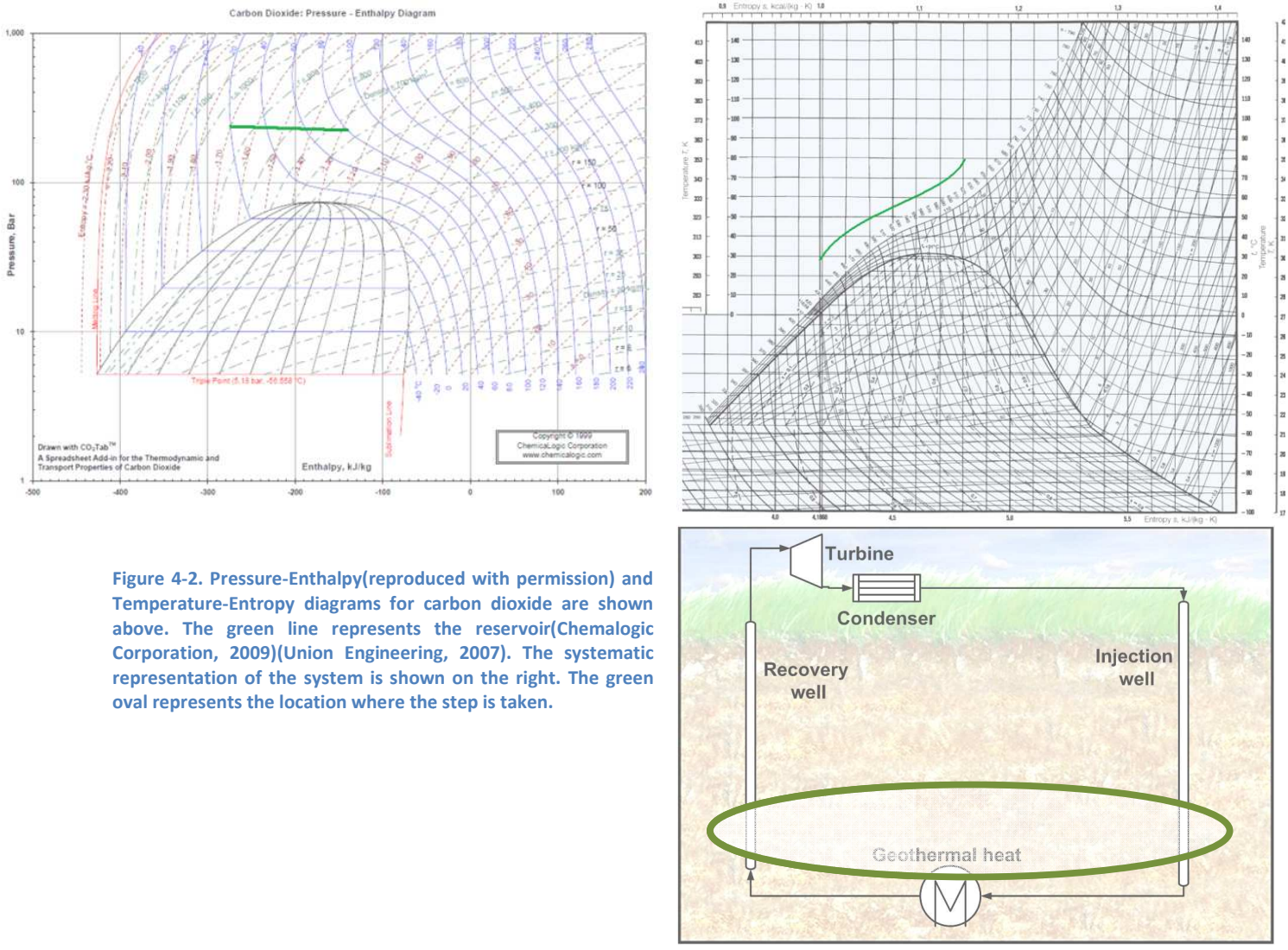

Figure 4-2. Pressure-Enthalpy(reproduced with permission) and Temperature-Entropy diagrams for carbon dioxide are shown above. The green line represents the reservoir(Chemalogic Corporation, 2009)(Union Engineering, 2007). The systematic representation of the system is shown on the right. The green oval represents the location where the step is taken.

4.2.3 Step 3: Temperature and pressure change in the wells

As stated in chapter 3, the wells are isenthalpic. A stepwise calculation is chosen to calculate the temperature and pressure difference in the wells as a result of increased depth. In the first step the pressure is reduced by 1 bar and the temperature is kept constant, where after the properties of carbon dioxide are recalculated. Thereafter the temperature is increased or decreased, depending on the well, with a small amount until the initial enthalpy is obtained. This process is repeated until the end of the reservoir. Figure 4.3 shows the taken step in a pressure-enthalpy, a temperature-entropy diagram and a graphical representation of the system.

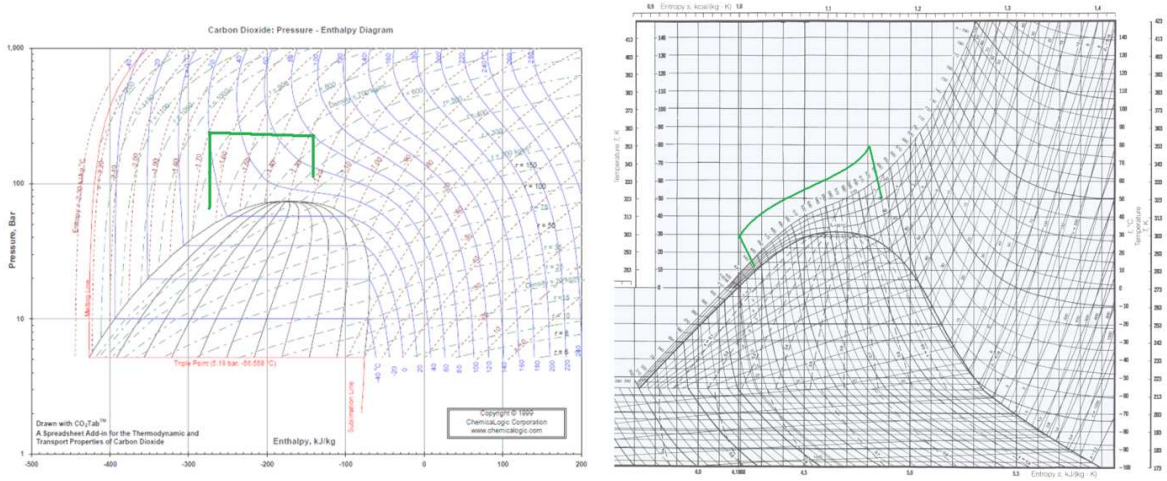

Figure 4-3. Pressure-Enthalpy(reproduced with permission) and Temperature-Entropy diagrams for carbon dioxide are shown above. The green line represents the injection well, the recovery well and the reservoir(Chemalogic Corporation, 2009)(Union Engineering, 2007). The systematic representation of the system is shown on the right. The green oval represents the location where the step is taken.

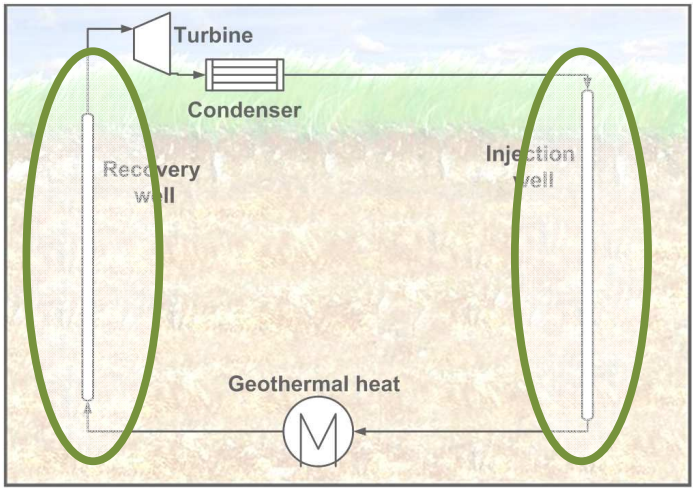

4.2.4 Step 4: The turbine

At this point the pressure and temperature at the end of the recovery well are known. However, no equations were available to calculate the turbine's end pressure. To calculate the end pressure of the turbine, a stepwise calculation is used. First of all, the pressure is reduced where after the temperature is decreased until the pressure and temperature decrease equal isentropic expansion. After either the minimum temperature of 304.1 K or the saturation line is reached, the temperature is increased until the enthalpy difference equals the initial enthalpy difference multiplied by the isentropic efficiency. These steps are repeated several times as shown in figure 4.4. Figure 4.5 shows the taken step in a pressure-enthalpy, a temperature-entropy diagram and a graphical representation of the system.

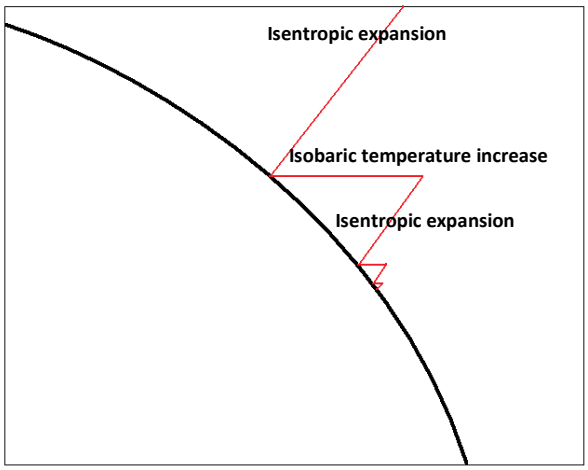

ıwise calculation of the turbine pressure e shown in an enlarged P-H diagram. The sents the saturation line and the red line alculation line of the specific enthalpy.

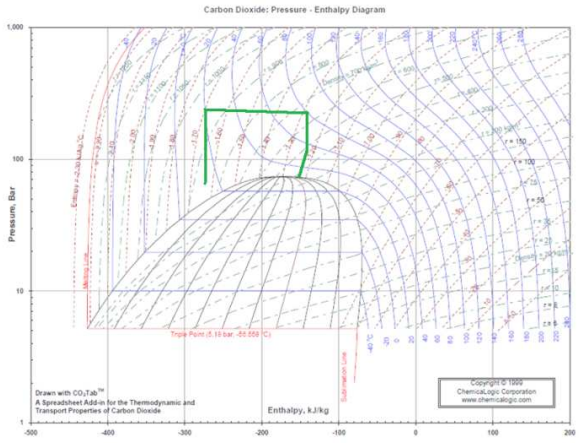

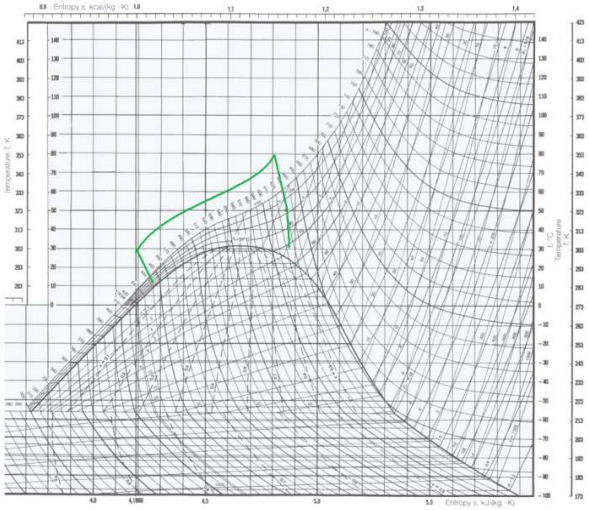

Figure 4-5. Pressure-Enthalpy(reproduced with permission) and Temperature-Entropy diagrams for carbon dioxide are shown above. The green line represents the injection well, the recovery well, the reservoir and the turbine(Chemalogic Corporation, 2009)(Union Engineering, 2007). The systematic representation of the system is shown on the right. The green oval represents the location where the step is taken.

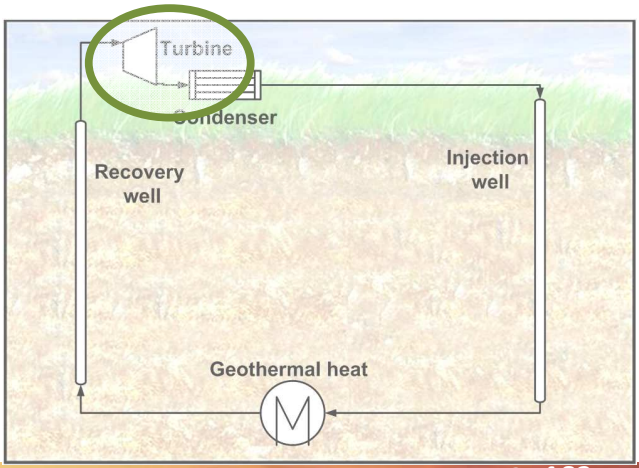

4.2.5 Step 5: The condenser

The last step of the cycle is the temperature reduction in the condenser. The condenser is independent on both flow and pressure. There is however a pressure based boundary condition. As stated in chapter 3, the minimum temperature in the condenser is 296 K. To guarantee that a liquid is formed in the condenser, the pressure has to be above a certain value. Figure 4.6 shows the specific enthalpy for carbon dioxide in the range of 1 to 100 bar.

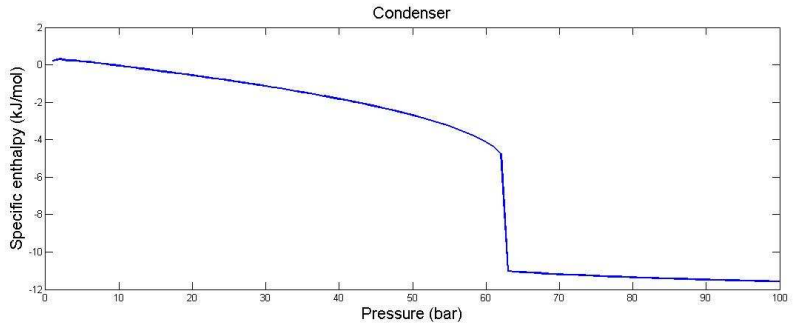

Figure 4-6. Specific enthalpy of carbon dioxide as a function of pressure (T=296 K)

Figure 4.6 shows a gradual decline in specific enthalpy while the pressure rises. When the pressure reaches 62 bar the specific enthalpy suddenly drops to -11 kJ/mol where after the gradual decrease continues. The sudden drop at 62 bar represents the phase change from gas to liquid at 296 K. This means that at the minimum temperature of 296 K the minimum required pressure to obtain a liquid equals 63 bar.

Figure 4.7 shows the taken step in a pressure-enthalpy, a temperature-entropy diagram and a graphical representation of the system. The cycle in this figure is not complete, as the system still needs to be balanced which will be done in step 6.

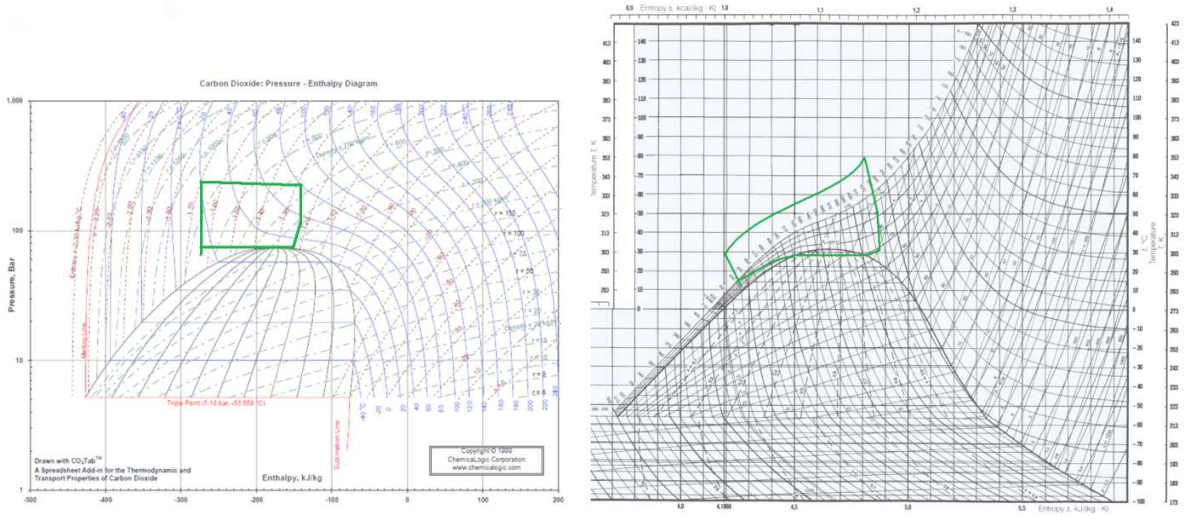

Figure 4-7. Pressure-Enthalpy(reproduced with permission) and Temperature-Entropy diagrams for carbon dioxide are shown above. The green line represents the whole cycle of the system before the system has been balanced(Chemalogic Corporation, 2009)(Union Engineering, 2007). The systematic representation of the system is shown on the right. The green oval represents the location where the step is taken.

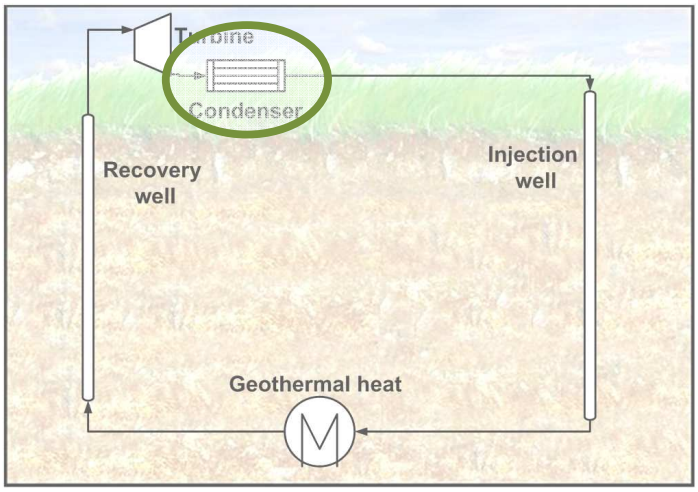

4.2.6 Step 6: Balancing the system

At this point the properties of carbon dioxide can be calculated for each part of the system. It is also possible to calculate the output and efficiency of the system. However, the end pressure of the condenser may not be the same as the inlet pressure of the injection well.

When the pressure at the end of the condenser is too high the flow is low and vice versa. As can be seen in figure 4.1, a higher flow means a larger recovery well pressure and thus a lower condenser pressure. The flowfactor can be used to balance the system. At the end of the first cycle the flowfactor is changed accordingly to the pressure difference. The new flowfactor will then be used for the second cycle. This process is repeated several times until the system is balanced. Figures 4.8 and 4.9 show the taken step in a pressure-enthalpy and a temperature-entropy diagram.

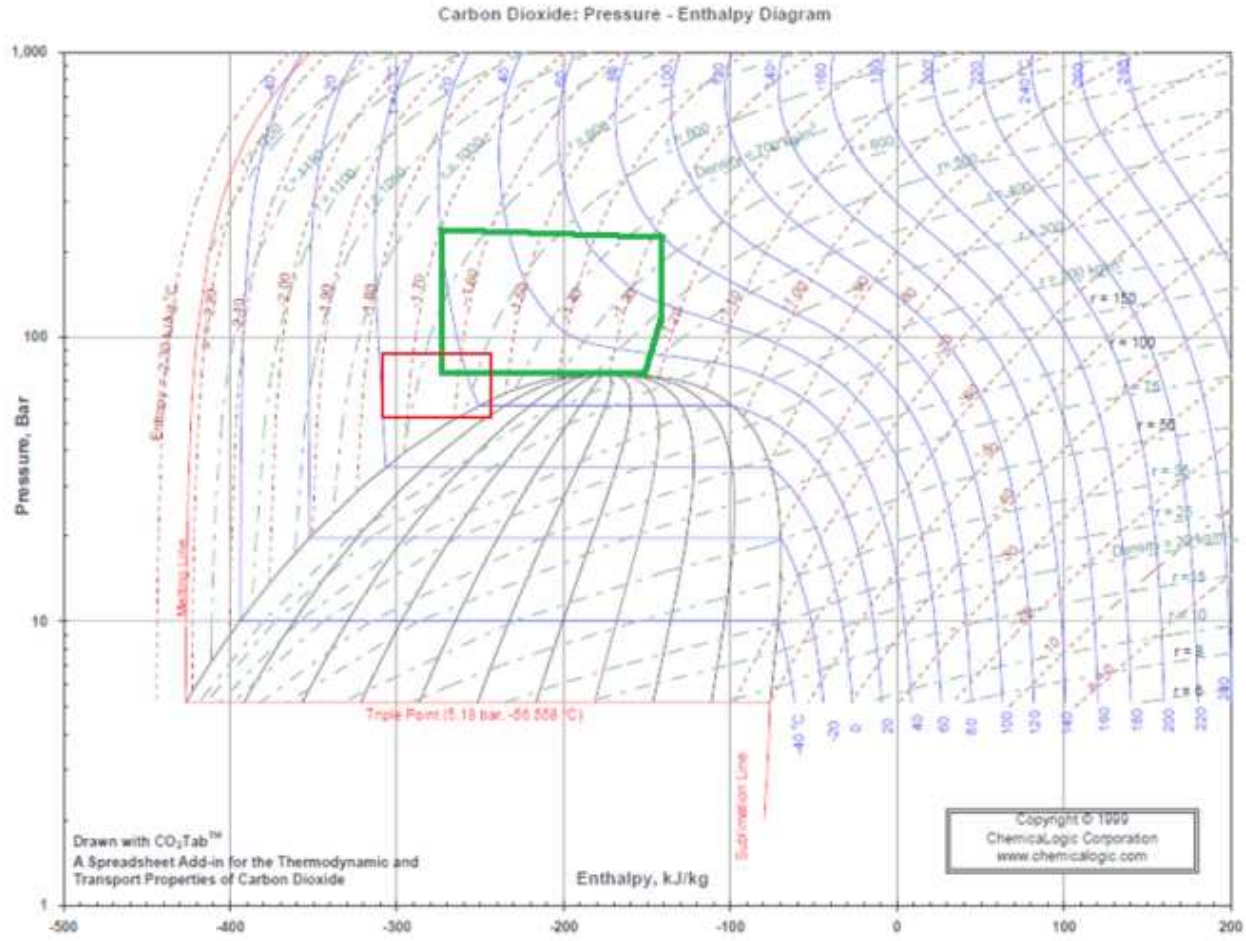

Figure 4-8. Pressure-Enthalpy(reproduced with permission) diagram for carbon dioxide. The green line represents the whole cycle of the system after the system has been balanced. The red square shows the area where the system is balanced using the flowfactor. (Chemalogic Corporation, 2009) (Reproduced with permission)

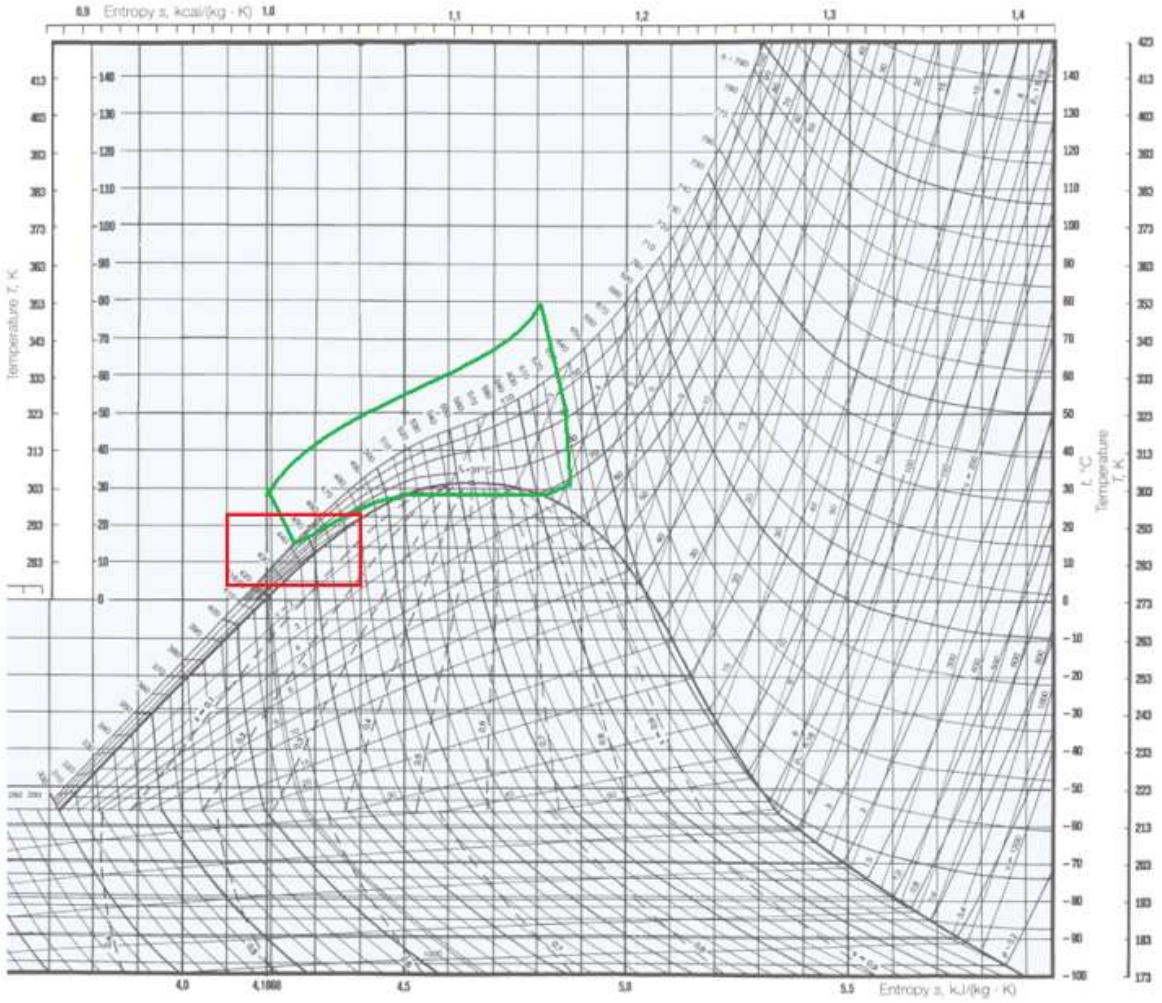

Figure 4-9. Temperature-Entropy diagrams for carbon dioxide. The green line represents the whole cycle of the system after the system has been balanced. The red square shows the area where the system is balanced using the flowfactor. (Union Engineering, 2007)

5 Results

This chapter contains the results from the calculations and modeling from the previous chapters. The main output of the system is shown in the amount of electricity produced, which is the goal of the system. However, the system's output can be described using all of the following aspects:

- Electrical output
- Thermal input
- Efficiency
- Well spacing
- Flow (mass and volume)

Several variables have to be defined before an output can be calculated. These variables are mainly location specific variables as properties of the reservoir. A complete list of variables that influence the output of the system are:

- Reservoir
  - Depth
  - Reservoir height
  - Geothermal gradient
  - Rock permeability
- Turbine
  - Lifetime
- Wells
  - Diameter

The impact of these variables on the system will be described below in the sensitivity analysis. However, before a sensitivity analysis can be performed, a base system needs to be defined. The values for this system have been discussed within IF technology and have been posed as being a reasonable average.

5.1 Base System in the Netherlands

The base system is designed using average temperature values for the Netherlands. The variables of the base system can be found in table 5.1.

Table 5.1. Variables used for base system in the Netherlands(Lokhorst, et al., 2007)

Variable	Value	Unit
Reservoir depth	2000	m
Reservoir height	100	m
Geothermal gradient	31	K/km
Permeability	10^{-13}	m^2
Turbine efficiency	80	%
Running hours per year	7750	hr/yr
Lifetime	50	yr
Well diameter	0.2	m

Output

The base system design as stated above results in a system which extracts 14.5 MW of heat from the soil and turns it into 0.48 MW electrical output resulting in a 3.3% overall efficiency. To maintain this output for at least 50 years with a runtime of 7750 hours per year, the wells need to be at least 1400 m apart from each other.

The properties at the different parts of the system for the base case of the Netherlands can be seen in Table 5.2. The numbers in table 5.2 can be seen in figure 5.1.

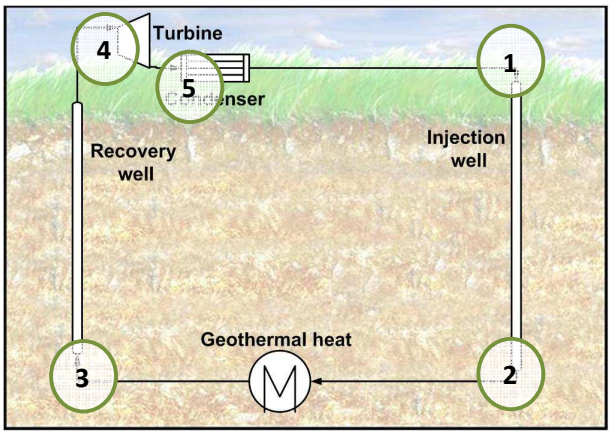

Figure 5-1. Systematic representation of the system. The numbers represent the locations from table 5.2.

Table 5.2. Properties of carbon dioxide at the start of the different steps in the system for the base case of the Netherlands.

Number	Location	Pressure	Temperature	Density	Enthalpy	Entropy
		Bar	*K*	*kg/m^3*	*kJ/mol*	*kJ/mol/K*
1	**Injection well**	74.05	296.0	788.0	-1.855	0.106
2	**Reservoir**	264.2	305.0	929.3	-1.855	0.103
3	**Recovery well**	244.2	347.5	715.0	2.276	0.116
4	**Turbine**	93.05	317.3	474.3	2.276	0.110
5	**Condenser**	74.05	303.9	303.9	2.137	0.119

5.2 Sensitivity analysis

The base system is designed using average values for the Netherlands. However, these values can be different for specific locations. Several sensitivity diagrams are made to visualize the effects of the variables on the output of the system. The sensitivity analysis will be performed for electrical output, overall efficiency, well spacing and mass flow. The last output, thermal input, can be calculated from the electrical output and overall efficiency.

5.2.1 Reservoir depth

The depth of the reservoir has been varied between 1000 m and 3000 m. 1000 m is chosen because it is slightly higher than the minimum depth required in the Netherlands of 718 m. The depth of 3000 m is chosen as upper limit to have the same increase as decrease in the sensitivity analysis and 3000 m still complies with aim of the research to analyze the possibility of low depth geothermal electricity production. The sensitivity diagram can be seen in figure 5.2.

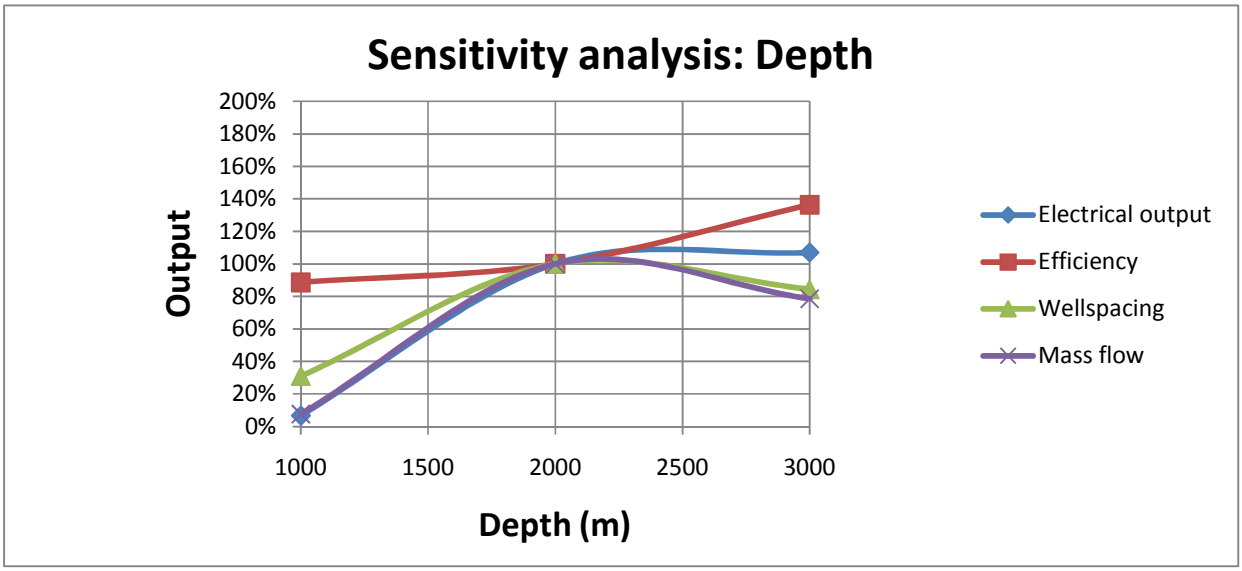

Figure 5-2. Sensitivity diagram for change in depth. A reservoir depth of 2000 m equals the base case for the Netherlands.

While the efficiency reduces only 10% at low depths, the overall electrical output is reduced by 90%. The larger temperature increase at larger depths results in a lower density at the recovery well which gives a higher volumetric flowrate. This larger volumetric flowrate results in a larger pressure difference in the recovery well which reduces the pressure difference over the reservoir reducing the overall mass flow. The temperature is higher at larger depths, resulting in a higher turbine entrance temperature, which results in a higher efficiency.

At shallow depths, the pressure difference in the turbine has a relative large effect on the total pressure difference. Therefore there is only a small amount of pressure difference left for the dynamic component in the wells resulting in a small flow rate. This small flowrate results in a small electrical output and a small well spacing. However, since there is less heat extracted from the reservoir, the overall efficiency stays nearly the same.

5.2.2 Reservoir height

The amount of energy that can be recovered from a reservoir depends on the volume of the reservoir, which depends on the height of the reservoir. Reservoirs can vary from several meters to several hundreds of meters. However, to keep the reservoir height realistic and relevant, a choice has been made to vary the height between 50 and 150 m, which is in the vicinity of the Barendrecht reservoirs(Shell CO2 Storage B.V., 2009). Figure 5.3 shows the sensitivity diagram for the variation in reservoir height.

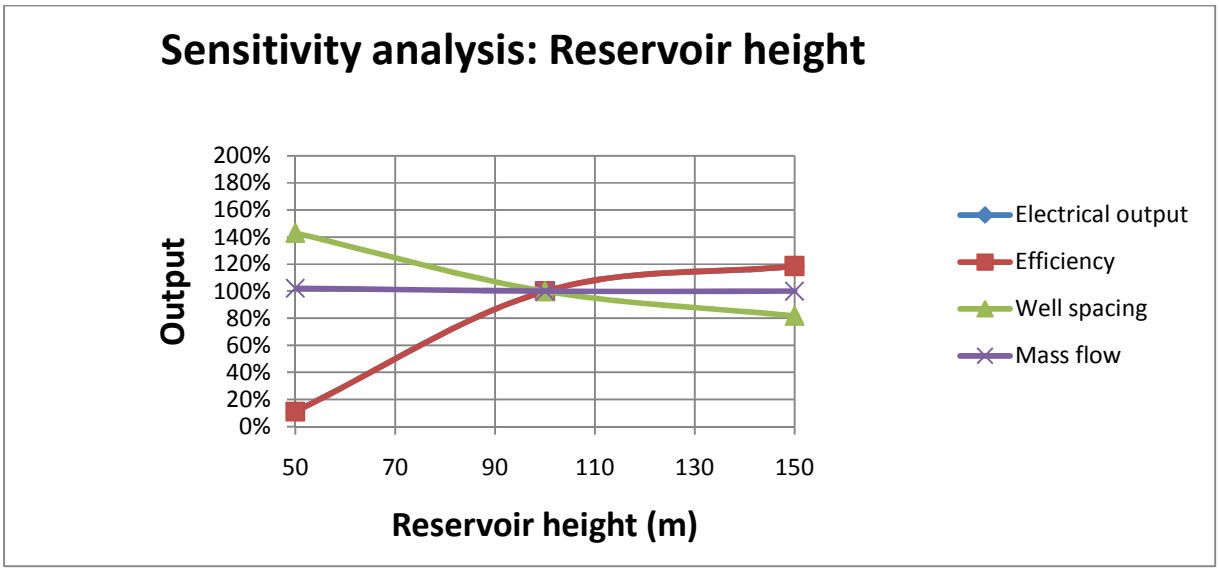

Figure 5-3. Sensitivity diagram for change in reservoir height. A reservoir height of 100 m equals the base case for the Netherlands.

A smaller height of the reservoir results in an increased well spacing as the same volume is required to maintain the energy production over the entire lifetime. However, a larger well spacing requires a larger pressure difference to maintain the mass flow. A larger pressure difference in the reservoir results in a smaller pressure difference over the turbine, reducing the output and overall efficiency. When the reservoir height is halved, the efficiency and electrical output are reduced with 85%.

A larger reservoir height has the opposite effect, but with reduced values.

5.2.3 Geothermal gradient

Lokhorst made an analysis of the geothermal gradient in the Netherlands where the results vary between less than 343 K to more than 363 K for a depth of 2000 m(Lokhorst, et al., 2007). To include the areas with the lowest and highest temperature in the Netherlands these temperatures have been enhanced by 10 degrees resulting in a geothermal gradient between 20 and 50 degrees per kilometer. The sensitivity diagram can be seen in figure 5.4.

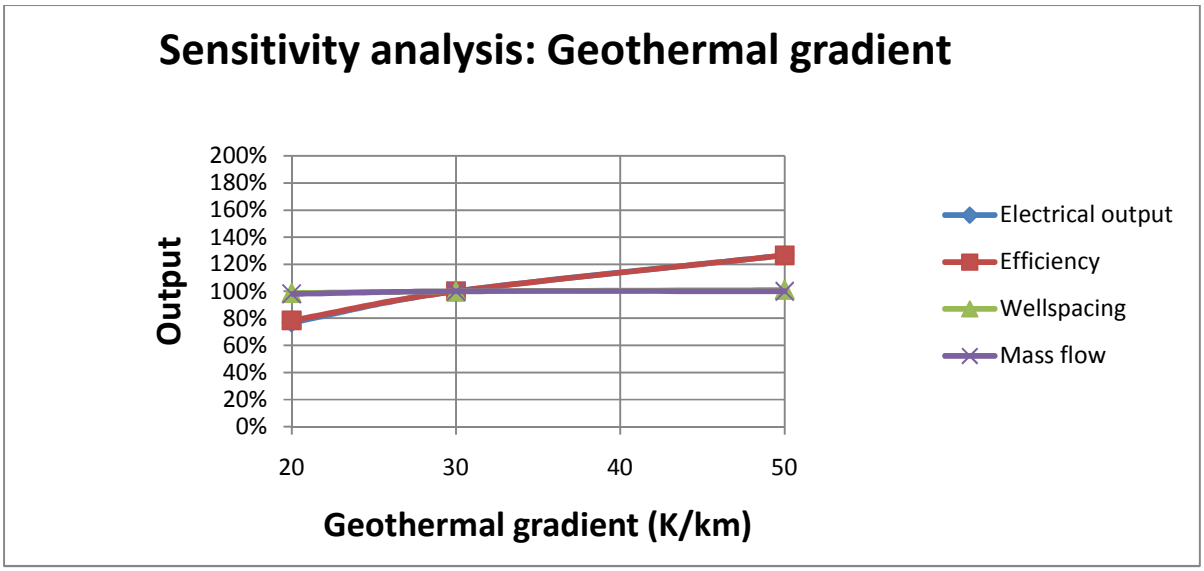

Figure 5-4. Sensitivity diagram for change in geothermal gradient. A geothermal gradient of 30 K/km equals the base case for the Netherlands.

A higher geothermal gradient causes a higher temperature at the end of the recovery well. This allows for more heat to be available in the turbine resulting in a higher efficiency and a higher electrical output. A lower geothermal gradient has the opposite effect.

At a geothermal gradient of 40 K/km a deviation from the increase in efficiency is seen. This deviation is caused by the fact that at this gradient the end temperature of the turbine is closer to the temperature of the surface water that at a gradient of 50 K/km. At a gradient of 50 K/km about 20% of the available temperature in the turbine is cooled away in the condenser due to the fact that the minimum pressure is reached.

5.2.4 Rock permeability

The permeability of the reservoir reflects its ability to transmit fluids. A higher permeability means the fluid will flow easier through the reservoir and less pressure is required to achieve the same flow. The permeability has been varied between $1.5*10^{-12}$ to $5*10^{-14}$ m^2, using 10^{-13} m^2 as around the average of the Netherlands[1]. The sensitivity diagram for permeability is shown in figure 5.5.

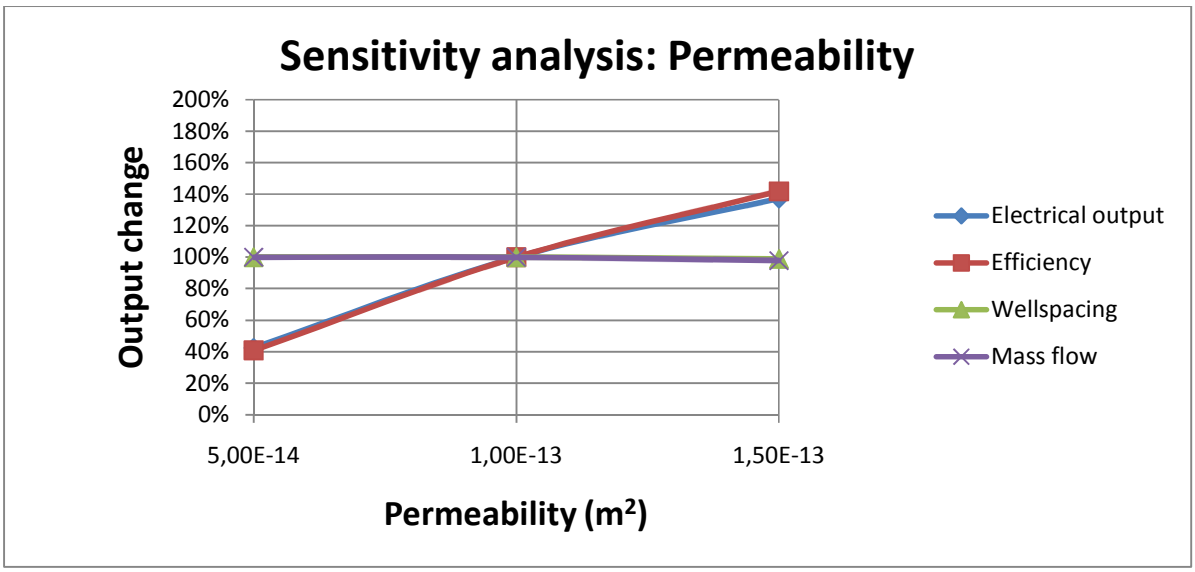

Figure 5-5. Sensitivity diagram for change in permeability. A permeability if 10^{-13} m^2 equals the base case for the Netherlands.

The sensitivity diagram for permeability shows that the permeability has hardly any effect on mass flow and well spacing. This is true for the fact that when the permeability changes less pressure is required to achieve the minimum flow. Therefore the end pressure of the injection well will be higher which results in a higher turbine output and a higher overall efficiency.

When the permeability gets too low the pressure difference in the reservoir gets too high, resulting in a low pressure difference of the turbine. Therefore the electricity output and efficiency reduces. However, as the pressure difference increase in the reservoir results in a pressure difference decrease in the turbine, with a 50% reduction in permeability there is hardly any pressure difference left in the turbine. Therefore the reduction in output with 50% decrease in permeability is larger than the addition of output with a 50% increase in permeability.

[1] Stated by IF Technology

5.2.5 Lifetime

The lifetime of a coal fired power plant(Rainforest Action Network, 2008) and a nuclear power plant go up to 50 years(Katona, et al., 2003). A similar lifetime for geothermal power production can increase its competitiveness. However, to analyze the effect of lifetime, the lifetime has been varied between 30 and 70 years. The sensitivity diagram for the change in lifetime can be seen in figure 5.6.

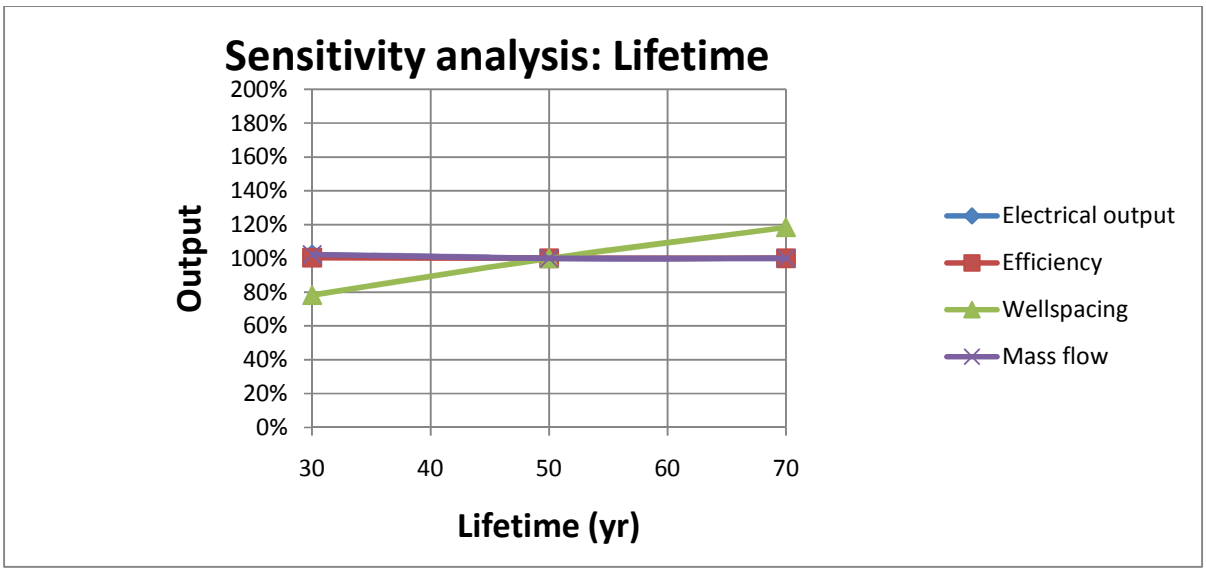

Figure 5-6. Sensitivity diagram for change in lifetime. A lifetime of 50 year equals the base case for the Netherlands.

The lifetime of the project has an effect on the well spacing of the system as a shorter lifetime results in less heat which needs to be extracted. While there are some effects on electrical output, efficiency and mass flow, they are hardly noticeable.

5.2.6 Well diameter

Figure 5.6 shows the sensitivity diagram for the changes in well diameter. A well diameter of 0.2 m is most often used in geological drillings[2]. To show sufficient variation and keep the well diameter within realistic bounds, a variation of 0.1 m has been chosen. Figure 5.7 shows the sensitivity diagram for the change in well diameter.

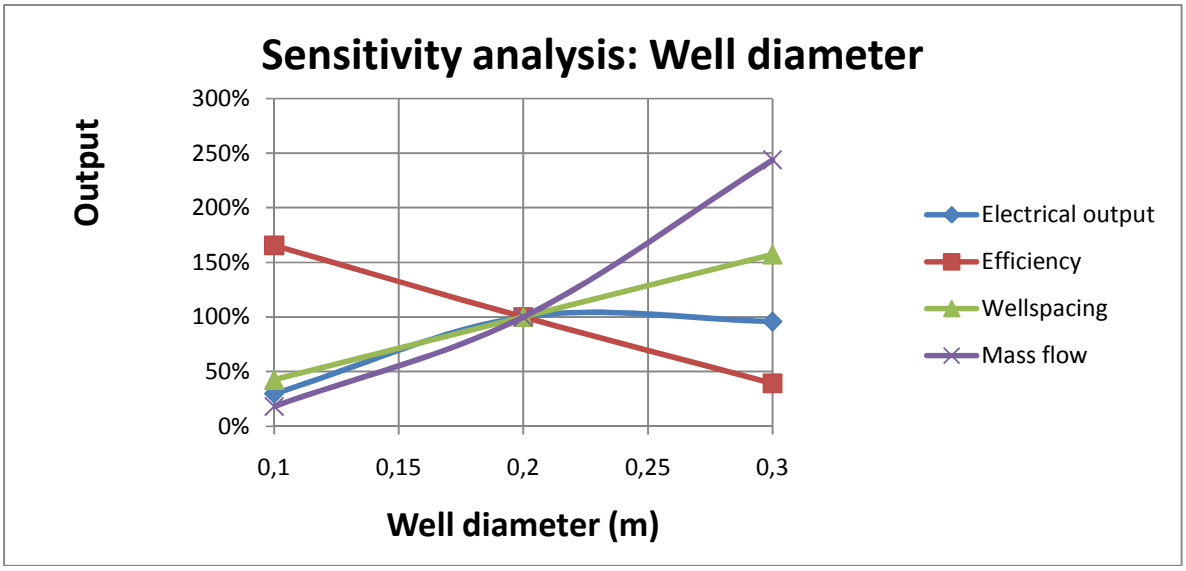

Figure 5-7. Sensitivity diagram for change in well diameter. A diameter of 0.2 m equals the base case for the Netherlands.

A larger well diameter allows for a larger flow and thus a larger well spacing. However, a larger flow also results in a larger pressure difference in the recovery well and a lower turbine entry pressure. The lower turbine pressure difference results in a lower efficiency. When the lower efficiency and higher flow rate are combined the result is an electrical output without noticeable change compared to the base diameter.

Reducing the well diameter results in a higher efficiency in the same way as a larger well diameter results in a lower efficiency. However, when the higher efficiency is combined with the reduced flow, the electrical output is reduced by about 70%.

[2] Stated by IF Technology

5.3 Optimal system

The optimal system is designed using the results of the sensitivity analysis. For every different variable the value is chosen which gives the highest electrical output. However, all variables are kept within a reasonable range. For example, a depth of 10 km most likely gives a much higher electrical output, but to implement a geothermal system at those depths surpasses the aim of this research and therefore a 3 km depth is chosen. Table 5.3 shows the values of the chosen variables.

Table 5.3. Variables used for optimal system

Variable	Value	Unit
Reservoir depth	3000	m
Reservoir height	150	m
Geothermal gradient	50	K/km
Permeability	$1.5*10^{-13}$	m^2
Turbine efficiency	80	%
Running hours per year	7750	hr/yr
Lifetime	50	yr
Well diameter	0.2	m

Output

The optimal system design as stated above results in a system which extracts 31 MW_{th} of heat from the soil and turns it into 5 MW_e electrical output resulting in a 16% overall efficiency. To maintain this output for at least 50 years with a runtime of 7750 hours per year, the wells need to be at least 950 meter apart from each other. The properties at the different parts of the system for the base case of the Netherlands can be seen in Table 5.4. The numbers in table 5.4 are shown in figure 5.8.

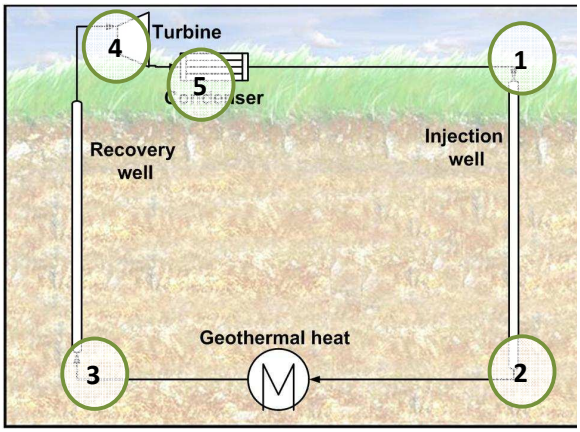

Figure 5-8. Systematic representation of the system. T numbers represent the locations from table 5.4.

Table 5.4. Properties of carbon dioxide at the start of the different steps in the system for the optimal system.

Number	Location	Pressure	Temperature	Density	Enthalpy	Entropy
		Bar	*K*	*kg/m³*	*kJ/mol*	*kJ/mol/K*
1	**Injection well**	64.00	296.0	1000	-2.852	0.106
2	**Reservoir**	353.4	307.3	962.9	-2.852	0.102
3	**Recovery well**	342.1	437.5	509.1	9.122	0.131
4	**Turbine**	181.4	405.6	325.9	9.122	0.135
5	**Condenser**	64.00	320.0	154.7	7.232	0.137

5.4 Validation

The results from this research are hard to compare with literature as there is no literature describing the a geothermal carbon dioxide system for electricity production. However, a comparison has been made with other low temperature supercritical power cycles and organic Rankine cycles(Yamaguchi, et al., 2006)(Chen, et al., 2006). These systems show efficiencies between which vary between 40% and 70% of Carnot efficiency(Nieuwlaar, et al., 2007-2009). The current system as described in this research shows efficiencies varying between 75% for the optimal case and 80% for the base case.

The system described in this research thus shows a slightly higher efficiency than the literature when all efficiencies are relative to Carnot. This can be explained by the fact that the current system does not require any work input to pump the fluid.

6 Safety, environment and financial analysis

This chapter is meant to give an analysis on the safety, health and environmental risks and a rough estimation on the costs of a geothermal carbon dioxide system. This analysis is far from complete, as a full thorough analysis goes beyond the aim of this research. To stay within the scope of the research and to ensure the quality of the analysis, the safety, health and environmental risks are largely based on the carbon dioxide storage project in Barendrecht(Shell CO2 Storage B.V., 2009).

6.1 Safety analysis

Chapter 6.1 will discuss the safety and health risks of geothermal carbon dioxide projects.

6.1.1 Risks

Carbon dioxide safety risks

Carbon dioxide is a harmless substance in most cases. As its material safety data sheet(MSDS) shows, carbon dioxide is not flammable, does not have any risk or safety phrases, hardly has any harmful effects on the ecology and even ingesting it does not cause serious harm(Air Liquide, 2007). The only danger that lies with carbon dioxide is the fact that its heaver than air. Whenever carbon dioxide is emitted in high concentrations there is a possibility that carbon dioxide will force the oxygen away.

Large scale carbon dioxide escape

Both the Monoun and Nyos incidents took place with a natural carbon dioxide field created by volcanic activities. These field are located tens of meters under the surface, which is a large difference compared with the current carbon dioxide storage projects which use depths of several kilometers. In addition to the large depths the carbon dioxide is stored in gas fields which are located underneath an impermeable layer of rock. The risk of the Monoun and Nyos incidents repeating themselves is therefore very small in carbon dioxide storage projects. Since the geothermal carbon dioxide project uses exactly the same reservoirs as carbon dioxide storage, the risk of large scale carbon dioxide escape is also very small.

Leakage

Both the Barendrecht project and the geothermal carbon dioxide project have a large distance of piping just below the surface. In the Barendrecht case the piping comes from the carbon dioxide capture location to the storage location. In the geothermal carbon dioxide project the additional piping goes from the recovery well to the injection well.

Small leakages can be easily detected by weekly inspection. Carbon dioxide leakage in the piping results in dying vegetation while carbon dioxide leakages in the turbine(geothermal carbon dioxide) or compressor(Barendrecht) can be detected by detection equipment(Shell CO2 Storage B.V., 2009).

Large leakages, so called blowouts, can be caused by pipe breaking or similar incidents. Carbon dioxide is expanded rapidly by flowing from a high pressure pipe to atmospheric pressure. This rapid expansion causes both an acoustic and visual warning. Rapid expansion of carbon dioxide causes the temperature

to drop very fast within a second, causing deposition of the water in the air. The water vapor in the air cools down so rapidly resulting in a white plume in the air. In this case, the system has remotely controlled valves which can be closed down to prevent the escape of large carbon dioxide quantities(Shell CO2 Storage B.V., 2009).

The last possibility of leakage is subsurface leakage which can theoretically take place through the impermeable layer, breaks in the impermeable layer, the surrounding of the reservoir or through the wells. According to the environmental impact assessment study from Barendrecht these scenarios are very unlikely to occur(Shell CO2 Storage B.V., 2009). However, when a geothermal carbon dioxide project is performed these risks have to be re-evaluated since the reservoir pressure is higher than in the carbon dioxide storage project which enhances the risks.

Subsidence

The pressure in a natural gas reservoir drops whenever the natural gas is extracted. The Barendrecht gas field dropped in pressure from 174 bar to 30 bar. This pressure drop can cause subsidence, where the earth's surface shifts downward. This can cause severe damage on buildings in the area(Commissie bodemdaling, 2010). Filling the gas field with carbon dioxide and thereby restoring its initial pressure stops the subsidence from continuing.

Long term overpressure

At the end of the lifetime of a geothermal carbon dioxide project the reservoir is filled with liquid carbon dioxide of 296 K. At a pressure of 250 bar the carbon dioxide has a density of 957 kg/m^3. However, when time passes the reservoir will slowly be heated up from the heat flux of the earth's core. After a certain amount of time the reservoir will be back at its old temperature. In the base case for the Netherlands the temperature will rise to 345 K. At the same pressure of 250 bar the density has lowered to 736 kg/m^3. This 30% reduction in density would usually mean a 43% increase in volume. However, the volume cannot increase since the reservoir is a closed system, resulting in an increase of pressure to 639 bar.

To ensure the reservoir does not have too much overpressure, the maximum allowed pressure has to be evaluated for each different case and the amount of carbon dioxide either must not exceed the maximum amount at the end of the system or the excess of carbon dioxide must be removed from the reservoir.

6.1.2 Safety conclusion

Carbon dioxide on itself is a nearly harmless substance(Air Liquide, 2007). The danger of carbon dioxide lies when the carbon dioxide is emitted in large quantities since carbon dioxide is heavier than air and can force the air away. However, the danger of large quantity carbon dioxide emission from a carbon dioxide storage project is very small(Shell CO2 Storage B.V., 2009).

Using carbon dioxide as a geothermal working fluid requires additional research to guarantee its safety. Reasons for this is the fact that the reservoir pressure is higher than with carbon storage projects and that the exact effect of long term storage after the projects lifetime has not been researched yet.

6.2 Environmental analysis

This project aims to combat climate change by both reducing the overall carbon dioxide concentration in the atmosphere by storing the carbon dioxide in geological reservoir and by producing carbon neutral electricity.

6.2.1 Carbon dioxide storage

The total amount of carbon dioxide stored underground and the amount of produced electricity greatly depends on the properties of the reservoir and the volume allocated to a doublet. The ground area allocated to a doublet is set to be equal to the area of the thermal front droplet as shown in section 3.2.3. The area is calculated as follows.

$$A = \frac{4\pi R^2}{3} \qquad \text{(Eq. 40)}$$

where:

A = Area, m^2
R = Thermal radius from section 3.2.3., m

The height of the reservoir is used to calculate the allocated volume per doublet. To calculate the amount of carbon dioxide which can be stored in the subsurface, an equation is proposed by van der Meer(Meer, et al., 2009).

$$M_{CO2\ stored} = VrR_nE\phi\rho \qquad \text{(Eq. 41)}$$

where

$M_{CO2\ stored}$ = Carbon dioxide storage capacity

Vr = Aquifer volume, m^3

R_n = Net to gross ratio, -

E = Efficiency factor, constant = 0.02, total storage efficiency stated by Meer(Meer, et al., 2009)

ϕ = Porosity, -

Base case for the Netherlands

The base case for the Netherlands has a well spacing of 1400 meter and a reservoir height of 100 meter. Therefore a single doublet has an allocated area of 2.1 km^2 and a volume of 0.21 km^3. To prevent overpressure in the reservoir after the carbon dioxide present is heated up, a pressure of 256 bar and a

temperature of 245 K is used which results in a density of 745 kg/m^3. This results in a total carbon dioxide storage potential of 153,000 ton per doublet.

Optimal case

The optimal case has a well spacing of 950 meter and a reservoir height of 150 meter. When using the same calculation as with the base case for the Netherlands above, the total carbon dioxide storage potential equals 106,000 ton per doublet.

6.2.2 Carbon neutral electricity

The production of electricity using a geothermal carbon dioxide system is carbon neutral. To compare the avoided carbon dioxide emission to the atmosphere a comparison is made with natural gas fired power plants. On average, natural gas fired power plants have a carbon dioxide emission of 380 g CO2/kWh(International Energy Agency, 2009). However, the average carbon dioxide emission from natural gas power generation in the Netherlands over the years 2005 to 2007 equals 294 g CO2/kWh(International Energy Agency, 2009), which will be used as comparison value.

Base case for the Netherlands

The base case for the Netherlands produces 0.48 MW per doublet with a runtime of 7750 hours per year. This totals an electricity production of 3.7 GWh per year without carbon dioxide emissions. When the same amount of electricity would have been produced using natural gas fired power plants the total carbon dioxide emissions would equal 1100 ton. This results in a total avoidance of 36000 ton carbon dioxide over the full 50 years lifetime of the system. This adds 36% of total carbon savings to a carbon dioxide storage project.

Optimal case

The same calculation method is used for the optimal case as used with the base case for the Netherlands. The total electricity production per doublet equals 38.5 GWh per year, resulting in a total avoided carbon dioxide emission of 11300 ton. This results in a total avoidance of 565,000 ton carbon dioxide over the full 50 years lifetime of the system, enhancing the carbon dioxide savings of a carbon dioxide storage project by 430%.

6.2.3 Environment conclusion

This project can be seen as an enhancement on carbon dioxide storage projects. When the system has a lifetime of 50 years the total amount of carbon that is stored in the reservoir can be enhanced by 36% for the base case and 430% for the optimal case by avoided carbon dioxide emissions due to carbon neutral electricity production.

6.3 Financial analysis

This chapter gives a rough estimation of the costs of a geothermal system using carbon dioxide as working fluid. This cost analysis is not meant to be a complete thorough analysis of every single component but is meant to give a first estimation of what this kind of system would cost.

The costs of a geothermal carbon dioxide system depend on the system size and design. To make a clear analysis a choice has been made for two different cases defined as both the base case and the optimal case from chapter 5; two different turbine placing designs where there will be a turbine for 2 doublets or a single turbine for every doublet; and two different pricing scenarios where either the costs are fully allocated to this system or where the costs are partially allocated to carbon dioxide storage. The total number equals 8 different scenarios. Table 6.1 shows an overview of the 8 scenarios.

Table 6.1. Scenarios used for calculating the costs

System number	Output (MWe)	Turbine	# turbines	Costs
1	1	Single turbine per 2 doublets	1	Full
2	1	Single turbine per 2 doublets	1	Partial
3	1	Single turbine per doublet	2	Full
4	1	Single turbine per doublet	2	Partial
5	10	Single turbine per 2 doublets	1	Full
6	10	Single turbine per 2 doublets	1	Partial
7	10	Single turbine per doublet	2	Full
8	10	Single turbine per doublet	2	Partial

6.3.1 Multiple wells

Half of the scenarios mentioned above used a single turbine per two doublets. This is only possible if a reservoir is large enough that multiple wells can be placed to enhance the output. However, when multiple wells are placed within range of each other, the droplet shaped thermal front will change(U.S. Department of Energy, 2001). The relations and equations involved are beyond the scope of this research. However, to analyze the effect of multiple wells in a single gas field, the assumption has been made that a recovery well is ignored in the fluid flow when the distance is equal or greater than 125% of the closest recovery well based on the injection well's location. This assumption is visualized in figure 6.1.

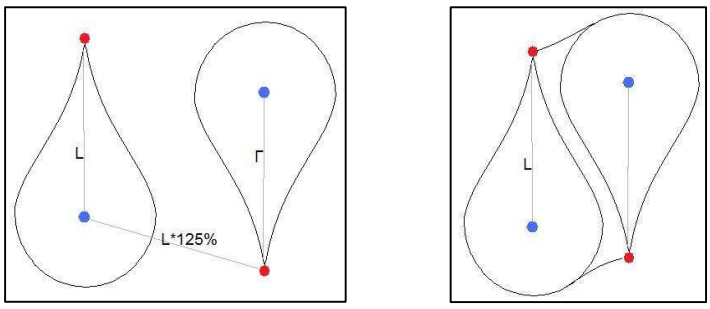

Figure 6-1. Left: Distance between left injection and right recovery well equals 125% of the well spacing L. Therefore the droplet shape is maintained. Right: The distance between the left injection well and right recovery well is too small and causes a different shape.

6.3.2 Costs

The costs have to be allocated to initial investments and periodic investments. Initial investments are all costs which have to be invested before the system starts running and consists mostly out of construction costs. The construction costs consist of surface piping, wells and turbines. Table 6.2 shows the quantity of piping, wells and turbines required.

Table 6.2. Total material required for the different systems

System number	m surface piping	# wells	# turbines	Turbine size (MWe)
1	4000	4	1	1x1
2	4000	2	1	1x1
3	2800	4	2	2x0.5
4	2800	2	2	2x0.5
5	2700	4	1	1x10
6	2700	2	1	1x10
7	1900	4	2	2x5
8	1900	2	2	2x5

Surface piping

The amount of surface piping is defined as the total length of piping required to transport the carbon dioxide from the recovery well to the turbine and from the turbine to the injection well. For an insulated pipe which has to withstand 70 bar of pressure the average price would be around €500 per meter(MATTHEW DAVIS Australia Pty. Ltd., 2008)(Charlotte Pipe and Foundry company, 2010) with no difference made between a pipe for a gas or a liquid since.

Wells

The number of wells is the same for every system, being 9 injection and 9 recovery wells. The price of a single well is usually around €1000 per meter(Stated by IF Technology, 2010). For a single 2000 meter well this would result in a total of €2,000,000. However, drilling wells has a 20% chance of failure rendering the well useless. Therefore the price of €1000 per meter has been divided by 0.8 to cover the failures. This results in a total price of €1250 per meter, €2,500,000 for a 2000 meter well and € 3,750,000 for a 3000 meter well.

For the systems where a part of the costs is allocated to a carbon dioxide storage project, the total number of wells is halved, since it is assumed that the injection wells of the storage project can be re-used for a geothermal carbon dioxide system.

Turbine and condenser

Using data from Nye Thermodynamics Corporation an equation has been formed to calculate the price per kW_e(Nye Thermodynamics Corporation, 2010), which is formed using turbines up to 20 MW. While this data contains only prices for gas turbines it is assumed that carbon dioxide turbines have similar costs.

$$M€ = 0.0004kWe + 0.4137 \quad (R^2=0.9738) \qquad \text{(Eq. 42)}$$

However, this is merely the costs for the turbine alone. No data was obtained after searching online and contacting companies about the costs for the condenser or the infrastructure for the turbine. Therefore, to still take these cost into account, the cost of the turbine have increased by 100%. This would result in M€1.6 to M€2.4 for the base scenario and M€8.8 to M€9.6 for the optimal scenario.

Periodic costs

Periodic costs consist mainly of operation and maintenance. For a standard heat and cold storage projects the periodic costs are about 2% of the initial costs. Because the system designs stated above go deeper than heat and cold storage projects and require more advanced turbines the periodic costs have been set to 2% initial and another 0.1% for each turbine which is placed. This results in 2.1% for the systems 1, 2, 5 and 6 to 2.2% for the systems 3, 4, 7 and 8.

Initial transport and compression costs

The systems with partial costs assume that the system is applied to an existing carbon dioxide storage project. The full cost system however, assumes that the carbon dioxide still needs to be stored in the reservoir. To store the carbon dioxide in the reservoir it needs to be transported to the storage site and compressed to inlet pressure. The transport costs of carbon dioxide vary with each separate location. However, on average in Western Europe it costs €3 per ton of carbon dioxide to transport the carbon dioxide from the capture location to the storage location(Hendriks, et al., 2004). When the carbon dioxide reaches the storage location it needs to be compressed to allow for injection in the reservoir. The compression of carbon dioxide costs around €7.5 per ton(Hendriks, et al., 2004).

Using the total carbon dioxide storage from chapter 6.2.1 of 153,000 ton for the base case and 106,000 for the optimal case, the additional cost for carbon dioxide transport and compression equal M€1.15 per doublet for the base case of the Netherlands and M€0.8 for the optimal case.

Overview

Table 6.3 shows the results when all the prices stated above are projected upon the different systems.

Table 6.3. Overview of costs per system

System number	CO2 transport and compression	Price surface piping	Price wells	Price turbines	Total[3]	Total per MW	Periodic costs	Periodic costs
	M€	*M€*	*M€*	*M€*	*M€*	*M€/MW*	-	*M€/yr*
1	€ 3,21	€ 2,00	€ 10,00	€ 1,63	€ 12,84	€ 12,84	2,10%	€ 0,27
2	€ 0,00	€ 2,00	€ 5,00	€ 1,63	€ 8,63	€ 8,63	2,10%	€ 0,18
3	€ 3,21	€ 1,40	€ 10,00	€ 4,08	€ 14,69	€ 14,69	2,20%	€ 0,32
4	€ 0,00	€ 1,40	€ 5,00	€ 4,08	€ 10,48	€ 10,48	2,20%	€ 0,23
5	€ 2,23	€ 1,35	€ 15,00	€ 8,83	€ 24,63	€ 2,46	2,10%	€ 0,52
6	€ 0,00	€ 1,35	€ 7,50	€ 8,83	€ 17,68	€ 1,77	2,10%	€ 0,37
7	€ 2,23	€ 0,95	€ 15,00	€ 9,65	€ 25,06	€ 2,51	2,20%	€ 0,55
8	€ 0,00	€ 0,95	€ 7,50	€ 9,65	€ 18,10	€ 1,81	2,20%	€ 0,40

[3] This includes carbon dioxide storage benefits

6.3.3 Transport heat loss

As stated in chapter 3.2.7, a longer distance between the recovery well and the turbine causes losses in temperature. For the base case, the heat loss equals around 6.5 W per meter(The Engineering Toolbox, 2005). For the optimal case the heat loss equals around 49 W per meter due a much larger temperature difference than the base case(The Engineering Toolbox, 2005).

For the base case the efficiency drop equals 4% for systems 1 and 2 and 2% for systems 3 and 4. However, for the optimal case, the efficiency drop equals 55% for systems 7 and 8 and 28% for the systems 9 and 10. The first reason for this is, as mentioned above, a much larger temperature difference. The second reason for this is the fact that the base case uses lower pressure and temperature in the turbine which results in a larger heat capacity for carbon dioxide. Systems 5, 6, 11 and 12 have no heat losses since a turbine can be placed near every recovery well negating the need for transportation between the recovery well and the turbine.

These efficiencies have been applied to the revenues of the systems in the calculation of the net present value.

6.3.4 Revenues

Electricity sales

The main goal of any electricity production is its sales, and with sales its profits. The price of electricity has been set to €0.085 per kWh. This price is taken from the revenues gained from selling renewable energy to Essent(Essent, 2010). The base system then would gain a total €218,000 per doublet per year. The optimal system would gain a total of €1,128,000 per doublet per year.

Carbon credits

Besides electricity sales the system also gains revenues from carbon credits. At first, the system gains credits for storing carbon dioxide in the reservoir and when the reservoir is filled the system gains carbon credits for producing renewable electricity.

The price per ton of carbon dioxide equals €13.08 at the end of March 2010(Point Carbon, 2010). The base system then gains a total revenue of €4,000,000 for storing 306,000 ton of carbon dioxide. The optimal system gains a total revenue of €2,770,000 for storing 212,000 ton of carbon dioxide. However, this is not the case for the scenarios with an odd number (1, 3, 5, …). Since these systems have the costs for carbon dioxide storage not allocated to the system they can also not allocate the revenues from carbon storage to the system.

The base system avoids a total of 1,100 ton of carbon dioxide per doublet per year. This equals a revenue of €14,400 per year. The optimal system avoids 11,300 ton of carbon dioxide per year totaling a revenue of €148,000 per doublet per year.

Overview

Table 6.4 shows an overview of the revenues of the different systems.

Table 6.4. Overview of revenues per system

System number	CO2 storage credits	CO2 avoided credits	Electricity sales	Total per year
	M€	*k€/yr*	*M€/yr*	*M€/yr*
1	€ 4,00	€ 28,78	€ 0,63	€ 0,66
2	€ 0,00	€ 28,78	€ 0,63	€ 0,66
3	€ 4,00	€ 28,78	€ 0,65	€ 0,67
4	€ 0,00	€ 28,78	€ 0,65	€ 0,67
5	€ 2,77	€ 295,61	€ 6,59	€ 6,88
6	€ 0,00	€ 295,61	€ 6,59	€ 6,88
7	€ 2,77	€ 295,61	€ 2,99	€ 3,28
8	€ 0,00	€ 295,61	€ 2,99	€ 3,28

6.3.5 Net present value / Pay back period

The main question which often arises with large investments is how long it takes before the investment is earned back. At the year 0, the total balance of the system equals the investments costs. Every subsequent year the profits are added and the periodic costs are subtracted. Whenever the balance equals 0 the investment has earned enough to compensate for its cost and the pay back period is reached. To calculate the net present value is calculated using the equation below (Blok, 2007).

$$NPV = \sum_{i=0}^{n} \frac{B_i - C_i}{(1+r)^i} \qquad \text{(Eq. 43)}$$

where:
n = Lifetime
R_i = Revenues in year i
C_i = Costs in year i
r = Discount rate

The NPV is calculated for 2 different discount rates. A discount rate of 10% is used for a private company and a discount rate of 4% is used for a public company. Figures 6.2 to 6.5 show the net present value for the base case and the optimal case using the different discount rates. The net present value graphs show the balance of the system at each year. The total net present value equals the balance of the system at the final year, the system's lifetime. If the net present value of a system is positive, the system is economically feasible(Blok, 2007).

Discount rate 10%

Figure 6.2 shows the NPV for the base case for the Netherlands when a discount rate of 10% is applied.

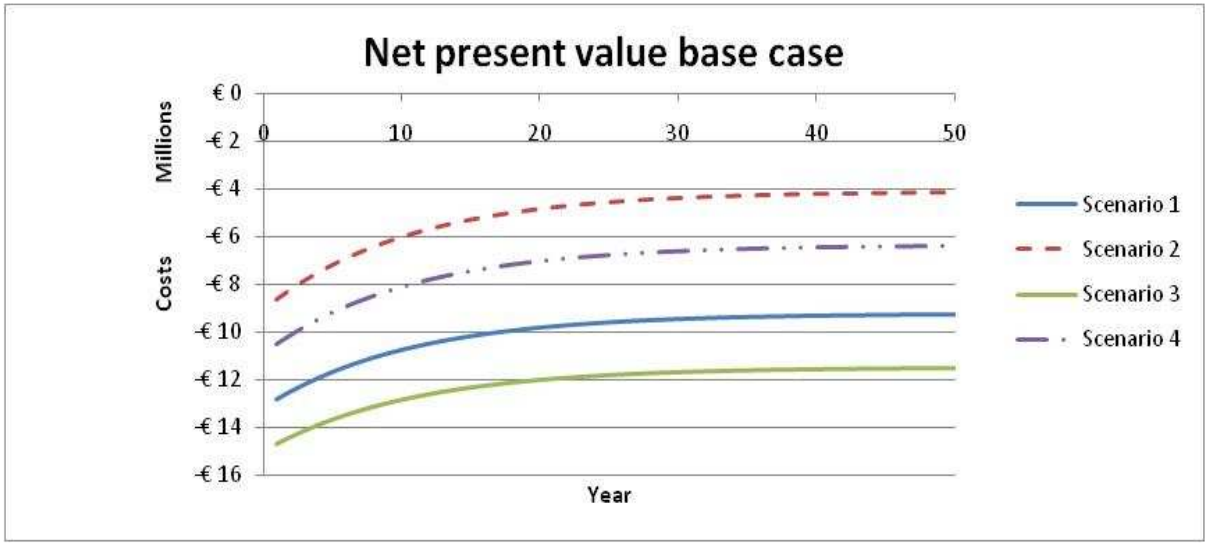

Figure 6-2. Net present value graph for the base system in the Netherlands over 50 years, using a 10% discount rate.

For the base case for the Netherlands is not economically feasible when a discount rate of 10% is used. Even when part of the system is allocated to a carbon storage project and the cheapest turbine placing is used, the outcome still is a negative NPV.

Figure 6.3 shows the NPV for the optimal case with a discount rate of 10%.

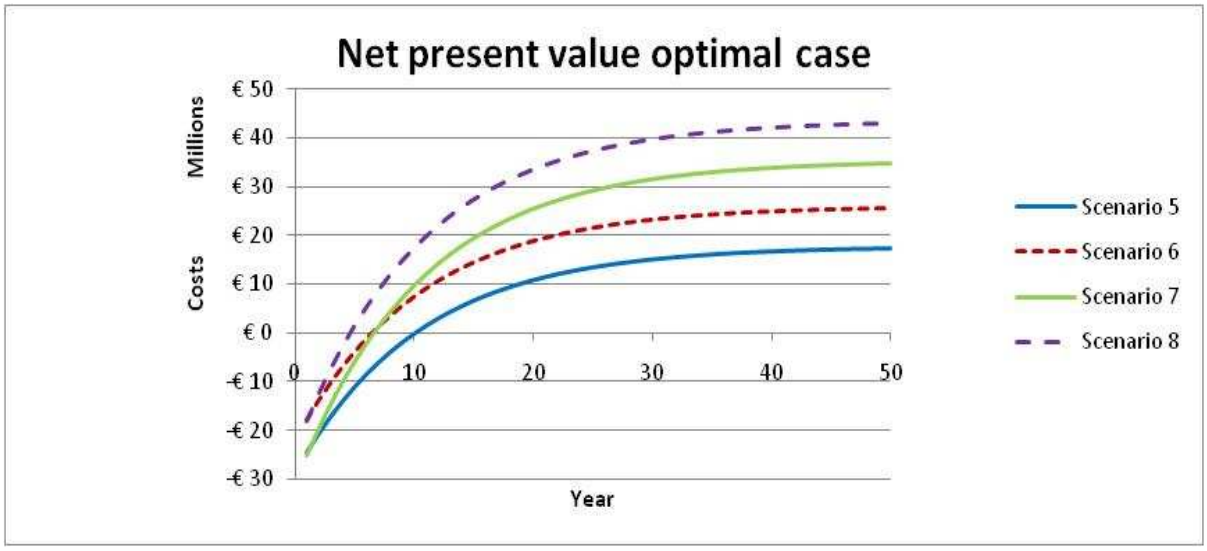

Figure 6-3. Net present value graph for the optimal system over 50 years using a 10% discount rate.

The NPV for the optimal case is positive for all scenarios with pay back periods between 5 and 11 years. The difference with the base case is caused by a higher electrical output of about a factor 10. Scenarios

5 and 7 are less profitable as scenarios 6 and 8, which have only part of their costs allocated to this system. This can be explained by the fact that the current carbon credit price is too low to make carbon storage economically feasible. The fact that scenario 8 gives a better result than scenario 6 is caused by the heat loss due to transport in scenario 6.

Discount rate 4%

Figure 6.4 shows the NPV for the base case for the Netherlands when a discount rate of 4% is applied.

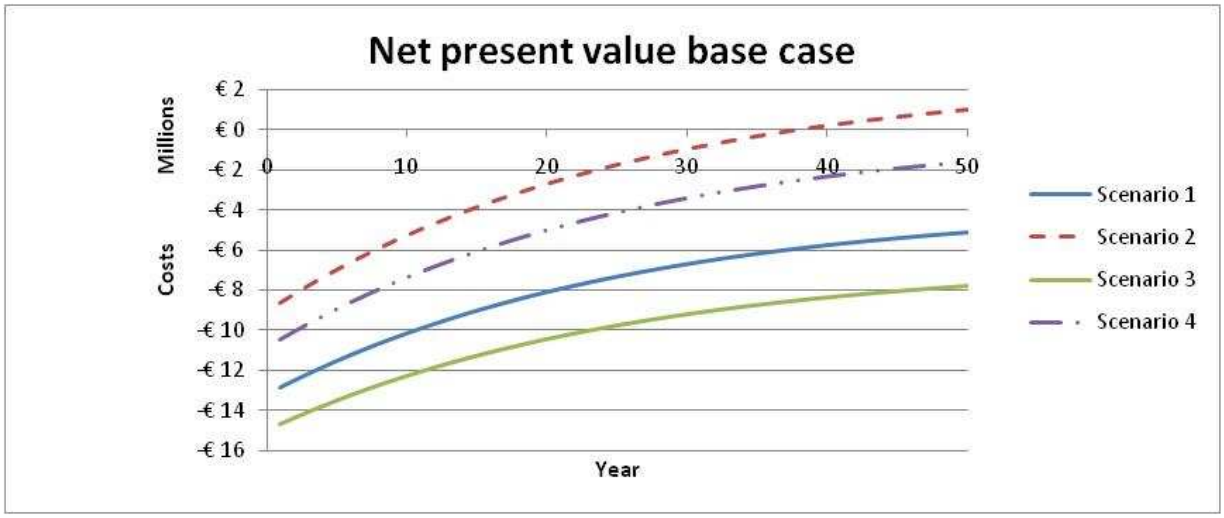

Figure 6-4. Net present value graph for the base system in the Netherlands over 50 years, using a 4% discount rate.

Out of the 4 base case scenarios, only scenario 2, partial costs with a single turbine for 2 doublets, has a positive NPV when a discount rate of 4% is used. A positive balance is achieved after 38 years. The other 3 scenarios are not economically feasible with a 4% discount rate.

Figure 6.5 shows the NPV for the optimal case with a discount rate of 4%.

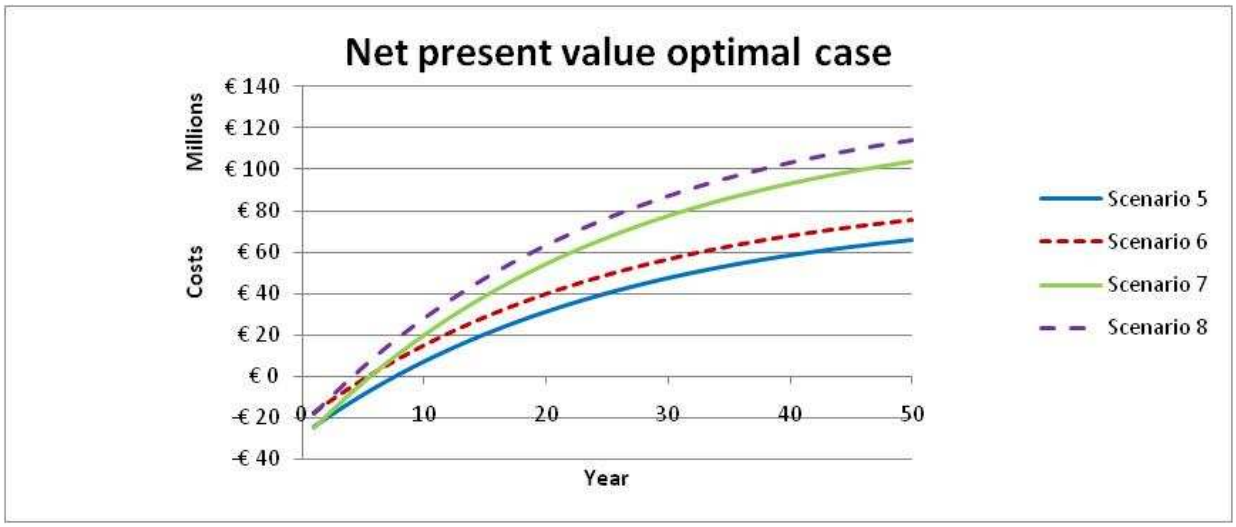

Figure 6-5. Net present value graph for the optimal system over 50 years, using a 4% discount rate.

The NPV for the optimal case is positive for all scenarios with pay back periods between 5 and 8 years. While there is not much difference in pay back period, the NPV value more than doubled.

The pay back period and the net present value for the different systems are shown in table 6.5.

Table 6.5. Pay back periods and net present values for the systems.

System	Pay back period	Net present value	Pay back period	Net present value
Discount rate	**4%**	**4%**	**10%**	**10%**
	yr	M€	yr	M€
1	>50	-€ 9.24	>50	-€ 5.09
2	>50	-€ 4.15	38	€ 1.01
3	>50	-€ 11.50	>50	-€ 7.53
4	>50	-€ 6.37	>50	-€ 1.35
5	11	€ 17.34	8	€ 65.78
6	7	€ 25.74	6	€ 75.85
7	7	€ 34.74	6	€ 103.76
8	5	€ 43.21	5	€ 113.98

6.3.6 Financial conclusion

As expected there is a large difference between the base case and the optimal case. The base case has lower investment costs, but also much lower profits. Out of all four scenarios for the base case for the Netherlands, only one scenario has a positive NPV, and only when a discount rate of 4% is used instead of 10%. The net present value for these systems vary from €-11,500,000 to €1,000,000. If a geothermal carbon dioxide system is built in a location with similar conditions as the base case for the Netherlands in this report, it will only be economically feasible if a system is built with a single turbine for multiple doublets and a discount rate of 4% is used.

The optimal case is different, since the efficiency losses are much larger. Therefore it is best to place a single turbine at every doublet. Also, the systems where only part of the costs is allocated to the project are more profitable than a system including carbon dioxide storage. The pay back periods for the optimal case vary between 5 and 11 years with net present values varying between €17,300,000 and €114,000,000.

6.4 Validation

For carbon capture and storage to be profitable the carbon price should be around $40 per ton(Earth2Tech, 2010), which equals around €30. To make the systems with an empty reservoir as profitable as the systems with a carbon storage project already taken place, the price of a carbon credit should equal €34.6.

The costs of the system have been made using a spreadsheet from IF Technology which is used to calculate the costs of heat and cold storage systems. While the costs for initial investments are different, the periodic costs are nearly the same. The remaining parts of the system are only based on literature. There is no other kind of validation done on the financial analysis since this was not the focus of the research.

7 Case study – Barendrecht Ziedewij

The Barendrecht carbon dioxide storage project has been a lot in the Dutch news lately. Also, much research has been done already on the area. Therefore, the Barendrecht area has been chosen as case study for this research.

7.1 The area

The area near Barendrecht has 2 gas fields which are planned to be filled with carbon dioxide, namely the smaller field at Barendrecht itself and the larger field at Barendrecht Ziedewij. The latter has the best properties for this research as the reservoir is 960 m deeper, 37 K warmer and 3 times as high as the smaller field. Table 7.1 shows the variables for the Barendrecht Ziedewij system.

Table 7.1 Variables for the Barendrecht Ziedewij system

Variable	Value	Unit
Reservoir depth	2630	m
Reservoir height	180	m
Geothermal gradient	27.11	K/km
Permeability	$1.7*10^{-13}$	m^2
Turbine efficiency	80	%
Running hours per year	7750	hr/yr
Lifetime	50	Yr
Well diameter	0.2	m

7.2 Output per doublet

The Barendrecht Ziedewij system design as stated above results in a system which extracts 17 MW_{th} of heat from the soil and turns it into 1.14 MW_e electrical output per doublet resulting in a 6.7% overall efficiency. To maintain this output for at least 50 years with a runtime of 7750 hours per year, the wells need to be at least 945 meter apart from each other.

7.3 Overall area potential

The Barendrecht Ziedewij area is 2200 by 1250 m and is oval shaped. This area allows for multiple doublets as shown in figure 7.1 with a maximum well spacing of 950 m.

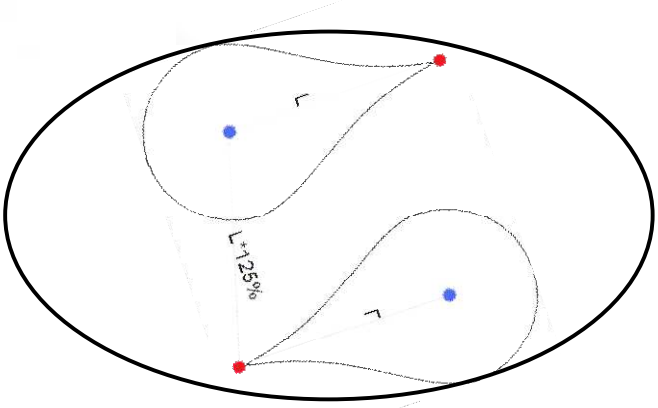

Figure 7-1. Systematic view of Barendrecht Ziedewij area with wells placed 950 m apart.

The placing of 2 doublets sets the output at 2.27 MW_e. The total domestic consumption of the Netherlands equals 24,300 GWh spread over 16,587,000 inhabitants(International Energy Agency, 2007)(CBS, 2010). This equals 1.47 MWh per person over one year. Barendrecht had 44,200 inhabitants which use on average a total of 64,800 MWh per year(Gemeente Barendrecht, 2007). When the geothermal carbon dioxide system runs for 7750 hours per year with an electrical output of 2.27 MW_e, the total amount would come at 17,600 MWh, which equals 27% of the total domestic consumption of Barendrecht.

7.4 Costs

Chapter 6 showed that the cheapest option is where every recovery well has its own turbine. Therefore it is chosen to place 2 turbines which connect a recovery well to an injection well. In total there are 2 turbines of 1.2 MW, 2 times 950 m of insulated piping and 2 recovery wells. The costs are M€ 0.95 for the piping, M€ 6.6 for the wells assuming the injection wells area already present and M€ 2.7 for the turbines resulting in a total investment of M€ 10.2. Operation and maintenance is set at 2.2% of the initial investment each year totaling €225,000.

Assuming a price of €0.085 per kWh, the system provides a total revenue from electricity sales of M€0.96 per year. This production of carbon neutral electricity avoids the emission of 5,200 ton of carbon dioxide per year, resulting in additional revenues from carbon credits of €67,500. When a discount rate of 10% is used, these revenues result negative NPV. Figure 7.2 shows the net present value for the system as described above. Using a lifetime of 50 years the net present value equals M€-2.9.

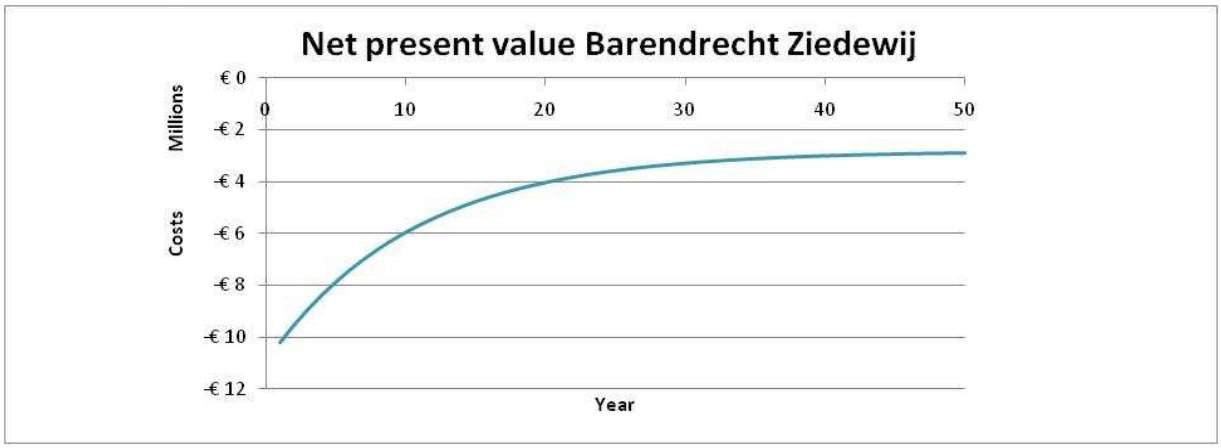

Figure 7-2. Net present value for the system in Barendrecht Ziedewij, using a 10% discount rate.

When the discount rate is lowered to 4%, the NPV is positive and equals M€5.6, resulting in a pay back period of 22 years. Figure 7.3 shows the NPV for the Barendrecht Ziedewij system using a discount rate of 4%.

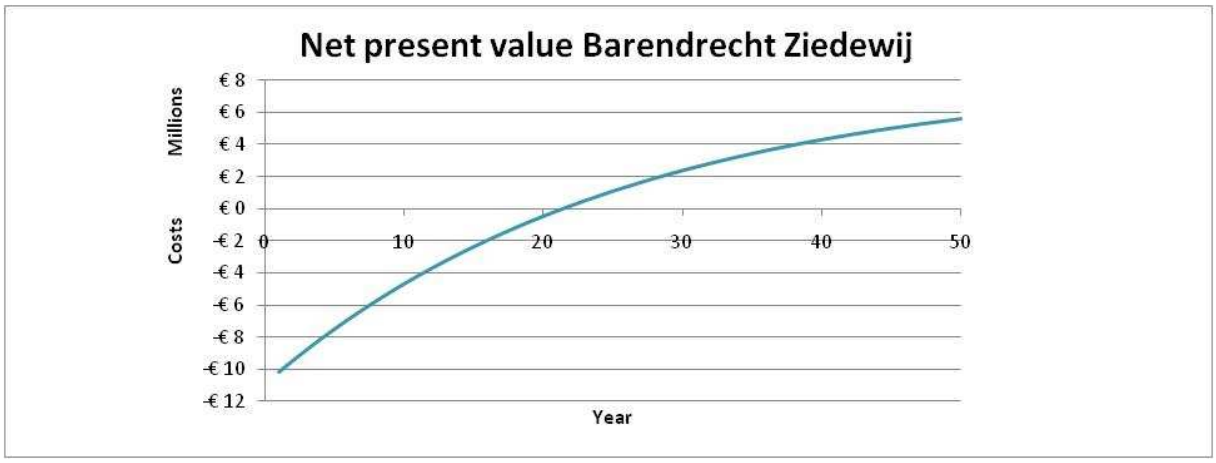

Figure 7-3. Net present value for the system in Barendrecht Ziedewij using a 4% discount rate.

7.5 Conclusion Barendrecht Ziedewij

Geothermal carbon dioxide can be a feasible option for the reservoir at Barendrecht Ziedewij. The total electricity production can go up to 27% of the domestic consumption in Barendrecht and can be maintained for 50 years. The total project will cost M€10.2, will be paid back in 22 years and has a net present value of M€5.6 when a discount rate of 4% is used. When the discount rate is increased to 10%, the NPV becomes negative. Therefore this could be a good addition to the current carbon storage project planned for the Barendrecht Ziedewij gas field if a low discount rate is used.

8 Conclusion

In this study the potential of a geothermal system using carbon dioxide as working fluid is investigated. The main result of this study is that it is possible to use carbon dioxide as working fluid in a geothermal system, based on technical feasibility.

A clear understanding of the behavior of carbon dioxide under increased pressure and temperature has been obtained. Hydrostatic pressure alone causes the carbon dioxide to pass the critical pressure below 800 meters. To reach the critical temperature even less depth is required than 800 m. The low critical point of carbon dioxide has many advantages. First of all, compared to water, supercritical carbon dioxide has a low viscosity resulting in less energy required to drive the flow of carbon dioxide through a geothermal reservoir. The second main advantage is that when carbon dioxide is extracted from the well it is still in supercritical form. The temperature difference in the reservoir results in a higher carbon dioxide density reduction compared to water. The density of carbon dioxide is lower in the recovery well resulting in less pressure difference in the recovery well compared to the injection well. Therefore, carbon dioxide is still supercritical once it reaches the surface. Supercritical carbon dioxide can then be led through a turbine to produce electricity without the need of a heat exchanger.

The system design is based on a transcritical power cycle. This cycle uses both supercritical and gaseous carbon dioxide to produce electricity. The only adaptation to this cycle is the adding of two wells. The carbon dioxide flows from the surface through an isenthalpic injection well to the reservoir. In the reservoir the liquid carbon dioxide gets heated up to supercritical state. After the reservoir the carbon dioxide flows back to the surface using an isenthalpic recovery well before it flows into a turbine. After the turbine the carbon dioxide is cooled to a liquid before the carbon dioxide re-enters the injection well.

The system is designed as a closed cycle steady state system where a mass flow of around 144 kilograms per second flow through the base system, which has been designed using average values for the Netherlands. The base system extracts 14 MW of heat from the soil and turns it into 0.48 MW electrical output resulting in a 3.3% overall efficiency. To maintain this output for at least 50 years with a runtime of 7750 hours per year, the wells need to be at least 1400 m apart from each other. However, increasing the geothermal gradient, depth, reservoir height, permeability, turbine efficiency or running hours result in a higher overall efficiency and electrical output. When all of the abovementioned variables are increased to reasonable amounts, the total electricity production goes up to 4.95 MW using an overall 16% efficiency and 950 m distance between the wells.

The environmental impact of a geothermal system using carbon dioxide is promising. Besides the fact that the implementation of such a system requires a gas field to be filled with carbon dioxide, the electricity produced with this system is carbon neutral. Compared to a natural gas fired power plants a single doublet can avoid between 11,000 and 565,000 ton of carbon dioxide over the lifetime of the project per doublet, depending on the properties of the reservoir.

The reservoir also has a big impact on the pay back period of the system. The depth of the reservoir has a linear relation with the costs of the wells, which equal 55% to 80% of the costs of the system. The turbine increases with increased temperature of the reservoir, while the amount of piping is nearly unaffected by the reservoir. However, the biggest impact on the pay back period and net present value of the system is the ratio between the profits of the system and the periodic costs. The base case of the Netherlands has slightly lower investment costs than the optimal case but also much lower profits resulting in pay back period starting at 38 years. The pay back period for the optimal system varies between 5 and 11 years, since it has higher investment costs but also much higher profits.

The system is applicable on both an empty reservoir as on a reservoir which is filled with carbon dioxide by a carbon storage project. However, the current carbon price of €13 per ton is too low to make carbon storage projects profitable. This causes the systems which are applied to an empty reservoir to have a higher pay back period than the systems which are applied to a carbon storage project. This can even cause the difference between a positive or negative net present value for the base case in the Netherlands.

Overall, the system as described in this research can make a good addition to an already existing carbon storage project. When the properties of the reservoir are good, the system can even become profitable combined with a carbon storage project. When this system is applied to the Barendrecht carbon storage project it results in a system with a pay back period of 22 years, when a discount rate of 4% is used, which avoids over 5,200 ton of carbon dioxide each year. The system can produce an amount of electricity which equals 27% of Barendrecht's domestic consumption.

Judged by the results of this study, it is advised to analyze the different aspects in more detail by further research. A geothermal system using carbon dioxide as working fluid can become an important player in the field of sustainable energy, as it shows a decent carbon neutral electricity production combined with pay back periods starting from 5 years. However, before the system can be implemented, several subjects have to be researched more thoroughly, which will be discussed in the next chapter.

9 Discussion and future work

While the system shows promising results, there is still much to do before the system can be applied to an empty gas field. This chapter will discuss the assumptions made in the research and the limitations of the system and will give some proposals for future work on this topic.

At first, the assumption is made that the system is a closed cycle steady state. A system involving an empty gas field is not a closed cycle, since the carbon dioxide in the gas field can flow to surrounding areas. As stated in (Pruess, 2006), where carbon dioxide and water are compared as heat transfer fluids, carbon dioxide losses are estimated at around 1 kg/s per MW of power generated. If there indeed are carbon dioxide losses during the system's lifetime, additional carbon dioxide must be added to the system to maintain the pressure and balance.

When the system is assumed a closed cycle there will be no contaminants entering the system. However, there will always be some degree of water present in a geological reservoir. As stated in this report, when carbon dioxide comes in contact with water a chemical reaction occurs forming carbonic acid. This carbonic acid can cause corrosion in the wells, which results in more friction and chances of leakage, and corrosion in the turbine, which can result in loss of efficiency, leakage or complete shutdown. The effects of contaminants should be researched thoroughly before the system is implemented.

While the system is designed as a steady state closed cycle, there is always a startup phase. It is not modeled in this research how carbon dioxide behaves in the system during the startup phase, as this was not the focus. However, it will take some time before the system reaches its balance described in chapter 4.

There are almost no calculations done on the condenser in the system, since it is assumed that enough surface water is available to cool the carbon dioxide to a liquid. However, the size of the condenser depends on the end temperature of the carbon dioxide and the flow in the system. The condenser should therefore be more thoroughly researched based on among others the size or the condenser, the type of condenser and the effects of summer and winter temperatures. It should also be analyzed that whether or not suitable energy can be captured from the cooling carbon dioxide, especially when the condenser is reached at the minimum pressure and high temperatures. Recovering this energy could enhance the system's efficiency by adding thermal energy as output.

The entire system is designed for a single doublet. An assumption on the usage of multiple wells is given in chapter 6, but not elaborated or backed up by mathematical relations. The flow patterns described in (U.S. Department of Energy, 2001) show several possible flow patterns for multiple wells. However, these patterns fall out of the scope of this research, but are important for future research. The placing of multiple wells can enhance the electrical output of the system, making it more attractive from an environmental and economical point of view.

What also should be research is the effect of differences in well diameters between the injection and recovery wells. In the current system design the injection and recovery well have the same diameter. For example, increasing the recovery well diameter while keeping the injection well diameter the same can result in a larger pressure difference over the turbine as the friction pressure increase in the recovery well is reduced. The effects of differences in well diameter should be combined with the effects of multiple wells, as both effects influence each other in a similar way.

The safety and financial analysis have been discussed in this study, but with very limited detail since this study is performed as a proof of concept based on technical feasibility. Therefore, more research is required on these field. The environmental impact assessment study from the Barendrecht carbon storage projects covers several of the safety issues which apply to a geothermal carbon dioxide project. However, many aspects still require more attention such as increased reservoir pressure, risk of a supercritical turbine or the recovery of carbon dioxide. The financial analysis must be done in more detail to get a better view of the costs of the system. For example, the current variation in pay back period, between 5 and more than 50 years, is much too broad. A more thorough and specific study on the costs and benefits of the system should be performed.

To summarize, there are still many subjects that require attention and can be used for further research. As shown in the conclusion, the system shows to be a promising addition to carbon dioxide storage projects and with an increased carbon credit price can become a promising system for sustainable power generation.

10 References

Air Liquide Safety Data Sheet: Carbon Dioxide [Report]. - Paris : Air Liquide, 2007.

Air Products Industry Co., Ltd Carbon Dioxide, technical data [Online] // Carbon Dioxide, technical data. - 2009. - February 12, 2010. - http://www.apithailand.com/carbon.html.

Appelo C.A.J. and Postma D. Geochemistry, groundwater and pollution [Book]. - Amsterdam : A.A. Balkema Publischers, 2005.

Atkins P. Physical Chemistry, 7th edition [Book]. - New York : Oxford University Press, 2002.

Bachu S. Sequestration of CO2 in geological media; Criteria and approach for site selection in response to climate change [Journal]. - [s.l.] : Energy conversion and management, 2000. - 9 : Vols. 41, pp. 953-970.

BBC Climate change [Online] // BBC Weather Centre. - July March, 2009. - 21. - http://www.bbc.co.uk/climate/evidence/carbon_dioxide.shtml.

Blok K. Introduction to energy analysis [Book]. - Amsterdam : Techne Press, 2007.

Broek M. van den, Faaij A. and Turkenburg W. Planning for an electricity sector with carbon capture and storage; Case of the Netherlands [Journal]. - Utrecht : International Journal of Greenhouse Gas Control, 2008. - Vols. 2, pp. 105-129.

Cayer A. [et al.] Analysis of a carbon dioxide transcritical power cycle using a low temperature source [Journal]. - Sherbrooke : Applied Energy, 2008. - Vols. 86, pp. 1055-1063.

CBS Bevolkingsteller [Online] // Centraal Bureau voor de Statistiek. - 2010. - March 21, 2010. - http://www.cbs.nl/nl-NL/menu/themas/bevolking/cijfers/extra/bevolkingsteller.htm.

Charlotte Pipe and Foundry company List price schedule XH-110 [Online] // Charlottepipe.com. - January 1, 2010. - March 19, 2010. - http://www.charlottepipe.com/Products/Assets/02A-Cast_Iron_List_Price/XH-110%20%281109%29.pdf.

Chemalogic Corporation Mollier Charts (Pressure-Enthalpy with constant Temperature, Density and Entropy Lines) [Online] // ChemicaLogic Corporation. - ChemicaLogic Corporation, May 29, 2009. - October 30, 2009. - http://www.chemicalogic.com/mollier/default.htm.

Chen Y. [et al.] A comparative study of the carbon dioxide transcritical power cycle compared with an organic rankine cycle with R123 as working fluid in waste heat recovery [Journal]. - Sigtuna : Applied Thermal Engineering, 2006. - Vols. 26, pp. 2142-2147.

Commissie bodemdaling Commissie bodemdaling door aardgaswinning Groningen [Online] // Commissie bodemdaling door aardgaswinning Groningen. - 2010. - March 19, 2010. - http://www.commissiebodemdaling.nl/.

Damen K., Faaij A. and Turkenburg W. Health, safety and environmental risks of underground CO2 storage; Overview of Mechanisms and current knowledge [Journal]. - Utrecht : Climate Change, 2006. - 1-3 : Vols. 74, pp. 289-318.

Daubert T.E. Chemical engineering thermodynamics [Book]. - Singapore : McGraw-Hill Educaction, 1986.

De Volkskrant Ambitieus klimaatakkoord G8 [Online]. - July 8, 2009. - August 10, 2009. - http://www.volkskrant.nl/buitenland/article1256037.ece/Ambitieus_klimaatakkoord_G8.

Dean J.A. Lange's Handbook of Chemistry [Book]. - Tennessee : McGraw-Hill, 1999. - Vol. 15.

Duan Z. and Sun R. An improved model calculating CO2 solubility in pure water and aqueous NaCL solutions from 273 to 533 K and from 0 to 2000 bar [Journal]. - California : Chemical geology : an international journal, 2002. - 3-4 : Vols. 193, pp. 257-271.

Duan Z., Moller N. and Weare J.H. An equation of state for the CH4-CO2-H2O system: 1. Pure systems from 0 too 1000 C and 0 to 8000 bar [Journal]. - California : Geochimica et Cosmochimica Acta, 1992. - Vols. 56, pp. 2605-2617.

Duan Z., Moller N. and Weare J.H. Molecular dynamics simulation of PVT properties of geological fluids and a general equation of state of nonpolar and weakly polar gases up to 2000 K and 20,000 bar [Journal]. - California : Geochimica et Cosmochimica Acta, 1992. - Vols. 56, pp. 3839-3845.

Earth2Tech Report: Carbon Price Needs to Be at $40 for Commercial CCS [Online] // Earth2Tech. - January 4, 2010. - March 12, 2010. - http://earth2tech.com/2010/01/04/report-carbon-price-needs-to-be-at-40-for-commercial-ccs/.

EMC Photosynthesis [Online] // Estrella Mountain Community College. - June 6, 2007. - November 11, 2009. - http://www.emc.maricopa.edu/faculty/farabee/BIOBK/BioBookPS.html.

Energieraad CO2-opslag Barendrecht: 'Ramp niet uit te sluiten' [Online] // Energieraad.nl. - December 16, 2008. - 19 March. - http://www.energieraad.nl/newsitem.asp?pageid=6222.

Essent Teruglevering van duurzame energie [Online] // Essent. - Essent, 2010. - March 11, 2010. - http://www.essent.nl/content/thuis/producten/stroom_en_gas/groene_stroom/teruglevering.jsp.

European Environment Commission Climate action [Online] // Climate action. - February 23, 2010. - March 12, 2010. - http://ec.europa.eu/environment/climat/climate_action.htm.

Fedyunina L.V. [et al.] Equations of state and thermodynamic properties of carbon dioxide and argo in the critical region [Journal]. - New York : Journal of engineering physics and thermophysics, 1992. - 1 : Vols. 61, pp. 902-908.

Feher A.G. The supercritical thermodynamic power cycle [Journal]. - [s.l.] : Energy conversion, 1968. - 2 : Vols. 8, pp. 85-90.

Gemeente Barendrecht Feiten en Cijfers [Online] // Gemeente Barendrecht. - Gemeente Barendrecht, July 1, 2007. - March 19, 2010. - http://www.barendrecht.nl/content.jsp?objectid=980&highlights=inwoneraantal.

Hamelink C. [et al.] Potential for CO2 sequestration and Enhanced Coalbed Methane production in the Netherlands [Report]. - Utrecht : NOVEM, 2001.

Hendriks C. and Graus W. Global carbon dioxide storage potential and costs [Report]. - Utrecht : Ecofys, 2004.

Hofmeister A.M.l Criss, R.E. Earth's heat flux revised and linked to chemistry [Journal]. - [s.l.] : Tectonophysics, 2004. - 1-4 : Vols. 409, pp. 199-203.

Hovorka S.D. [et al.] Quick-look assessments to identify optimal CO2 EOR storage sites [Journal]. - [s.l.] : Environmental geology, 2008. - 8 : Vols. 54, pp. 1695-1706.

IF Technology Examples of thermal conductivity and volume-related specific heat capacity of the underground a approx 20 C [Journal].

IF Technology NCM methode. - [s.l.] : IF Technology, 2009.

International Energy Agency CO2 emissions from fuel combustion [Report]. - Paris : International Energy Agency, 2009.

International Energy Agency Electricity/Heat in Netherlands in 2007 [Online] // Internation Energy Agency. - 2007. - February 12, 2010. - http://www.iea.org/stats/electricitydata.asp?COUNTRY_CODE=NL.

Katona T. [et al.] Lifetime-Management and Operational Lifetime Extension at Paks Nuclear Power Plant [Conference] // 17th International Conference on Structural Mechanics in Reactor Technology. - Prague : Nuclear Power plant ltd., 2003.

Koninklijk Nederlands Meteorologisch Instituut Jaaroverzichten - Archief [Online] // Klimatologie. - 2010. - February 26, 2010. - http://www.knmi.nl/kd/maand_en_seizoensoverzichten/.

Lokhorst A. and Wong Th,E. Goethermal energy; geology in the Netherlands [Journal]. - [s.l.] : Royal Netherlands Academy of Arts and Sciences, 2007. - Vols. pp. 341-346.

Marland Global, regional, and national CO2 emissions [Online] // PEW Center on global climate change. - 2007. - March 30, 2010. - http://www.pewclimate.org/docUploads/images/Historical-Emissions.preview.JPG.

MATTHEW DAVIS Australia Pty. Ltd. Carbon Steel Pipe (Welded & Seamless) [Online] // Matthewdavis.com. - 2008. - February 12, 2010. - http://www.matthewdavis.com.au/downloads/15-%20American%20Pipe%201-3-08.pdf.

Meer L.G.H. van der and Yavuz F. CO2 storage capacity calculations for the Dutch subsurface [Journal]. - [s.l.] : Energy procedia, 2009. - 1 : Vols. 1, pp. 2615-2622.

Milicentraal Groene stroom [Online] // Alles over energie en milieu in het dagelijks leven. - Milicentraal, 2007. - February 24, 2010. - http://www.milieucentraal.nl/pagina.aspx?onderwerp=Groene%20elektriciteit.

Ministerie van VROM Evaluatienota Klimaatbeleid 2005; Onderweg naar Kyoto [Report]. - Den Haag : Ministerie van VROM, 2006.

Ministerie van VROM Groen licht voor beperkte CO2-opslag Barendrecht [Online] // Ministerie van volkshuisvesting, Ruimtelijke Ordening en Milieubeheer. - November 18, 2009. - March 18, 2010. - http://www.vrom.nl/pagina.html?id=45208.

National Institute of Standards and Technology Thermophyscial properties of fluid systems [Online] // Thermophyscial properties of fluid systems. - 2008. - October 11, 2009. - http://webbook.nist.gov/chemistry/fluid/.

Nationmaster.com CO2 emissions per capita per country [Online] // Nationmaster.com. - 2003. - December 11, 2009. - http://www.nationmaster.com/graph/env_co2_emi_percap-environment-co2-emissions-per-capita.

Nieuwlaar E. and Sark W. van Readers and handouts from courses of Sustainable Development - Energy and Resources program [Book]. - Utrecht : Utrecht University, 2007-2009.

nu.nl Barendrecht krijgt co2 opslag [Online] // nu.nl. - November 18, 2009. - March 10, 2010. - http://www.nu.nl/binnenland/2125450/barendrecht-krijgt-co2-opslag.html.

Nye Thermodynamics Corporation Gas Turbine Prices by Output [Online] // Gas Turbine Prices by Output. - 2010. - February 12, 2010. - www.gas-turbines.com/trader/outprice.htm.

Paterson L. [et al.] Numerical modeling of pressure and temperature profiles including phase transitions in carbon dioxide wells [Conference] // 2008 SPE Annual technical conference and exhibition. - Denver : SPE international, 2008.

Pitzer K. [et al.] The Volumetric and Thermodynamic Properties of Fluids. II. Compressibility Factor, Vapor Pressure and Entropy of Vaporization [Journal]. - California : Journal of the American Chemical Society, 1955. - 13 : Vols. 77, pp. 3433-3440.

Point Carbon Point Carbon - Providing critical insights into energy and environmental markets [Online] // Point Carbon - Providing critical insights into energy and environmental markets. - 2010. - March 24, 2010. - www.pointcarbon.com.

Pruess K. Enhanced Geothermal Systems (EGS) using CO2 as working fluid; A novel approach for generating renewable energy with simltaneous sequestration of carbon [Journal]. - Berkeley : Geothermics, 2006. - Vols. 35, pp. 351-367.

Pruess K. Enhanced geothermal systems (EGS) using CO2 as working fluid; A novel approach for generating renewable energy with simultaneous sequestration of carbon [Journal] // Elsevier. - 2006.

Pruess K. Enhanced Geothermal Systems(EGS): Comparing water and CO2 as heat transmission fluids. - Berkeley : Lawrence Berkeley National Laboratory, 2008. - Vols. LBNL Paper LBNL-63627.

Pruess K. Numerical somulation of CO2 leakage from a geologic disposal reservoir, including transitions from super- to sub-critical conditions and boiling of liquid CO2 [Journal]. - Berkeley : SPE Journal, 2003. - 2 : Vols. 9, pp. 237-248.

Qouilin S. Experimental Study and Modeling of a Low Temperature Rankine Cycle for Small Scale Cogeneration [Report]. - Liège : Université de Liège, 2007.

Rainforest Action Network The biggest cause of climate change: Coal fired power plants [Report]. - San Francisco : Rainforest Action Network, 2008.

Recktenwald G.W. Matlab Programming [Book]. - Portland : Portland State University, 2001.

Saleh B. [et al.] Working fluids for low-temperature organic Rankine cycles [Journal]. - [s.l.] : Energy, 2005. - 7 : Vols. 32, pp. 1210-1221.

Sandri R and Wong J.K.S. An emperical equation of state for gaseous carbon dioxide covering a very wide range of temperature and pressure [Journal]. - [s.l.] : The Canadian Journal of Chemical Engineering, 1969. - 3 : Vols. 47, pp. 211-212.

Shell CO2 Storage B.V. MER "Ondergrondse opslag van CO2 in Barendrecht"; Rapport [Report]. - Den Haag : Sheel CO2 Storage B.V., 2009.

Sonová H. and Procházka J. Calculations of compressed carbon dioxide viscosities [Journal]. - Prague : Industrial & Chemical Engineering Research, 1993. - Vols. 32, pp. 3162-3169.

Sterner M. and Pitzer K. An equation of state for carbon dioxide valid from zero to extreme pressures [Journal]. - Bayreuth : Contribution Mineral Petrol, 1994. - Vols. 117, pp. 362-374.

The Engineering Toolbox Heat Loss Diagrams of Insulated Pipes [Online] // Resources, Tools and Basic Information for Engineering and Design of Technical Applications!. - 2005. - February 23, 2010. - http://www.engineeringtoolbox.com/heat-loss-insulated-pipes-d_1152.html.

The MathWorks MATLAB and Simulink for Technical Computing [Online] // Accelerating the pace of engineering and science. - 2010. - January 14, 2010. - http://www.mathworks.com.

TNO Bouw en Ondergrond Voorstel rapportage-vereisten geologische evaluatie aardwarmte project [Report]. - Utrecht : TNO, 2009.

TNO Renewed interest in geothermal energy [Online] // TNO, Kennis voor zaken. - TNO, 2007. - February 23, 2010. - http://www.tno.nl/content.cfm?context=markten&content=product&laag1=187&laag2=160&item_id=1047.

TNO, Ministerie van economische zaken Geothermie [Online] // NL Olie- en gasportaal. - 2010. - February 18, 2010. - http://www.nlog.nl/nl/home/geothermy.html.

Tsiklis D. Measurements and calculation of the molar volume and thermodynamic properties of carbon dioxide at high pressures and temperatures [Conference] // 1st International Conference Calorimetry and Thermodynamics. - Warsaw : [s.n.], 1969. - Vols. pp. 649-658.

U.S. Department of Energy Doublets and other allied well patterns [Book]. - California : U.S. Department of Energy, 2001.

U.S. Environmental protection agency Clean energy; Natural gas [Online] // EPA. - www.epa.gov.

Union Engineering Properties of carbon dioxide [Report]. - Koblenz : Kohlensäure-Industrie e.V., 2007.

United Nations Environment Programme Environmental due diligence process for geothermal energy systems [Report]. - Lund : Base, 2002.

Vukolovich M.P., Altunin V.V. and Timoshenko N.I. The themodynamic properties of carbon dioxide at temperatures of 0-1000 C and pressures up to 100 bar [Journal]. - [s.l.] : Atomnaya Énergiya, 1963. - 3 : Vols. 15, pp. 210-214.

Willemsen A. and Drijver B. Ondergrondse berging opgelost CO2; Haalbaarheidsstudie [Report]. - Arnhem : IF Technology, 2008.

Yamaguchi H [et al.] Solar energy powered Rankine cycle using supercritical CO2 [Journal]. - Kyoto : Applied Thermal Engineering, 2006. - Vols. 26, pp. 2345-2354.

Zhenhao Duan Research Group Thermodynamic properties of carbon dioxide [Online] // Thermodynamic properties of carbon dioxide. - Zhenhao Duan Research Group, 2006. - October 7, 2009. - http://www.geochem-model.org/models/co2/.

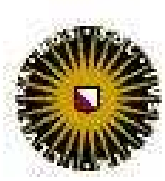

Universiteit Utrecht

Appendices

1 Appendix 1. Used equations

1.1 Nomenclature

Variable	Explanation	Unit	Value
(i)	Reference to simple fluid(1) or reference fluid(2)	-	-
a,b,c,d,e	Parameters in equations	-	-
B_i	Benefits in year i	€	-
C^i	Costs in year i	€	-
C_p	Specific heat capacity	J kg^{-1} K^{-1}	-
f	Fugacity	-	-
f	Friction constant	-	-
f_{ret}	Retardation factor	-	-
g	Gravitational constant	m s^{-2}	9.80665
h	Height	m	-
hr	Reservoir height	M	-
H	Enthalpy	kJ mol^{-1}	-
H_0	Enthalpy of ideal gas	kJ mol^{-1}	-
k	Heat conductivity	W K^{-1} m^{-3}	-
L	Length	m	-
M	Molar mass	kg mol^{-1}	44.01
NPV	Net present value	€	-
P	Pressure	bar	-
Pc	Critical pressure	bar	73.825
Pr	Reduced pressure	-	-
Psat	Starated pressure	Bar	-
Q	Heat source	W m^{-3}	-
R	Gas constant	J K^{-1} mol^{-1}	8.314472
Re	Reynolds number	-	-
Rn	Net to gross ratio	-	1
r_i	Distance from the middle of the pipe	m	
r_p	Radius of the pipe	m	-
r	Discount rate	%	-
S	Entropy	kJ mol^{-1}	-
S_0	Entropy of ideal gas	kJ mol^{-1}	-
T	Temperature	K	-
Tl	Lifetime	Yr	-
t	Time	s	-
tf	Running hours	hr/yr	-
Tc	Critical temperature	K	304.1
Tr	Reduced temperature	-	-
U	Internal energy	kJ mol^{-1}	-
V	Volume	m^3	-
v	Velocity	m s^{-1}	-
Vr	Reduced volume	-	-

Vr	Reservoir volume	m^3	-
Z	Compressibility factor	-	-
η	Dynamic viscosity	Pa s	-
η_0	Dynamic viscosity ideal gas	Pa s	-
ρ	Density	kg m^{-3}	-
ρ_r	Reduced density	-	-
ϕ	Fugacity coefficient	-	-
Φ	Fluid flow	m^3 s^{-1}	-
ϕ	Efficiency factor CO2 storage	-	0.02
ɯ	Acentric factor	-	0.22394
$ɯ^{(2)}$	Acentric factor reference	-	0.3978

1.2 Parameters

Equation of state from (Sterner, et al., 1994)

$$a_{ij} = \begin{bmatrix} 0 & 0 & 0.18261340E+7 & 0.79224365E+2 & 0 & 0 \\ 0 & 0 & 0 & 0.66560660E-4 & 0.57152798E-5 & 0.30222363E-9 \\ 0 & 0 & 0 & 0.59957845E-2 & 0.71669631E-4 & 0.62416103E-8 \\ 0 & 0 & -0.13270279E+1 & -0.15210731E+0 & 0.5364244E-3 & -0.71115142E-7 \\ 0 & 0 & 0.12456776E+0 & 0.49045367E+1 & 0.98220560E-2 & 0.55962121E-5 \\ 0 & 0 & 0 & 0.75522299E+0 & 0 & 0 \\ -0.39344644E+12 & 0.90918237E+8 & 0.42776716E+6 & -0.22347856E+2 & 0 & 0 \\ 0 & 0 & 0.40282608E+3 & 0.11971628E+3 & 0 & 0 \\ 0 & 0.22995650E+8 & -0.78971817E+5 & -0.63376456E+2 & 0 & 0 \\ 0 & 0 & 0.95029765E+5 & 0.18038071E+2 & 0 & 0 \end{bmatrix}$$

$$b_{ij} = a_{ij} \cdot \begin{bmatrix} T^{-4} \\ T^{-2} \\ T^{-1} \\ T^{0} \\ T^{1} \\ T^{2} \end{bmatrix}$$

Equation of state from (Duan, et al., 1992)

$$c_{ij} = \begin{bmatrix} 8.99288497E-2 \\ -4.94783127E-1 \\ 4.77922245E-2 \\ 1.03808883E-2 \\ -2.82516861E-2 \\ 9.49887563E-2 \\ 5.20600880E-4 \\ -2.93540971E-4 \\ -1.77265112E-3 \\ -2.51101973E-5 \\ 8.93353441E-5 \\ 7.88998563E-5 \\ -1.66727022E-2 \\ 1.39800000E+0 \\ 2.9600000E-2 \end{bmatrix}$$

Viscosity calculation from (Sonová, et al., 1993)

$$d_{ij} = \begin{bmatrix} 0.248566120 & 0.004894942 \\ -0.37330060 & 1.22753488 \\ 0.363854523 & -0.774229021 \\ -0.063907075 & 0.142507049 \end{bmatrix}$$

Enthalpy and entropy calculation from (Daubert, 1986)

$$e_{ij} = \begin{bmatrix} 0.1181193 & 0.2026579 \\ 0.265728 & 0.331511 \\ 0.154790 & 0.027655 \\ 0.030323 & 0.203488 \\ 0.236744 & 0.0313385 \\ 0.0186984 & 0.0503618 \\ 0.0 & 0.01901 \\ 0.042724 & 0.041577 \\ 0.155488E-4 & 0.48736E-4 \\ 0.623689E-4 & 0.0740336E-4 \\ 0.65392 & 1.226 \\ 0.060167 & 0.03754 \end{bmatrix}$$

1.3 General equations

1.3.1 Pressure increase in a pipe

(TNO Bouw en Ondergrond, 2009)

$$\Delta P = -\rho_{P,T} g \Delta h - \Delta h \frac{f \rho v^2}{2D}$$

$$f = \left[1.14 - 2log\left(\frac{\varepsilon}{D} + \frac{21.25}{Re^{0.9}}\right)\right]^{-2}$$

$$Re = \frac{Dv\rho}{\mu}$$

$$\Delta P = -\rho_{P,T} g \Delta h - \Delta h \frac{f \rho v^2}{2D}$$

1.3.2 Flow through a porous medium

(TNO Bouw en Ondergrond, 2009)

$$\Delta P = Q_v \frac{\mu}{2\pi k h_r Rn}\left(ln\left(\frac{L}{r}\right)\right)$$

$$Q_v = \frac{\Delta P}{\frac{\mu}{2\pi k h_r Rn}\left(ln\left(\frac{L}{r}\right)\right)}$$

1.3.3 Dynamic viscosity

(Sonová, et al., 1993)

$$\eta = \eta_0 \left(\sum_{i=1}^{4}\sum_{j=1}^{2} d_{ij} \frac{\rho_r^i}{T_r^{j-1}}\right)$$

1.3.4 Heat transfer

(Paterson, et al., 2008)

$$q_{w,well} = \frac{4\pi k_{i,g}(\Delta T_{av})}{ln\left(\frac{4\alpha_{t,g} t}{\sigma r_c^2}\right)}$$

$$\frac{dT}{dh} = \frac{q_{w,well}}{Q_m C_p}$$

1.3.5 Energy content of a reservoir

(U.S. Department of Energy, 2001)

$$E = Q_v t_f \Delta T C_{p,f}$$

1.3.6 Well spacing

(U.S. Department of Energy, 2001)

$$L = \sqrt{\frac{3T_l Q_v t_f}{\pi h_r f_{ret} \phi}} \qquad (Eq.\ 44)$$

1.3.7 Pressure distribution

$$\Delta P_{Injection} = \Delta P_{Reservoir} + \Delta P_{Recovery} + \Delta P_{Turbine}$$

$$f_{flow} = 100 \frac{\Delta P_{recovery}}{\Delta P_{injection}} = 100 \frac{\Delta P_{recovery,hydrostatic} + \Delta P_{recovery,flow}}{\Delta P_{injection,hydrostatic} + \Delta P_{injection,flow}}$$

1.3.8 Storage potential

(Meer, et al., 2009)

$$M_{CO2\ stored} = V r R_n E \phi \rho$$

1.3.9 Net present value

(Blok, 2007)

$$NPV = \sum_{i=0}^{n} \frac{B_i - C_i}{(1+r)^i}$$

1.4 CO2 properties equations

1.4.1 Equation of state for CO2

(Sterner, et al., 1994)

$$\frac{P}{RT} = \rho + b_1\rho - \rho^2\left(\frac{b_3 + 2b_4\rho + 3b_5\rho^2 + 4b_6\rho^3}{(b_2 + b_3\rho + b_4\rho^2 + b_4\rho^3 + b_5\rho^4)^2}\right) + b_7\rho^2 e^{-b_8\rho} + b_9\rho^2 e^{-b_{10}\rho}$$

(Duan, et al., 1992)

$$Z = \frac{PV}{RT} = \frac{P_r V_r}{T_r} = 1 + \frac{B}{V_r} + \frac{C}{V_r^2} + \frac{D}{V_r^4} + \frac{E}{V_r^5} + \frac{F}{V_r^2}\left(\beta + \frac{\gamma}{V_r^2}\right) e^{\left(-\frac{\gamma}{V_r^2}\right)}$$

$$B = c_1 + \frac{c_2}{T_r^2} + \frac{c_3}{T_r^3} \qquad D = c_7 + \frac{c_8}{T_r^2} + \frac{c_9}{T_r^3}$$

$$F = \frac{c_{13}}{T_r^3}$$

$$C = c_4 + \frac{c_5}{T_r^2} + \frac{c_6}{T_r^3} \qquad E = c_{10} + \frac{c_{11}}{T_r^2} + \frac{c_{12}}{T_r^3}$$

1.4.2 Compressibility factor

(Duan, et al., 1992)

$$Z = \frac{P}{\rho RT}$$

(Daubert, 1986)

$$z^{(i)} = \frac{P_r V_r}{T_r} = 1 + \frac{Bz}{V_r} + \frac{Cz}{V_r^2} + \frac{Dz}{V_r^5} + \frac{e_{i,8}}{T_r^3 V_r^2}\left(e_{i,11} + \frac{e_{i,12}}{V_r^2}\right) e^{-\frac{e_{i,12}}{V_r^2}}$$

1.4.3 Volume

(Duan, et al., 1992)

$$V = \frac{ZRT}{P}$$

1.4.4 Reduced volume, pressure and temperature

(Duan, et al., 1992)

$$V_r = \frac{VP_c}{RT_c}$$
$$P_r = \frac{P}{P_c}$$
$$T_r = \frac{T}{T_c}$$

1.4.5 Fugacity coefficient

(Daubert, 1986)

$$ln\,(\phi)^{(i)} = Z^{(i)} - 1 - ln\left(Z^{(i)}\right) + \frac{Bz}{V_r} + \frac{Cz}{2V_r^2} + \frac{Dz}{5V_r^5} + \frac{e_{i,8}}{2T_r^3 e_{i,12}}\left(e_{i,11} + 1 - \left(e_{i,11} + 1 + \frac{e_{i,12}}{V_r^2}\right)\right)e^{-\frac{e_{i,12}}{V_r^2}}$$
$$Bz = e_{i,1} - \frac{e_{i,2}}{T_r} - \frac{e_{i,3}}{T_r^3} - \frac{e_{i,4}}{T_r^3}$$
$$Cz = e_{i,5} - \frac{e_{i,6}}{T_r} + \frac{e_{i,7}}{T_r^3}$$
$$Dz = e_{i,9} + \frac{e_{i,10}}{T_r}$$

1.4.6 Acentric factor

(Pitzer, et al., 1955)

$$\omega = -log_{10}\left(\frac{P_{sat}}{P_c}\right) - 1 \quad at \;\; T_r{=}0.7$$

1.5 Thermodynamic equations

1.5.1 Specific enthalpy

(Daubert, 1986)

$$H = H_0 - \frac{RT_c}{M}\left(\frac{\overline{H}^0 - \overline{H}}{RT_c}\right)$$

$$\left(\frac{\overline{H}^0 - \overline{H}}{RT_c}\right) = \left(\frac{\overline{H}^0 - \overline{H}}{RT_{c,0}}\right)^{(1)} + \frac{\omega}{\omega^{(2)}}\left(\left(\frac{\overline{H}^0 - \overline{H}}{RT_{c,h}}\right)^{(2)} - \left(\frac{\overline{H}^0 - \overline{H}}{RT_{c,0}}\right)^{(1)}\right)$$

$$\left(\frac{\overline{H}^0 - \overline{H}}{RT_{c,0}}\right)^{(i)} = -T_r\left(z^{(i)} - 1 - \frac{e_{i,2} + \frac{2e_{i,3}}{T_r} + \frac{3e_{i,4}}{T_r^2}}{T_r V_r} - \frac{e_{i,6} + \frac{3e_{,73}}{T_r^2}}{2T_r V_r^2} - \frac{e_{i,10}}{5T_r V_r^5} + \frac{3e_{i,8}}{2T_r^3 e_{i,12}}\left(e_{i,11} + 1 - \left(e_{i,11} + 1 + \frac{e_{i,12}}{V_r^2}\right)e^{\left(-\frac{e_{i,12}}{V_r^2}\right)}\right)\right)$$

$$z^{(i)} = \frac{P_r V_r}{T_r} = 1 + \frac{Bz}{V_r} + \frac{Cz}{V_r^2} + \frac{Dz}{V_r^5} + \frac{e_{i,8}}{T_r^3 V_r^2}\left(e_{i,11} + \frac{e_{i,12}}{V_r^2}\right)e^{-\frac{e_{i,12}}{V_r^2}}$$

$$Bz = e_{i,1} + \frac{e_{i,2}}{T_r} + \frac{e_{i,3}}{T_r^3} + \frac{e_{i,4}}{T_r^3}$$

$$Cz = e_{i,5} + \frac{e_{i,6}}{T_r} + \frac{e_{i,7}}{T_r^3}$$

$$Dz = e_{i,9} + \frac{e_{i,10}}{T_r}$$

$$H_0 = C_p\frac{(T - 273)}{M}$$

1.5.2 Enthalpy ideal gas

(Daubert, 1986)

$$h_0 = A + BT + CT^2 + DT^3 + ET^4 + FT^5$$

1.5.3 Specific entropy

(Daubert, 1986)

$$S = S_0 - \frac{R}{M}\left(\frac{\overline{S}^0 - \overline{S}}{R}\right)$$

$$\frac{\overline{S}^0 - \overline{S}}{R} = \frac{\overline{H}^0 - \overline{H}}{RT_c} + ln\left(\frac{f}{P}\right) + ln(P)$$

$$S_0 = \frac{R\, ln\left(\frac{V}{\rho_{P=1,T=273}}\right)}{M}$$

1.5.4 Entropy ideal gas

(Daubert, 1986)

$$S_0 = S_{0,298K} + \int_{298}^{T} \frac{C_{P0}dT}{T}$$

1.5.5 Internal energy

(Atkins, 2002)

$$U = H - PV$$

1.5.6 Heat capacity ideal gas

(Daubert, 1986)

$$Cp_0 = B + 2CT + 3DT^2 + 4ET^4 + 5FT^4$$

1.6 Thermodynamic representation

(Cayer, et al., 2008)(Nieuwlaar, et al., 2007-2009)(Feher, 1968)

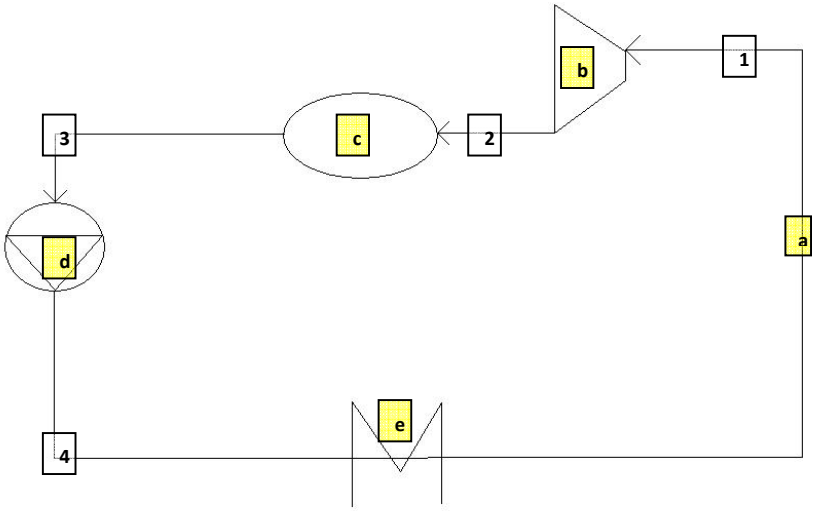

a) Recovery well

The recovery well is the location where the CO2 is recovered from the reservoir. The well is located after the heat source and before the turbine. No efficiency or energy calculations required.

b) TPC Turbine

The turbine is the place where the electricity is generated.

$$\eta_t = \frac{h_1 - h_2}{h_1 - h_{2,is}}$$

$$\dot{W}_t = \dot{m}_{CO_2}(h_1 - h_2)$$

c) Condenser

In the condenser, the gaseous CO2 is cooled down until it becomes a liquid. The temperature of the system is arranged here.

$$\dot{Q}_{out} = \dot{m}_{CO_2}(h_2 - h_3)$$

d) Pump/injection well

The pump/injection well is the location where the CO2 is pumped in the geothermal well. This is also the place where the pressure for the system is arranged.

$$\eta_p = \frac{h_3 - h_4}{h_3 - h_{4,is}}$$

$$\dot{W}_p = \dot{m}_{CO_2}(h_4 - h_3)$$

e) Heat source

The heat source is the geothermal well, where the heat is extracted from the earth.

$$\dot{Q}_{in} = \dot{m}_{CO_2}(h_1 - h_4)$$

The overall system is represented by the following equations:

$$w = \frac{\dot{W}_t - \dot{W}_p}{\dot{m}_{CO_2}}$$

$$w = \frac{\dot{m}_{CO_2}(h_1 - h_2) - \dot{m}_{CO_2}(h_3 - h_4)}{\dot{m}_{CO_2}} = (h_1 - h_2) - (h_4 - h_3)$$

$$\eta = \frac{\dot{W}_t - \dot{W}_p}{\dot{Q}_{in}}$$

2 Appendix 2. Matlab codes

The matlab program is designed as multiple .m files:

1. GeothermalCO2.m: The first overall matlab file creates the matrices and plots of the final system. This .m file combines the 4 different steps in the system and merges them.
2. rhocalc6: This .m file calculates the following properties of CO2: density, volume, compressibility factor and fugacity.
3. pitzer3: Using the method from Pitzer, this .m file calculated the thermodynamic properties of CO2 as enthalpy, internal energy and entropy.
4. reservoirenergycontent: This .m file uses the equations from Twidell and Weir to calculate the energy content of the reservoir.
5. GeoConstants: GeoConstans is a .m file consisting of all constants of the system.

2.1 GeothermalCO2.m

```
% Final program calculating the properties of CO2 in the
geothermal system
%
%
% Author: Dave Janse
% Last modification date: 01-04-2010


% ~~~~ PROGRAM: ~~~~
%% clearing all content
clear

% %% temp stuff to make this work
%
% Wellspacingavg=1000;
% scounter=0;


%% Loading tables if required

% load TABLEP.txt
% fprintf('loaded TABLET.txt\n');
% load TABLET.txt
% fprintf('loaded TABLECp.txt\n');
% load TABLECp.txt
% fprintf('loaded TABLErho.txt\n');
% load TABLErho.txt
% fprintf('loaded TABLEH.txt\n');
% load TABLEH.txt
% fprintf('loaded TABLES.txt\n');
% load TABLES.txt
% fprintf('loaded TABLEU.txt\n');
% load TABLEU.txt
% fprintf('loaded TABLEV.txt\n');
% load TABLEV.txt
% fprintf('loaded TABLEPhi.txt\n');
% load TABLEPhi.txt
% fprintf('loaded TABLEZ.txt\n');
% load TABLEZ.txt
% PTABLE=TABLEP(1,:);
% PTABLE=transpose(PTABLE);
% % 30:10:300;
% TTABLE=TABLET(:,1);
% 250:10:500;

%% entering initial and boundary conditions

%General
cycli=3; %the amount of full cycles
counter=1; %counter to show percentage of calculation, reset at
use
Tge=30; %temperature gradient in (K/km)
hs=100; %calculation steps (meter/step)
Ti=296; %temperature after condensor (K)
h=2000; %well heighth (m)
Pi=73; %pressure after condensor (bar)

% Wells
Rt=0.2; %diameter of the well (m)
```

```
% Turbine
effi=0.80; %turbine efficiency
Pvalve=115; %pressure at valve before turbine (bar)
Runfact=7750; %runtime in (hr/yr)
Lifetime=50; %lifetime of the system (yr)

% Reservoir
resheight=100; %height of the reservoir (m)
poro=0.05; %porosity of the reservoir
CProck=2.2; %heat capacity of Rock (kJ/kg/K)
L=1500; %Initial Wellspacing
Wellspacing=round(sqrt(L^2/2)/hs)*hs; %initial Wellspacing
perm=1e-13; %permeabilitiy
RatioBN=1; %Gross-net ratio
rhoROCK=2800; %density of the rock

%% Setting initial values
T=Ti;
P=Pi;
GeoConstants
CO2properties
TIMEfac=1;
resultSTEP=0;
ForVAR=1;
ForCYC=10;
Pfact=0;
PfactCOUNT=0;
ResCORRECTION=0;
cycleXcounter=0;
Perror=0;


for Rx=1:3 %this can be used if a the effect of a variable
requires checking
switch Rx
    case 1
        perm=0.5*10^-12
    case 2
        perm=10^-13
    case 3
        perm=5*10^-14
end

flowFACTOR=55; %Reser flowfactor
for cycleX=1:3; %Define the number of cycles
P=Pi; %set initial pressure
PstartINJ=P;
T=296; %set initial temperature
CO2properties %Calculate CO2 properties

if abs(Perror)>0.05 %Change flowfactor is required
    if Perror>0
        flowFACTOR=round(flowFACTOR*(90+Perror)/90);
    elseif Perror<0
        flowFACTOR=round(flowFACTOR*(50+Perror)/50);
    end
end
if flowFACTOR<35 %Minimum flowfactor
    flowFACTOR=35;
end
flowmaxcalc %Calculate the maximum flow
flowrate=Qm/rho2;
A=pi*Rt; %surface of well cross-cut (m2)
deltaP=(flowrate*Muxx/(2*pi*perm*resheight*RatioBN)*log(Wellspa
cing/(Rt/2)))/10^5; %Pressure difference in the reservoir

%% injection well
P=Pi;
PstartINJ=P;
T=296;
CO2properties
HxINJ=HCmol;
SstartINJ=Smol;
HstartINJ=HCmol;
RstartINJ=rho2;
TstartINJ=T;
% calculate the properties of CO2 in the injection well
for ForINJ=1:hs:h
    CO2properties
    flowrateINJ=Qm/rho2*3600;
    v=4*flowrateINJ/(pi*Rt^2)/3600;
    P=P+rho2*9.81*hs*10^-5+0.015*rho2*v^2/(2*Rt)*10^-5*hs;
%Pressure increase
    CO2properties
    TxINJ=0; %Isenthalpic temperature change
    while TxINJ==0
        T=T+0.1;
        CO2properties
        if HCmol>HxINJ;
            TxINJ=1;
        end
    end
    resultSTEP=resultSTEP+1;
    variableWRITE
end
PendINJ=P
TendINJ=T;
```

```
HendINJ=HCmol;
RendINJ=rho2;
SendINJ=Smol;
% fprintf('Finished: injection well\n')

%% reservoir
wellspacing %Calculate the required well spacing
PendRES=PendINJ-deltaP
PstartREC=PendRES;
P=PendRES;
T=283.5+Tge*h/1000+4; %Set reservoir temperature
TendRES=T;
CO2properties
HendRES=HCmol;
% fprintf('Finished: reservoir\n')

%% recovery well
P=PstartREC;
CO2properties
SstartREC=Smol;
HstartREC=HCmol;
TstartREC=T;
RstartREC=rho2;
HxREC=HCmol;
% calculate the properties of CO2 in the injection well
for ForREC=1:hs:h
    CO2properties
    flowrateREC=Qm/rho2*3600;
    v=4*flowrateREC/(pi*Rt^2)/3600;
    P=P-rho2*9.81*hs*10^-5-0.015*rho2*v^2/(2*Rt)*10^-
5*hs;%Pressure decrease
    CO2properties
    TxREC=0;%Isenthalpic temperature change
    while TxREC==0
        T=T-0.1;
        CO2properties
        if HCmol<HxREC;
            TxREC=1;
        end
    end
    resultSTEP=resultSTEP+1;
    variableWRITE
end
PendREC=P;
TendREC=T;
SendREC=Smol;
HendREC=HCmol;
RendREC=rho2;
H1=HCmol;
S1=Smol;
% fprintf('Finished: recovery well\n')

%% turbine
P=PendREC;
T=TendREC;
CO2properties;
Sx=Smol;
Hx=HCmol;
cnt=0;
for Cyc=1:2 %number of turbine steps
xx=0;

cntx=0;
while xx==0 %isentropic expansion


    xxxx=0;
    if Cyc>1
    while xxxx==0 %Apply turbine efficiency
        T=T+0.001;
        CO2properties
        if HCmol>H1-(H1-H2)*effi
            xxxx=1;
            T=T-0.001;
        end
    end
    end


    P=P-0.2;
    fprintf('P= %g',P)
    fprintf('; T= %g',T)
    fprintf('; H= %g',HCmol)
    fprintf('; S= %g\n',Smol)
    cnt=cnt+1;
    Ans(cnt,1)=P;
    Ans(cnt,2)=T;
    Ans(cnt,3)=HCmol;
    Ans(cnt,4)=Smol;
    xxx=0;
    Hx(cnt,1)=HCmol;
    while xxx==0 %calculate isentropic temperature
        T=T-0.01;
        CO2properties;
        if Smol<Sx
            xxx=1;
            T=T+0.01;
            CO2properties;
```

```
        end
    end
    Hx(cnt,2)=HCmol;

    if Hx(cnt,2)>Hx(cnt,1);
        cntx=cntx+1;
        if cntx==6;
            xx=1;
            P=Ans(cnt-5,1);
            T=Ans(cnt-5,2);
        end
    else
        cntx=0;
    end



    %end conditions for the turbine
    if abs(Hx(cnt,2)/Hx(cnt,1))>1.3;
        xx=1;
    end
    if abs(Hx(cnt,2)/Hx(cnt,1))<0.7;
        xx=1;
    end
    if Hx(cnt,2)>Hx(cnt,1)+0.25;
        xx=1;
    end
    if P<64;
        xx=1;
    end
    if T<Tc
        if P>Pc
            xx=1;
        end
    end

end
P=P+0.2;
CO2properties;
H2=min(Hx(:,2));
end



PendTUR=P;
SendTUR=Smol;
HendTUR=HCmol;
TendTUR=T;
RendTUR=rho2;
```

```
Pi=P;
T=293;
% fprintf('Finished: turbine\n')
CO2properties
S2=Smol;

Hverschil=(H1-H2)*effi;
%% condensor
% T=T-5;
% fprintf('Finished: condensor\n')
T=296;
Ti=T;
if P<64; Pi=64;
end


%% finishing
Perror=PendTUR-PstartINJ;
fprintf('Pressure difference between turbine and injection well
inlet: %g\n', Perror)
MWth=Qm*(HendRES-HendINJ)/0.04001/1000;
end

%writing the results
Result(Rx,1)=Perror;
Result(Rx,2)=PendINJ;
Result(Rx,3)=PendRES;
Result(Rx,4)=PendREC;
Result(Rx,5)=Qv;
Result(Rx,6)=Qm;
Result(Rx,7)=Rt;
Result(Rx,8)=TendINJ;
Result(Rx,9)=TendREC;
Result(Rx,10)=S1-S2;
Result(Rx,11)=Wellspacing;
Result(Rx,12)=Qm*Hverschil/0.04401/1000*7750/8760/MWth;
Result(Rx,13)=Qm*Hverschil/0.04401/1000;
Result(Rx,14)=deltaP;
Result(Rx,15)=Hverschil;
Result(Rx,16)=Hverschil/(HendRES-HendINJ);
end
```

2.2 rhocalc6.m

```
% ~~~~ Geothermal CO2 system ~~~~
% This program is a part of the geothermal CO2 system
```

```
% calculating the properties of CO2 with specific pressure
% and temperature using the equation of state from Duan et al.
%
% Author: Dave Janse
% Last modification date: 01-04-2010



%loading constants
GeoConstants


fff=0; %resetting while loop condition
Vr=1; %setting initial reduced volume
while fff==0
    if Vr>10^4; % boundary condition to make sure Vr doesnt get
too high
        Vr=1;
    end
    if Vr<-10^4; % boundary condition to make sure Vr doesnt
get too low
        Vr=-1;
    end
    %calculating reduced pressure using set or previously
calcated reduced
    %volume

Pr2=(1+B/Vr+C/Vr^2+D/Vr^4+E/Vr^5+F/Vr^2*(b(14)+(b(15)/Vr^2))*ex
p(-b(15)/Vr^2))/Vr*Tr;

Zd=(1+B/Vr+C/Vr^2+D/Vr^4+E/Vr^5+F/Vr^2*(b(14)+(b(15)/Vr^2))*exp
(-b(15)/Vr^2));

    %comparing calculated and defined reduced pressure
    CalcVr=round(Pr*1000)/round(abs(Pr2)*1000);
    %changing of reduced volume based on above comparison
    if CalcVr<1
        Vr=Vr*1.001;
    elseif CalcVr>1;
        Vr=Vr*0.999;
    else
        fff=1; %ending the while loop when correct reduced
volume is found
    end
end


Vc=R/100*Tc/Pc; %critical volume calculation
Vmol=Vr*Vc/1000; %molar volume calculation

rho2=1/Vmol*0.04401; %density calculation (kg/m3)
rho=rho2/0.044001/10^6; %density calculation (mol/dm3)

pitzer3 %Calculating the enthalpy with the current properties
HCmolx=HCmol;
if HCmol<1 %comparing whether the enthalpy is above or below
the critical point
    rho2=501;
end

if rho2>500; %comparing whether or not the density is high
enough for change in EOS
% Calculate rho using Sterner for liquid
rho3=1; %initial value for the iteraion
P1=(rho3+a(1).*rho3.^2-
rho3.^2.*(a(3)+2.*a(4).*rho3+3.*a(5).*rho3.^2+4.*a(6).*rho3.^3)
./(a(2)+a(3).*rho3+a(4).*rho3.^2+a(5).*rho3.^3+a(6).*rho3.^4).^
2+a(7).*rho3.^2.*exp(-a(8).*rho3)+a(9).*rho3.^2.*exp(-
a(10).*rho3)).*R.*T.*10;
f=0; %reset while loop value
while f==0;
        if round(P1.*100)<round(P.*100);
            % If pressure1 is too low, density should be higher
        rho3=rho3.*1.001;
        P1=(rho3+a(1).*rho3.^2-
rho3.^2.*(a(3)+2.*a(4).*rho3+3.*a(5).*rho3.^2+4.*a(6).*rho3.^3)
./(a(2)+a(3).*rho3+a(4).*rho3.^2+a(5).*rho3.^3+a(6).*rho3.^4).^
2+a(7).*rho3.^2.*exp(-a(8).*rho3)+a(9).*rho3.^2.*exp(-
a(10).*rho3)).*R.*T.*10;
        else
        if round(P1*100)>round(P*100);
            % If pressure1 is too high, density should be lower
            rho3=rho3.*0.9999;
            P1=(rho3+a(1).*rho3.^2-
rho3.^2.*(a(3)+2.*a(4).*rho3+3.*a(5).*rho3.^2+4.*a(6).*rho3.^3)
./(a(2)+a(3).*rho3+a(4).*rho3.^2+a(5).*rho3.^3+a(6).*rho3.^4).^
2+a(7).*rho3.^2.*exp(-a(8).*rho3)+a(9).*rho3.^2.*exp(-
a(10).*rho3)).*R.*T.*10;
        else
            f=1; % If pressure is good, end the while loop
        end
    end
end
 rho=rho3; %enter the value calculated with Sterner EOS as
density


% displaying rho, density
rho2=rho*0.044001*10^6;
```

```
end %end if for gas/liquid

%calculating specific enthalpy, entropy, fugacity and
compressibility
%factor
pitzer3

% calculating V, volume
V=Z*R*T/P*10; %cc/mol
% Vr=V*Pc/R/Tc/10;
V=V/1000000;

% Internal energy
Umol=HCmol-P*V*100;


%defining the physical state of the CO2
if P<Pc
    if HCmol>-7
        State=('Superheated gas');
    else
        State=('Subcooled liquid');
    end
elseif P>Pc
    if T>Tc
        State=('Supercritical');
    else
        State=('Subcooled liquid');
    end
end
```

2.3 pitzer3.m

```
% ~~~~ Geothermal CO2 system ~~~~
% This program is a part of the geothermal CO2 system
% calculating the specific enthalpy of a real gas by
% using Pitzer's method
%
% Author: Dave Janse
% Last modification date: 01-04-2010



%% Calculation of Vr for simple fluid
Vr=1000; % Initial value for reduced volume
%Caculate reduced pressure
Prx=(1+(aa(1)-aa(2)/Tr-aa(3)/Tr^2-aa(4)/Tr^3)/Vr+(aa(5)-
aa(6)/Tr+aa(7)/Tr^3)/Vr^2+(aa(9)+aa(10)/Tr)/Vr^5+aa(8)/(Tr^3*Vr
^2)*(aa(11)+aa(12)/Vr^2)*exp(-aa(12)/Vr^2))*Tr/Vr;
f=0; % Reset while loop value
while f==0
    Px=round(Pr*100)/round(abs(Prx)*100); %comparison between
actual reduced pressure and calculated reduced pressure
    if Prx<0
        Vr=Vr*0.9; %If calculated reduced pressure is too low,
Vr is reduced
            Prx=(1+(aa(1)-aa(2)/Tr-aa(3)/Tr^2-
aa(4)/Tr^3)/Vr+(aa(5)-
aa(6)/Tr+aa(7)/Tr^3)/Vr^2+(aa(9)+aa(10)/Tr)/Vr^5+aa(8)/(Tr^3*Vr
^2)*(aa(11)+aa(12)/Vr^2)*exp(-aa(12)/Vr^2))*Tr/Vr;
    elseif Px>5
            Vr=Vr*0.9;
            Prx=(1+(aa(1)-aa(2)/Tr-aa(3)/Tr^2-
aa(4)/Tr^3)/Vr+(aa(5)-
aa(6)/Tr+aa(7)/Tr^3)/Vr^2+(aa(9)+aa(10)/Tr)/Vr^5+aa(8)/(Tr^3*Vr
^2)*(aa(11)+aa(12)/Vr^2)*exp(-aa(12)/Vr^2))*Tr/Vr;
     elseif Px>2
            Vr=Vr*0.99;
            Prx=(1+(aa(1)-aa(2)/Tr-aa(3)/Tr^2-
aa(4)/Tr^3)/Vr+(aa(5)-
aa(6)/Tr+aa(7)/Tr^3)/Vr^2+(aa(9)+aa(10)/Tr)/Vr^5+aa(8)/(Tr^3*Vr
^2)*(aa(11)+aa(12)/Vr^2)*exp(-aa(12)/Vr^2))*Tr/Vr;
    elseif Px>1
            Vr=Vr*0.999;
            Prx=(1+(aa(1)-aa(2)/Tr-aa(3)/Tr^2-
aa(4)/Tr^3)/Vr+(aa(5)-
aa(6)/Tr+aa(7)/Tr^3)/Vr^2+(aa(9)+aa(10)/Tr)/Vr^5+aa(8)/(Tr^3*Vr
^2)*(aa(11)+aa(12)/Vr^2)*exp(-aa(12)/Vr^2))*Tr/Vr;
     elseif Px==1 %If calculated reduced pressure is good, loop
is ended
            f=1;
     elseif Px<1
            Vr=Vr*1.001; %If calculated reduced pressure is too
high, Vr is increased
            Prx=(1+(aa(1)-aa(2)/Tr-aa(3)/Tr^2-
aa(4)/Tr^3)/Vr+(aa(5)-
aa(6)/Tr+aa(7)/Tr^3)/Vr^2+(aa(9)+aa(10)/Tr)/Vr^5+aa(8)/(Tr^3*Vr
^2)*(aa(11)+aa(12)/Vr^2)*exp(-aa(12)/Vr^2))*Tr/Vr;
     elseif Px>0.01;
            Vr=Vr*1.01;
            Prx=(1+(aa(1)-aa(2)/Tr-aa(3)/Tr^2-
aa(4)/Tr^3)/Vr+(aa(5)-
aa(6)/Tr+aa(7)/Tr^3)/Vr^2+(aa(9)+aa(10)/Tr)/Vr^5+aa(8)/(Tr^3*Vr
^2)*(aa(11)+aa(12)/Vr^2)*exp(-aa(12)/Vr^2))*Tr/Vr;
     else
```

```
            Vr=Vr*1.1;
            Prx=(1+(aa(1)-aa(2)/Tr-aa(3)/Tr^2-
aa(4)/Tr^3)/Vr+(aa(5)-
aa(6)/Tr+aa(7)/Tr^3)/Vr^2+(aa(9)+aa(10)/Tr)/Vr^5+aa(8)/(Tr^3*Vr
^2)*(aa(11)+aa(12)/Vr^2)*exp(-aa(12)/Vr^2))*Tr/Vr;
     end
end
%calculate the compressibility factor for the simple fluid
(CO2)
Z0=Pr*Vr/Tr;
Z0=(1+(aa(1)-aa(2)/Tr-aa(3)/Tr^2-aa(4)/Tr^3)/Vr+(aa(5)-
aa(6)/Tr+aa(7)/Tr^3)/Vr^2+(aa(9)+aa(10)/Tr)/Vr^5+aa(8)/(Tr^3*Vr
^2)*(aa(11)+aa(12)/Vr^2)*exp(-aa(12)/Vr^2));
%Calculate the simple fluid part for the enthalpy calculation
Hx0=-Tr*(Z0-1-(aa(2)+(2*aa(3)/Tr)+(3*aa(4)/Tr^2))/(Tr*Vr)-
(aa(6)-
3*aa(7)/Tr)/(2*Tr*Vr^2)+aa(10)/(5*Tr*Vr^5)+3*aa(8)/(2*Tr^3*aa(1
2))*(aa(11)+1-(aa(11)+1+aa(12)/Vr^2)*exp(-aa(12)/Vr^2)));
Vr1=Vr; %save the calculated reduced volume

%% Calculation of VrR for heavy reference fluid
VrR=Vr1; %Continue with the iterations
PrRx=(1+(bb(1)-bb(2)/TrR-bb(3)/TrR^2-bb(4)/TrR^3)/VrR+(bb(5)-
bb(6)/TrR+bb(7)/TrR^3)/VrR^2+(bb(9)+bb(10)/TrR)/VrR^5+bb(8)/(Tr
R^3*VrR^2)*(bb(11)+bb(12)/VrR^2)*exp(-bb(12)/VrR^2))*TrR/VrR;
count=1;
while f==1
if VrR>999999; %Boundary for maximum reduced volume
    VrR=1;
end
Px=round(PrR*100)-round(PrRx*100);
    if PrRx<0
        VrR=VrR*0.9;%If calculated reduced pressure is too low,
Vr is reduced
            PrRx=(1+(bb(1)-bb(2)/TrR-bb(3)/TrR^2-
bb(4)/TrR^3)/VrR+(bb(5)-
bb(6)/TrR+bb(7)/TrR^3)/VrR^2+(bb(9)+bb(10)/TrR)/VrR^5+bb(8)/(Tr
R^3*VrR^2)*(bb(11)+bb(12)/VrR^2)*exp(-bb(12)/VrR^2))*TrR/VrR;
    elseif Px>5
            VrR=VrR*0.9;
            PrRx=(1+(bb(1)-bb(2)/TrR-bb(3)/TrR^2-
bb(4)/TrR^3)/VrR+(bb(5)-
bb(6)/TrR+bb(7)/TrR^3)/VrR^2+(bb(9)+bb(10)/TrR)/VrR^5+bb(8)/(Tr
R^3*VrR^2)*(bb(11)+bb(12)/VrR^2)*exp(-bb(12)/VrR^2))*TrR/VrR;
     elseif Px>2
            VrR=VrR*0.99;
            PrRx=(1+(bb(1)-bb(2)/TrR-bb(3)/TrR^2-
bb(4)/TrR^3)/VrR+(bb(5)-
bb(6)/TrR+bb(7)/TrR^3)/VrR^2+(bb(9)+bb(10)/TrR)/VrR^5+bb(8)/(Tr
R^3*VrR^2)*(bb(11)+bb(12)/VrR^2)*exp(-bb(12)/VrR^2))*TrR/VrR;
    elseif Px>1
            VrR=VrR*0.999;
            PrRx=(1+(bb(1)-bb(2)/TrR-bb(3)/TrR^2-
bb(4)/TrR^3)/VrR+(bb(5)-
bb(6)/TrR+bb(7)/TrR^3)/VrR^2+(bb(9)+bb(10)/TrR)/VrR^5+bb(8)/(Tr
R^3*VrR^2)*(bb(11)+bb(12)/VrR^2)*exp(-bb(12)/VrR^2))*TrR/VrR;
     elseif Px==1 %If calculated reduced pressure is good, loop
is ended
            f=2;
     elseif Px<1
            VrR=VrR*1.001; %If calculated reduced pressure is
too high, Vr is increased
            PrRx=(1+(bb(1)-bb(2)/TrR-bb(3)/TrR^2-
bb(4)/TrR^3)/VrR+(bb(5)-
bb(6)/TrR+bb(7)/TrR^3)/VrR^2+(bb(9)+bb(10)/TrR)/VrR^5+bb(8)/(Tr
R^3*VrR^2)*(bb(11)+bb(12)/VrR^2)*exp(-bb(12)/VrR^2))*TrR/VrR;
     elseif Px>0.01;
            VrR=VrR*1.01;
            PrRx=(1+(bb(1)-bb(2)/TrR-bb(3)/TrR^2-
bb(4)/TrR^3)/VrR+(bb(5)-
bb(6)/TrR+bb(7)/TrR^3)/VrR^2+(bb(9)+bb(10)/TrR)/VrR^5+bb(8)/(Tr
R^3*VrR^2)*(bb(11)+bb(12)/VrR^2)*exp(-bb(12)/VrR^2))*TrR/VrR;
     else
            VrR=VrR*1.1;
            PrRx=(1+(bb(1)-bb(2)/TrR-bb(3)/TrR^2-
bb(4)/TrR^3)/VrR+(bb(5)-
bb(6)/TrR+bb(7)/TrR^3)/VrR^2+(bb(9)+bb(10)/TrR)/VrR^5+bb(8)/(Tr
R^3*VrR^2)*(bb(11)+bb(12)/VrR^2)*exp(-bb(12)/VrR^2))*TrR/VrR;
     end
end
%calculate the compressibility factor for the reference fluid
(n-octane)
Zh=(Zd-Z0)/(Omg0/Omgh)+Z0;
Z1=(Zd-Z0)/Omg0;

%recalculte the compressibility factor for the reference fluid
as
%validation
Zh2=(1+(bb(1)-bb(2)/TrR-bb(3)/TrR^2-bb(4)/TrR^3)/VrR+(bb(5)-
bb(6)/TrR+bb(7)/TrR^3)/VrR^2+(bb(9)+bb(10)/TrR)/VrR^5+bb(8)/(Tr
R^3*VrR^2)*(bb(11)+bb(12)/VrR^2)*exp(-bb(12)/VrR^2));
Zh=Zh2;
%Calculate the reference fluid part for the enthalpy
calculation
Hxh=-TrR*(Zh-1-(bb(2)+(2*bb(3)/TrR)+(3*bb(4)/TrR^2))/(TrR*VrR)-
(bb(6)-
3*bb(7)/TrR)/(2*TrR*VrR^2)+bb(10)/(5*TrR*VrR^5)+3*bb(8)/(2*TrR^
```

```
3*bb(12))*(bb(11)+1-(bb(11)+1+bb(12)/VrR^2)*exp(-
bb(12)/VrR^2)));
Vr2=VrR;

%% Pressure effect on enthalpy
HxC=(Hx0+Omg0/Omgh*(Hxh-Hx0));
H0=aaa(1)+aaa(2)*T+aaa(3)*T^2+aaa(4)*T^3+aaa(5)*T^4+aaa(6)*T^5;
% enthalpy ideal gas (kj/kg)
H0mol=H0*0.04401; % enthalpy ideal gas (kj/mol)
HC=H0-R*Tc/44.01*HxC; % enthalpy real gas (kj/kg)
HCmol=HC*0.04401; % enthalpy real gas (kj/mol)


%% fugacity coefficient

% Fugacity coefficient carbon dioxide part
pB=aa(1)-aa(2)/Tr-aa(3)/Tr^2-aa(4)/Tr^3;
pC=aa(5)-aa(6)/Tr+aa(7)/Tr^3;
pD=aa(9)+aa(10)/Tr;
pE=(aa(8)/(2*Tr^3*aa(12)))*(aa(11)+1-
(aa(11)+1+(aa(12)/Vr^2))*exp(-aa(12)/Vr^2));
lnPhi0=Z0-1-log(Z0)+pB/Vr+pC/(2*Vr^2)+pD/(5*Vr^5)+pE;

% Fugacity coefficient reference fluid part
pBR=bb(1)-bb(2)/TrR-bb(3)/TrR^2-bb(4)/TrR^3;
pCR=bb(5)-bb(6)/TrR+bb(7)/TrR^3;
pDR=bb(9)+bb(10)/TrR;
pER=(bb(8)/(2*TrR^3*bb(12)))*(bb(11)+1-
(bb(11)+1+(bb(12)/VrR^2))*exp(-bb(12)/VrR^2));
lnPhih=Zh-1-log(Zh)+pBR/VrR+pCR/(2*VrR^2)+pDR/(5*VrR^5)+pER;



% Fugacity coefficient calculation
lnPhiX=lnPhi0+Omg0/Omgh*(lnPhih-lnPhi0); % fugacity
lnPhi=exp(lnPhiX); % fugacity coefficient

%% entropy calculation
SxC=HxC*Tc/T+lnPhiX+log(P*10^2);

%entropy calculation for an ideal gas
S0=((aaa(2)*log(T)+2*aaa(3)*T+3/2*aaa(4)*T^2+4/3*aaa(5)*T^3+5/4
*aaa(6)*T^4)-
(aaa(2)*log(298)+2*aaa(3)*298+3/2*aaa(4)*298^2+4/3*aaa(5)*298^3
+5/4*aaa(6)*298^4))*44.01+213.74;

% entropy
S=S0/44.01-(R/44.01)*SxC;
Smol=S*0.04401;

% write compressibility factor and fugacity coefficient
Z=Z0;
phi=lnPhi;
fug=log(phi*P*10^5);
```

2.4 wellspacing.m

```
% Calculation of the wellspacing
P=PendINJ;
T=Ti;
TABLEinterp;

Retardation=1+(((1-poro)*CProck)/(poro*Cp/rho2)); %retardation
factor
WHILEflowrate=1;
flowmaxcalc
P=PendINJ;
T=Ti;
TABLEinterp;
Wellspacing=sqrt((Lifetime*Runfact*Qm/rho2*3600*3)/(pi*resheigh
t*Retardation*poro)); %Apply well spacing equation
```

2.5 GeoConstants.m

```
% ~~~~ Geothermal CO2 system ~~~~
% This program is a part of the geothermal CO2 system
% containing all the constants used in the calculations
%
%
% Author: Dave Janse
% Last modification date: 01-04-2010

Tc=304.1282; %Critical temperature
Pc=73.773; %Critical pressure
PcR=Pc; %Critical pressure reference
TcR=Tc; %Critical temperature reference
VcR=4.3071e-3; %Critical volume reference
TrR=T/TcR; %Reduced temperature reference
PrR=P/PcR; %Reduced pressure reference
Tr=T/Tc; %Reduced temperature
Pr=P/Pc; %Reduced pressure
R=8.314472; %Gas constant
```

```
Rduan=R/100; %Gas constant in Duan EOS units
Omg0=0.22394; %Acentric factor CO2
Omgh=0.3978; %Acentric factor n-octane reference
boltz=1.381e-23; %Boltzman constant
planck=6.626e-34; %Planck constant

% Coefficients for equations of state
% Sterner EOS
c=[0 0 1.8261340e6 7.9224365e1 0 0; ...
    0 0 0 6.6560660e-5 5.7152798e-6 3.0222363e-10; ...
    0 0 0 5.9957845e-3 7.1669631e-5 6.2416103e-9; ...
    0 0 -1.3270279 -1.5210731e-1 5.3654244e-4 -7.1115142e-8;
...
    0 0 1.2456776e-1 4.9045367 9.8220560e-3 5.5962121e-6; ...
    0 0 0 7.5522299e-1 0 0; ...
    -3.9344644e11 9.0918237e7 4.2776716e5 -2.2347856e1 0 0; ...
    0 0 4.0282608e2 1.1971627e2 0 0; ...
    0 2.2995650e7 -7.8971817e4 -6.3376456e1 0 0; ...
    0 0 9.5029765e4 1.8038071e1 0 0];
Tm=[T^-4; T^-2; T^-1; 1; T; T^2];
a=c*Tm;

% Sterner EOS for function only
a1=1.8261340e6.*T.^-1+7.9224365e1;
a2=6.6560660e-5+5.7152798e-6.*T+3.0222363e-10.*T.^2;
a3=5.9957845e-3+7.1669631e-5.*T+6.2416103e-9.*T.^2;
a4=-1.3270279.*T.^-1-1.5210731e-1+5.3654244e-4.*T-7.1115142e-
8.*T.^2;
a5=1.2456776e-1.*T.^-1+4.9045367+9.8220560e-3.*T+5.5962121e-
6.*T.^2;
a6=7.5522299e-1;
a7=-3.9344644e11.*T.^-4+9.0918237e7.*T.^-2+4.2776716e5.*T.^-1-
2.2347856e1;
a8=4.0282608e2.*T.^-1+1.1971627e2;
a9=2.2995650e7.*T.^-2-7.8971817e4.*T.^-1-6.3376456e1;
a10=9.5029765e4.*T.^-1+1.8038071e1;

% Duan EOS
b=[8.99288497e-2;...
    -4.94783127e-1;...
    4.77922245e-2;...
    1.03808883e-2;...
    -2.8251686e-2;...
    9.49887563e-2;...
    5.20600880e-4;...
    -2.93540971e-4;...
    -1.77265112e-3;...
    -2.51101973e-5;...
    8.93353441e-5;...
    7.88998563e-5;...
    -1.66727022e-2;...
    1.39800000;...
    2.96000000e-2];
B=b(1)+b(2)/Tr^2+b(3)/Tr^3;
C=b(4)+b(5)/Tr^2+b(6)/Tr^3;
D=b(7)+b(8)/Tr^2+b(9)/Tr^3;
E=b(10)+b(11)/Tr^2+b(12)/Tr^3;
F=b(13)/Tr^3;

% Coefficients for Sonová viscosity equation
AA=[0.248566120 0.004894942;...
    -0.373300660 1.22753488;...
    0.363854523 -0.774229021;...
    -0.0639070755 0.142507049];

% data for Pitzer calculation for Enthalpy/Entropy
% Data for CO2
aa=[0.1181193;...
    0.265728;...
    0.154790;...
    0.030323;...
    0.0236744;...
    0.0186984;...
    0;...
    0.042724;...
    0.155488e-4;...
    0.623689e-4;...
    0.65392;...
    0.060167];

% Date for n-octane reference
bb=[0.2026579;...
    0.331511;...
    0.027655;...
    0.203488;...
    0.0313385;...
    0.0503618;...
    0.016901;...
    0.041577;...
    0.48736e-4;...
    0.0740336e-4;...
    1.226;...
    0.03754];

% data for ideal enthalpy/entropy calculation
aaa=[11.11374 0.479107 0.762156e-3 -0.35936e-6 0.084744e-9 -
0.05775e-13];
```